1997

Winter/spring steady-state water balances for a palustrine forested wetland located in southeastern Virginia

Daniel Otis Redgate
College of William and Mary - Virginia Institute of Marine Science

WINTER/SPRING STEADY-STATE WATER BALANCES FOR A PALUSTRINE FORESTED WETLAND LOCATED IN SOUTHEASTERN VIRGINIA

A Thesis

Presented to

The Faculty of the School of Marine Science

The College of William and Mary in Virginia

In Partial Fulfillment

Of the Requirements for the Degree of

Master of Arts

---

by

Daniel Otis Redgate

1997

APPROVAL SHEET

This thesis is submitted in partial fulfillment of
the requirements for the degree of

Master of Arts

Daniel O. Redgate

Approved, August 1997

Carlton H. Hershner, Ph.D.
Committee Chairman/Advisor

James E. Perry III, Ph.D.

William G. Reay, Ph.D.

Thomas C. Juster, Ph.D.
Department of Geology
University of South Florida - Tampa

Michael J. Focazio, Ph.D.
Water Resources Division
U. S. Geological Survey

TABLE OF CONTENTS

LIST OF TABLES

LIST OF FIGURES

ABSTRACT

The seasonal hydrodynamics of a flatwoods ecosystem containing winter-wet woods, ridges and sinkholes was investigated to evaluate net groundwater flow from or between winter-wet woods and adjacent land features. Short-term, steady-state climatic water balances were generated from water table elevations recorded during the winter recharge season and into mid-summer. Net precipitation (P_n) input to the water balance was estimated by published equations applied to measurements of gross precipitation (P_g), and evapotranspiration (ET) was calculated by the equilibrium model from climatic measurements taken on site. Total cumulative P_g for the study period of October 17, 1994 to June 21, 1995. was 694 ± 42 mm, and total ET was 480 ± 96 mm. The winter and spring were drier than normal, resulting in negligible surface water outflow from the study area. Daily ET went from a seasonal low in December and January of approximately 0.6 mm/day to a high of approximately 4 to 5 mm/day in June. Based on these climatic measurements, forty-five balances with an average duration of 42 days were calculated using the water level data from 17 wells located in wet flatwoods, ridges, and sinkholes. Six balances between October 1994 and mid-March 1995 had a mean ratio of ET:P_n of 43%, thus leaving an average of 57% of P_n for groundwater recharge. In this time period, all features showed net groundwater outflow in excess of the pooled standard error. Water balances that included a dry period from mid-March to mid-April or subsequent balances in June had ET:P_n ratios >100%, indicating an additional water input to the climatic balance besides precipitation. Since significant regional, groundwater inflow is unlikely from both preliminary observations of nested piezometers and landscape setting of the study area, the excess water may have resulted from an overestimation of ET losses or unmeasured changes in soil moisture storage. A balance between P_n and ET existed from late April through May when ET:P_n ratios were closer to 100%. The steady-state, climatic water balances show that: 1) soil moisture excesses and deficits due to seasonal inequalities in rates of P and ET are not represented simply by changes in soil water volume as vertical fluctuations in water table level in the study area. Net groundwater flow exits the study area in winter and spring; and, 2) vegetation of the flatwoods ecosystem may not be transpiring at a potential rate due to soil moisture limitation. The residuals of the climatic balances and their associated standard errors did not show significant differences between landscape features. This information could be obtained by performing water balances where direction and magnitude of groundwater flow are measured as well as on-site estimates of canopy interception.

WINTER/SPRING STEADY-STATE WATER BALANCES FOR A PALUSTRINE FORESTED WETLAND LOCATED IN SOUTHEASTERN VIRGINIA

1.0 INTRODUCTION AND STUDY OBJECTIVES

The world climate can be subdivided into regional patterns characterized by a unique seasonal distribution and annual balance of precipitation (P) and evapotranspiration (ET). The processes of P and ET are a function of climate, such as radiation, atmospheric circulation and topography; vegetation, such as plant physiology and root morphology; and geology, such as soil genesis and aquifer permeability. To provide a rational framework for the definition of climatic regions, Thornthwaite (1948) introduced a moisture index based on a soil moisture budget of P and potential ET (PET). He defined PET as the rate of ET expected from dense, short vegetation with non-limiting soil moisture. Non-climatic surface controls on ET such as variation in the type of soil or vegetation can influence the rate of ET significantly. A standardized surface (e.g., the combination of soil surface, exterior plant surfaces, and plant mesophyll tissue that act as the source of water vapor) like the one suggested by Thornthwaite serves to isolate the influence of the regional meteorology on climatic patterns. As a result, Thornthwaite's functional classification of climate coupled an index of moisture availability with the standard statistical indices of meteorological elements, helping to explain patterns in landscape hydrology, and the distribution and growth of vegetation.

The humid subtropical climate of southeastern Virginia exhibits a near balance between annual P and PET. Approximately 75% of the annual precipitation of this region can be lost in ecosystems where ET equals PET (Thornthwaite 1948). Precipitation has a fairly uniform seasonal distribution with a slight peak in July and August whereas PET follows a sinusoidal distribution (Figure 1). Seasonal PET rates are dictated largely by

Figure 1. Normal monthly gross precipitation (Gross P), and potential evapotranspiration (PET) by the Thornthwaite method. Normals calculated for Norfolk, Virginia for the period of record 1961 to 1990.

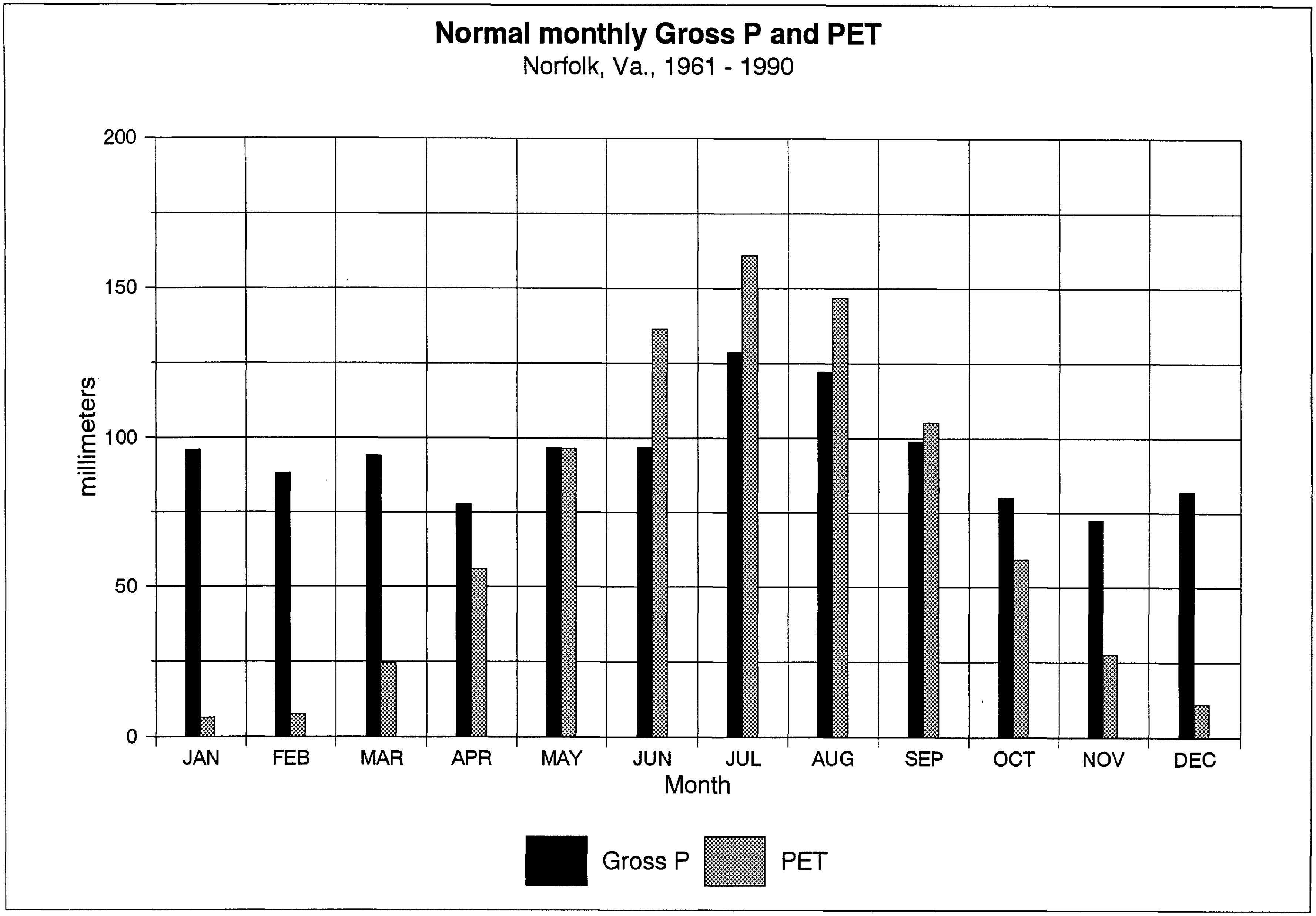

Normal monthly Gross P and PET
Norfolk, Va., 1961 - 1990
millimeters
200
150
100
50
0
JAN
FEB
MAR
APR
MAY
JUN
JUL
AUG
SEP
OCT
NOV
DEC
Month
Gross P
PET

climate and biota and therefore peak in summer and decline in winter. Taken together, the difference between these vertical water fluxes decreases soil moisture storage during the summer when ET > P. In early summer, while soil moisture is adequate, the rate of ET may equal or approach potential conditions. If soil moisture decreases enough to cause moisture stress in the vegetation, an increase in stomatal resistance reduces transpiration to some "actual" ET rate (AET) that is less than potential. In fall, a decrease in atmospheric and radiative moisture demand and biological activity reduces ET below P, resulting in recharge of soil moisture to a maximum in early spring.

The spatial and temporal balance of P and ET (i.e., the net vertical water flux) has a significant effect on distribution and magnitude of surface runoff and groundwater flow (i.e., the "lateral" water flux, for the purpose of this discussion). When P/ET > 1, increased soil moisture decreases the available pore space for infiltrating water and increases the likelihood of ponding and surface runoff generation. Higher water table position when coupled with steeper gradients in water table slope increases groundwater flow and streambank discharge. In turn, the rates of surface and subsurface water flows influence the rate and distribution of ET and, on a regional scale, of P as well. Reduced lateral flows increase the residence time of precipitated water in an ecosystem, increasing soil water availability and consequently the rate of ET. Many wetlands are called "water pumps" because they lose over two-thirds of their annual water inputs to ET (Richardson and McCarthy 1994). On a larger areal scale, landscapes with high soil moisture content affect the atmospheric transfers of sensible and latent heat, and in turn regional precipitation patterns.

A summary of vertical and lateral water flows for an ecosystem is useful in determining the function of that ecosystem within a landscape. Studies in ecosystem hydrodynamics explore the processes by which various ecosystems partition water inflows into different types of storage and outflows. In Figure 2, a conceptual hydrologic model of an ecosystem depicts typical water inflows and outflows along with areas of water storage. The presence and movement of water both transforms and transports the abiotic and biotic components of the ecosystem. Therefore, it is not surprising that variation in the sources and sinks of water for an ecosystem strongly influences its structure and function. Wetlands are of particular interest in landscape hydrology due to the greater interaction between subsurface, surface and atmospheric waters. In the Chesapeake Bay watershed, as is typical of the eastern United States, palustrine forested wetlands comprise more than half the total wetland acreage (Tiner et al. 1994). On the coastal plain of southeast Virginia, a large subset of palustrine forested wetlands are referred to as "flatwoods" or "winter-wet woods", and are characterized by low permeability soils and level topography. The range of hydroperiods for flatwoods varies from a seasonally flooded/saturated regime, which qualifies as a federal jurisdictional forested wetland, to a non-jurisdictional, mesic forest that is temporarily saturated. As a result of their borderline, jurisdictional wetland hydrology, and, in addition, their large areal extent and often high development potential, flatwoods have undergone considerable modification and destruction. The future of the current federal protection of the more mesic flatwoods is being debated as economic pressures to modify these wetlands intensifies. Investigations into the hydrology of flatwoods will yield information with which to assess the function and value of these areas, with respect to surface runoff generation, groundwater recharge and discharge, and biological diversity. A better scientific understanding of flatwood ecosystems will contribute to a more informed and effective management of these natural resources.

Figure 2. Conceptual hydrologic model of a vegetated ecosystem (modified from Duever, 1988).

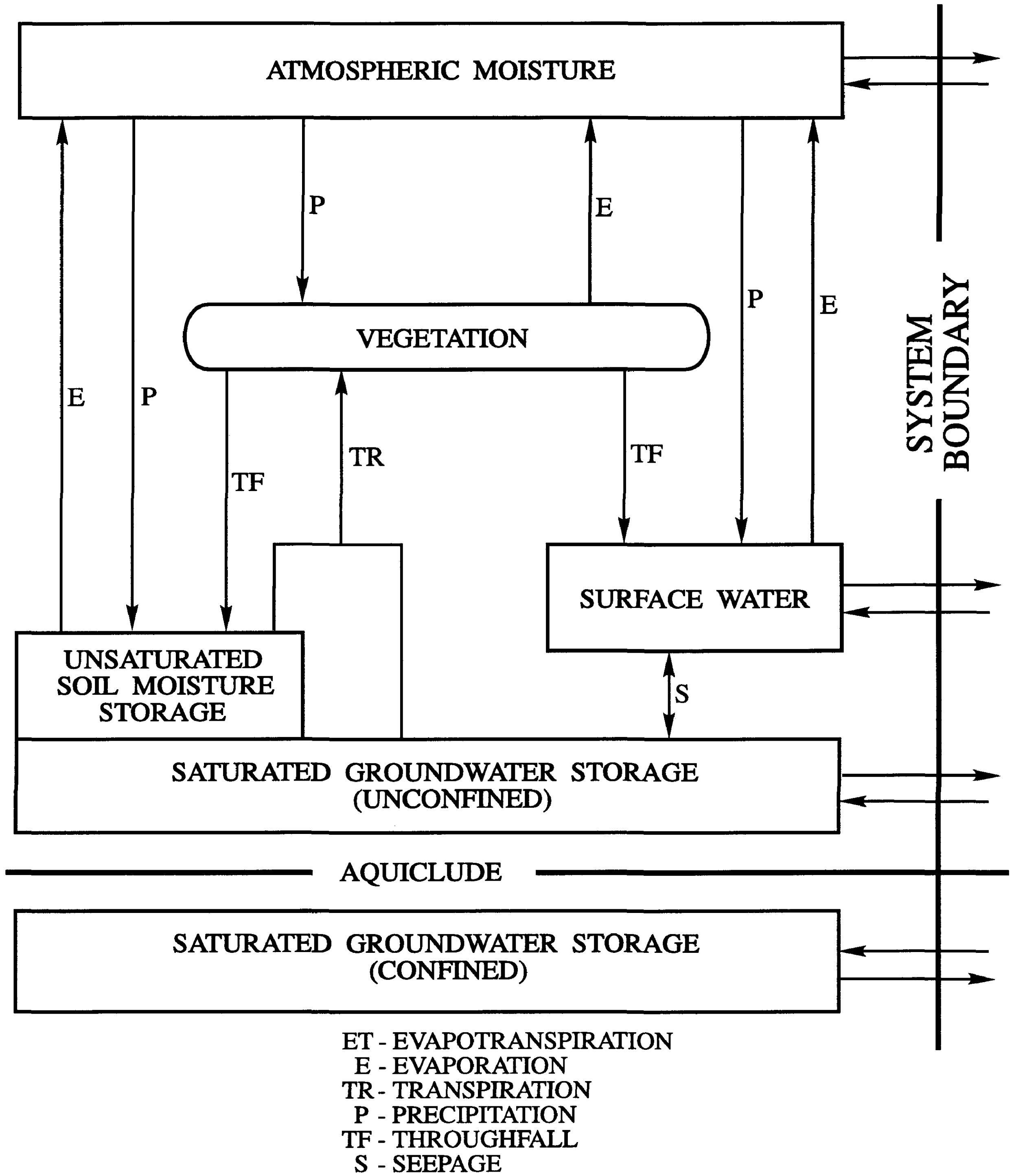

Figure 2. Conceptual hydrologic model of a vegetated ecosystem (modified from Duever, 1988).

The purpose of this research was to assess the potential for groundwater exchange between the flatwood and its adjacent landscape features. The degree of hydrologic connectivity between the flatwood and surrounding landscape was thought to be minimal after large fluctuations in seasonal water table levels were observed in flatwoods. In that, the seasonal change in storage of the water table aquifer could account for the annual water surplus between P and ET. Groundwater inflows are likely to be small for most flatwoods, because many of these flatwoods exist on broad, interstream terraces. Thus, P is probably the dominant water influx, and the major source of seasonal recharge to the water table aquifer. I hypothesized that the amount of water partitioned to lateral flows would be a small proportion of P on the basis that: 1) non-limiting soil moisture of a forested wetland causes ET to approach PET; and, 2) annual P and PET are similar in a humid subtropical climate. The relatively flat topography of the land surface combined with low permeability soils would reduce the rate of groundwater flow, and increase the residence time of soil moisture. Given no change in storage and an absence of surface water flows, a climatic water balance where P minus ET equals a residual representing net groundwater flow provides a method to examine the seasonal variation of P, ET and net groundwater flows. The primary objective was to determine whether water fluxes in wet flatwoods are dominated by vertical pathways with little groundwater flow to surrounding land features, and that seasonal inequalities in inflows and outflows result in a change in storage predominantly. However, on a seasonal basis, the P:ET ratio fluctuates. Currently, it is unclear the extent to which seasonal inequalities in P and ET are partitioned to groundwater flow or change in water storage. A high ratio of P:ET during the winter and early spring would provide an opportunity for storage increases and possibly higher groundwater flows. A low ratio of P:ET through the spring and summer would have an opposite effect. If seasonal water surplus and deficit is exchanged within aquifer storage, then the residual of a climatic balance with a steady-state storage variable should not be significantly different from zero.

Application of short-term, steady-state water balances to seasonal water table fluctuations provides a way to differentiate between changes in soil water volume and groundwater flow. Steady-state analysis involves setting one variable constant while varying others. This variable may be selected because it is difficult to measure, has a large uncertainty, or for the purpose of observing how remaining variables correlate given the constant variable. Depending on the site, change in volume over time for the storage component of the water balance can be difficult and error prone. The volume of water held in a given depth of the surficial, unconfined aquifer and overlying capillary zone is found by the measurement of aquifer specific yield as well as soil moisture distribution with depth. If two points in time are selected when the water table is at the same elevation, a water balance for the intervening time period may be modeled as steady state, thus avoiding the measurement and accompanying error of specific yield and soil moisture. However, this model requires the assumption that equal volumes of soil moisture exist above the water table at both times. Since soil moisture distribution with depth can vary given identical water table levels, this assumption represents a potential source of error in steady-state water balance calculations. Although this error is mentioned in water balance literature, the use of equal water table levels to define steady state is common practice, and this source of error is either unrecognized or considered negligible.

Having defined steady-state water balances, it is now easier to comprehend how dividing the hydroperiod of a wetland, or its annual hydrograph of phreatic water level, into short time periods can provide insight into the pathways and rates of wetland water flows. Certain types of wetlands exhibit little variation in the quantities or directions of flow for different seasons or climatic events. A short-term balance conducted at different times in the year would yield similar results for sources and sinks for water flow and associated rates and volumes. Other wetlands have seasonal hydrodynamics whereby flows of different origin (e.g., atmospheric, riverine, wind-driven tides, groundwater) may vary both in quantity and spatial distribution. In this instance, short-term balances can serve to isolate time periods and quantify the relative importance of the budget components. For instance, the hydroperiod of a riverine wetland may be dominated by groundwater flows during the winter and surface flow in the spring and summer. An annual balance may show that the groundwater and surface water components are equal quantities, but the timing and duration of the different flows would not be known. Yet this information is essential when questions are raised concerning the effect of various water flows on the physiochemical environment of the wetland and ecology of the area or region.

The hydroperiod of winter-wet woods shows a considerable change in storage volume of soil moisture during the year and a strong influence by P and ET fluxes. The extent of surface and groundwater flows are less predictable since they are dependent on site specific characteristics such as geology, soil development, and geomorphology of the surrounding landscape. This study focused on quantifying net groundwater flow during the winter 1994/spring 1995 water table recharge period when almost no surface flows occurred. Under these conditions, short-term, steady-state balances of P and ET on a monthly or seasonal basis with no surface flows yielded net groundwater flow for the study area.

The secondary objective of this study was to compare the water balance residuals, or net groundwater flow, between the different land features (i.e., flatwoods, sinkholes, and upland ridges). A large difference in residuals may indicate local groundwater flow between these land features or to surrounding areas, or spatial variation in the loss of water to deeper regional groundwater flow. In a homogeneous media, the water table would be a subdued expression of the topography. The ridges and possibly the flatwoods would have higher hydraulic heads than surrounding areas, resulting in flow downward and away from these features. Sinkholes would serve as a focus for groundwater flow due to their lower hydraulic head. In this case, the ridges and flatwoods would be groundwater recharge areas, and the sinkholes would be discharge areas. However, the land features in the study area have different soil types and permeability's, and, therefore, seasonal water table configuration may differ considerably from surface topography.

2.0 BACKGROUND

2.1 Water Balance Review

A water balance where the storage volume is at steady state calculates inflows and outflows of water from a soil volume over a period of time that begins and ends at the same water table level. The duration of a balance may be hours (e.g., the daily fluctuation of the water table in response to ET and groundwater recharge), months (e.g., a seasonal or annual hydroperiod), or years (e.g., the evaluation of a water balance model against long-term measurements). The components of the steady-state water balance can be expressed as the symbolic equation:

$$0 = \Delta V = P_n + S_i + G_i - ET - S_o - G_o \qquad (1)$$

where:

ΔV = change in volume of water storage, equals 0 at steady state
P_n = net precipitation
S_i = surface water inflow
G_i = groundwater inflow
ET = evapotranspiration
S_o = surface water outflow
G_o = groundwater outflow

Investigations using short time periods in which inflows must balance outflows offer several advantages for research of ecosystem hydrodynamics. Short duration permits greater resolution of temporal variations in hydrologic flows. Information on seasonal and event-based dynamics in water flows and storage is lost within an annual water balance. Second, data correlating the hydrologic response of the ecosystem to specific meteorological conditions, when gathered at different phases of the ecosystem's hydroperiod is useful in calibrating process-oriented hydrologic simulation models. Third, an investigator limited by time and materials need not measure the specific yield of the water table aquifer for estimation of the change in storage owing to the steady-state condition.

Yin and Brook (1992) used short-term, steady-state water balances of the Okefenokee Swamp watershed to evaluate four methods for estimating PET. Instead of the full water balance equation, the authors estimated AET from the difference in P and S_o. By definition of a watershed, natural surface water inputs do not occur. It was assumed that groundwater flow did not cross the surface boundaries of the watershed. In addition, G_o was eliminated from consideration after previous studies into the groundwater hydrology of the swamp had shown a total water loss of only 0 to 6%.

Using historical records of precipitation, S_o and water table level, Yin and Brook calculated watershed AET for 56 time periods lasting an average of 10.6 months that satisfied steady-state conditions. Under the assumption that watershed AET approximates PET due to shallow groundwater levels and abundant surface water ponding, watershed AET was compared to the PET estimates of four popular temperature-based methods, Thornthwaite, Holdridge, Blaney and Criddle, and pan evaporation. The results of the study showed that all methods were in close agreement in estimating PET. The Thornthwaite method offered the highest R^2 value while the Blaney-Criddle method gave the lowest root mean square error and therefore had the highest overall accuracy.

Monthly climatic water balances (i.e., $B = P - PET - \Delta V$, where B is net groundwater flow plus the sum of the errors of the components) of Thunder Bay, a Carolina bay located on the Upper Coastal Plain of western South Carolina, demonstrated significant groundwater flows between the bay and surrounding land which contradicted the popular belief that the bays were perched systems (Lide et al. 1995). In their research, a steady-state model was not necessary due to the availability of pond stage data for the calculation of ΔV. Precipitation was measured on site, and surface flows did not occur. ET was assumed to equal PET and was calculated by the Thornthwaite method. Groundwater flow was estimated by the residual (B). Given knowledge of the water table configuration around the Bay and a large residual, preliminary findings on the degree and direction of net groundwater flow were possible. The results suggest that the bay is predominantly a source of net groundwater outflow with episodes of net groundwater inflow during periods of above average rainfall and higher than normal water table levels.

Estimating a component of the water balance, especially groundwater flow or ET, as a residual is a common practice in studies of ecosystem hydrology (LaBaugh 1986). However, this method may have a large uncertainty, which, in some cases, may exceed net groundwater flow, G_n, thus making the direction of flow uncertain. As the sum of the other balance components, the residual produces an estimate of the unmeasured component subject to errors of measurement related to other components (Winter 1981). Therefore, a relatively small percent error in the measurement of a large flow becomes significant when used to estimate a smaller residual. For example, the average annual rainfall for York Co., Virginia is 1118 mm. If the measurement of P has a standard error of 112 mm (i.e., a relative error of 10%) and ET, if assumed to be 75% of annual **P** or 839 mm, has a standard error of 168 mm (i.e., a relative error of 20%), then the difference of these two amounts is 279 mm with a standard error of 202 mm, resulting in a large relative error of 72%. From this example, it is easy to see that additional error in components of the budget can lead to a standard error that is greater than the residual.

In addition to the propagation of error, a second limitation to calculating a balance component by a residual applies to throughflow systems where both inflow and outflow of either surface water or groundwater are not measured. In these situations, the residual represents the net flow only (Winter 1981). The limitations of this method can be illustrated by the following examples. First, a floodplain area where P, ET, and groundwater inflow and outflow are measured but a flood event responsible for surface water inflow and outflow is not measured. Second, a bog where P, ET, and surface flows are measured but groundwater inflows and outflows are not. In both of these hypothetical studies, the net flow calculated by the residual will have an uncertainty from the errors of the other components. Since the magnitude of the net flow will be less than the magnitudes of either inflow or outflow, the resulting estimate will have a greater relative error for a given uncertainty. The study by Lide et al. on Thunder Bay did not measure groundwater flows to or from the bay. However, the investigators did measure the water table slope, and therefore could associate the residual of the climatic balance with a direction of flow.

A water balance that uses the residual as an estimate of a hydrologic component should be subjected to an error analysis. Otherwise, as demonstrated above, it is unclear how measurement errors may have affected confidence in the estimate. Errors associated with various water flows may add to, subtract from, or compensate for each other. This study measured P and ET and calculated net groundwater flow by difference. A review of the errors associated with the measurement of P and ET was conducted in order to quantify confidence in the groundwater flow estimate. Errors in measurement and estimation of P and ET can be separated into two categories: measurement and regionalization (Winter 1981). Measurement errors exist due to faulty instrumentation, sampling design, or data collection whereas errors by regionalization occur when point measurements are extrapolated over a time-space continuum (Winter 1981).

2.2 Precipitation Measurement and Error Analysis

Measurement accuracy for point precipitation is commonly affected by evaporation, adhesion, color, inclination of orifice, splash, wind, technique of catch measurement, gage damage, and height of orifice above ground (Corbett 1967, Winter 1981). Significant evaporation of rainfall catch can occur in gages exposed to higher wind speeds, radiation or aridity, or located in remote stations where servicing occurs infrequently. Sample errors from adhesion are proportional to the surface area of the collector and the interior of the receiving tank if appropriate. Precipitation is most accurately measured when the gage orifice is oriented parallel to the slope of the ground surface.

Wind exposure is considered the largest potential source of error (Corbett 1967). The turbulence created by wind flowing over and around the gage decreases rainfall catch. As wind speed generally increases with height above ground, error from turbulence is augmented by raising the height of the gage above the soil surface. A more accurate catch results from the construction of a windshield that channels air flow around the gage to prevent updrafts next to the orifice (Corbett 1967). Alternatively, surrounding vegetation can provide a uniform obstruction to wind exposure. If the gage is located within a forest clearing, the U.S. Weather Bureau advises that the height of the trees above the gage should not exceed about twice their distance from the gage (i.e. about a 60 degree angle from the orifice to the top of the tree) (Corbett 1967). Other studies suggest placing a gage no closer to an object than the object's height which translates into a 45-degree cone of projection from the gage orifice (Corbett 1967).

Extending point measurements of precipitation into an areal average results in errors of regionalization. Confidence in an areal estimate is a function of spatial variability of rainfall, amount and duration of storm events, density of gage network and size of area. As a rule, error increases with shorter sampling periods and decreases with higher gage density, longer duration storms, and larger area (Winter 1981). With increasing areal mean precipitation (i.e., storm size), absolute error increases while the coefficient of variation decreases (Corbett 1967, Winter 1981).

Storm type, or the mechanism by which precipitation is formed, greatly affects spatial and temporal variability of precipitation (Corbett 1967, Winter 1981). The two basic mechanisms of storm generation are convection and stratiform, which differ in the rapidity with which precipitation particles develop and the magnitudes of vertical air motion associated with the precipitating cloud (Smith 1993). Orographic lifting can be considered a third precipitation mechanism, although it exhibits both convective and stratiform properties.

Convective precipitation is identified with vertical air motions that are locally strong, precipitation particles that form at the cloud base, and rapid development of precipitation (Smith 1993). As might be expected, this precipitation mechanism is associated with the highest rainfall variability (Corbett 1967). Stratiform precipitation differs from convective by having weak, vertical air motion, precipitation particles that form at the top of the cloud system, and longer development time for precipitation (Smith 1993). A more uniform rainfall pattern emerges from these large scale frontal storms that are often associated with extratropical cyclones (Corbett 1967, Smith 1993).

Corbett (1967) cites a number of studies of convective rainfall conducted on the relatively flat terrain of central Illinois. One study found rainfall gradients of 0.8 inches per mile for convective storms. A second study investigating variability of gage catch as a function of distance between gages demonstrated average differences of about 1.5% for gages 6 ft apart increasing to about 2.5% for gages 600 ft apart. A third study relates deviation between areal mean rainfall and a point observation at the areal center to the average storm size. Based on their results, the average deviation (X, in inches) between areal mean rainfall for an area (A, in mi^2) and point measurement (P, in inches) at areal center can be found by the equation:

$$X = -2.011 + 0.54\ P^{0.5} + 0.29\ \mathrm{Log}\ A \tag{2}$$

Using a common storm size of 15 mm (0.60 in), this relation predicts a deviation of 0.80 mm (5.2%) for an estimate of mean areal rainfall from a point measurement located at the center of a 5.3-km^2 area (2.0 mi^2). The area used in the previous example corresponds to the area of a circle that encompasses the present research area and is centered on the rain gage used for this study.

Gross precipitation (P_g) incident upon a forested ecosystem is intercepted by the canopy and redistributed as throughfall (T), stemflow (S_f), plant water uptake, and evaporation (E). Throughfall is both rain that has fallen unimpeded to the forest floor and intercepted rain that subsequently drips from the vegetative canopy. Water reaching the soil by flowing down the stems of vegetation is called stemflow. Water adhering to the foliage can be taken up by the plant or evaporated back to the atmosphere. The interception of rainfall by the vegetative canopy can represent significant losses to the water balance of an ecosystem. A 10% to 30% reduction of gross rainfall by interception is common, with some old growth canopies intercepting as much as 57% (Zinke 1967).

Helvey and Patric (1965) compared independent studies of interception in the hardwoods of the eastern United States, and found that predicted values for throughfall and stemflow were remarkably consistent over different sampling locations and canopy species. An average relation of T to P_g was calculated for mature, mixed hardwood stands by averaging equations from the literature and weighting them by the respective number of gages used. Using an approximate 95% confidence interval, Helvey and Patric concluded that 12 of 14 growing season equations and 7 of 9 dormant season equations were not significantly different. In the absence of detailed local throughfall studies, T (mm) could be estimated from measurements of P_g per storm (mm) by the equations:

$$\text{Growing Season:} \quad T = 0.901\ P_g - 0.79 \tag{3}$$

$$\text{Dormant Season:} \quad T = 0.914\ P_g - 0.38 \tag{4}$$

In addition, their review of the literature found that net precipitation (P_n), the portion of P_g entering the soil column, can be reasonably estimated by the measurement of T alone because litter interception and stemflow appear to compensate each other.

The interception loss from needle-leaved trees is greater than for broad-leaved trees (Zinke 1967). Needle-leaved trees have a greater leaf area index (LAI), the ratio of projected leaf area per unit ground surface area, and therefore greater interception storage and opportunity for evaporation during rain (Waring and Schlesinger 1985, Zinke 1967). Roth and Chang (1981) studied throughfall in four major southern pine species, loblolly (Pinus taeda L.), longleaf (P. palustris Mill), shortleaf (P. echinata Mill) and slash (P. elliottii Engelm). Loblolly pine allowed the least amount of throughfall, longleaf the greatest, and shortleaf and slash pines were not significantly different. Their resultant equation for predicting T (mm) from P_g (mm) in loblolly pine stands was:

$$T = 0.790\ P_g + 1.397 \tag{5}$$

which provides estimates of T that correspond closely with the results of previous studies, including Helvey (1971). Similar in method to the weighted equations produced by Helvey and Patric (1965) for hardwoods of eastern United States, Helvey calculated a weighted average equation from separate observations under loblolly canopy that predicts T (mm) from P_g (mm):

$$T = 0.80\ P_g - 0.25 \tag{6}$$

In a summary of measurement error for precipitation, Winter (1981) estimates errors from the gage itself to be from 1% to 5%. Errors due to placement or exposure range from 5% to 15% for long-term data and potentially 75% for individual storms. Calculating T from P_g using equations from the literature introduces two additional sources of uncertainty in estimating P_n, the standard error of the equation and its extrapolation to a new setting. First, the accuracy of the weighted throughfall equations from Helvey and Patric (1965) and Helvey (1971) are unknown, but, due to the summary nature of the equations, the standard errors are likely to be higher than those of the equations derived by Roth and Chang (1981) for example. The linear equations found for longleaf, shortleaf, loblolly and slash pine canopies have standard errors of 10.1%, 9.1%, 11.4%, and 8.4%, respectively, for an average of 9.8%. Second, the application of the literature equations to a site other than those used to generate the relationship introduces an unknown degree of uncertainty. Without a calibration of the equation through site-specific measurements, the estimate is likely to have greater uncertainty than was found in the source studies, although a conclusion of Helvey and Patric (1965) was that additional error may not be very large. With these considerations in mind, the throughfall estimate, which is equivalent to P_n for the purposes of this study, was assigned an error of 15% for use in the short-term, steady-state water balances.

2.3 Evapotranspiration Measurement and Error Analysis

Selection of a model for calculating ET is guided in part by availability of meteorological measurements. For this study, a weather tower was erected within the study area, and equipped with instruments to monitor net radiation, air temperature and relative humidity, wind speed and direction. This is a commonly used instrument array, because several ET models can be used and evaluated based on data from a minimum amount of instruments and thus investment. During the time period of this study, a malfunctioning relative humidity sensor prevented the application of a more sophisticated model such as the Penman-Monteith equation, and narrowed the selection to a model that correlates either air temperature or solar radiation with the rate of ET. Temperature-based methods such as those developed by Thornthwaite (1948), Hargreaves (1975), and Blaney and Criddle (1950) are commonly used to estimate PET. The high popularity of these methods is due to the widespread availability of the required meteorological parameters. In general, they use monthly temperature statistics as a basis on which to apply modifications for vegetation type, regional and monthly means of solar radiation, percent cloudiness, relative humidity, and wind speed. Recent and historical monthly temperature and other weather indices are readily available from most weather stations.

The success of temperature-based models in estimating ET is due to the correlation between temperature and radiation, the primary forcing function in the rate of evaporation (Slatyer and McIlroy 1961, Shuttleworth 1991). Relatively accurate seasonal and annual estimates of PET have been obtained by Rykiel (1984), Yin and Brook (1992), and Richardson and McCarthy (1994). A higher accuracy in these empirical models is obtained by either calibrating against a more robust and accurate ET model, or by partitioning an accurate annual estimate into monthly values weighted by local, more site specific meteorological parameters (e.g., biotemperature, pan evaporation). The empiricism of the temperature-based models limits their accuracy when applied to new systems with differing general climates, soil types, surrounding landscapes, and vegetation. If calibration for local conditions cannot be performed, the temperature-based methods are not recommended and should be used only when temperature is the only measurement available (Slatyer and McIlroy 1961, Shuttleworth 1991).

Radiation-based ET models are simplifications of the Penman-Monteith model which can be expressed as:

$$ET = \frac{Q_E}{\rho_w \lambda} = \frac{1}{\rho_w \lambda} \cdot \frac{\Delta Q_A + \rho_a c_p \delta e / r_a}{\Delta + \gamma (1 + r_s / r_a)} \tag{7}$$

where:

- Q_E = latent heat flux, in MJ m^{-2} day^{-1}
- ρ_w = density of water, in kg m^{-3}
- λ = latent heat of vaporization, in MJ kg^{-1}
- Δ = slope of the saturation vapor pressure curve (defined at ambient air temperature), in kPa C^{-1}
- Q_A = available energy, in MJ m^{-2} day^{-1}
- ρ_a = density of air, in kg m^{-3}
- c_p = specific heat of moist air at constant pressure, in kJ kg^{-1} C^{-1}
- δe = vapor pressure deficit in the air, in kPa
- γ = psychrometric constant, in kPa C^{-1}
- r_a = aerodynamic resistance, in s m^{-1}
- r_s = surface resistance, in s m^{-1}

Essentially, the Penman-Monteith model combines factors influencing the climatic evaporative demand (i.e., available energy and vapor pressure deficit) with the biologic and aerodynamic resistances to this demand. In this way, the model can estimate actual

ET for ecosystems with different plant species and soil moisture regimes given the appropriate values for the resistances. The most significant term of the Penman-Monteith model is Q_A, the energy available for partitioning into latent or sensible heat, which can be expressed as the result of an energy budget for a unit volume of an ecosystem with an extensive vegetative canopy:

$$Q_A = Q_N - Q_G - Q_S - Q_P - Q_C \tag{8}$$

where:

Q_N = net incoming radiant energy
Q_G = outgoing heat conduction into the soil
Q_S = energy stored within the volume (e.g., vegetation)
Q_P = energy absorbed by biochemical processes
Q_C = energy loss by horizontal air movement

The last two terms of (8), Q_P and Q_C, are usually not included in water balance work. First, Q_P is approximately 2% of Q_N (Shuttleworth 1993). Second, net energy losses by horizontal advection, Q_C, are minimized or eliminated by locating study sites within large, homogeneous landscapes. For instance, the forested area used in this study lies within a large forested tract consisting of both municipal water reservoir watershed and national park. The fetch, which is defined by Monteith and Unsworth (1990, pp.233) as the distance of traverse across a uniformly rough surface, for the study site was approximately 1.83 km (1.14 mi) where the tract was broken by either the reservoir or housing developments. The recommended fetch is expressed as a ratio of fetch distance to boundary layer depth, and, depending on the roughness elements of the transpiring surface, generally increases for increasing roughness. Fluctuations in the energy storage term, Q_S, occur through changes in the temperature and vapor pressure of the atmospheric volume, temperature of vegetation, and temperature of a shallow soil layer. Significant fluctuations of Q_S occur diurnally, seasonally, and between weather systems. This term is neglected in long-term studies since the net change in energy storage approaches zero. Two factors remove soil heat conduction (Q_G) from the energy balance of a forested swamp. First, the canopy allows little radiant energy to reach the soil surface, and second, the high soil moisture creates a strong sink for the conversion of remaining incident energy to latent heat rather than sensible soil heat flux (Slatyer and McIlroy 1961).

An empirical relation exists between Q_A, the radiation term, and δe, the vapor pressure deficit or atmospheric term, such that the Penman-Monteith model can be rewritten as the radiation term alone multiplied by a coefficient, α:

$$ET = \frac{Q_E}{\rho_w \lambda} = \frac{\alpha}{\rho_w \lambda} \cdot \frac{\Delta Q_A}{\Delta + \gamma} \tag{9}$$

where α has been experimentally determined to equal 1.26 for conditions of potential evaporation over water and PET over saturated soils and short crops in the absence of advection (Priestley and Taylor 1972). Both bare soils and short vegetation when supplied with abundant water exert little surface control over evaporation (Munro 1979) and therefore show a strong coupling between short-term fluctuations in radiation and latent heat flux (McNaughton and Black 1973). However, tall vegetation is more aerodynamically rough than shorter crops and therefore supports stronger turbulent mixing between the evaporating surface and the atmosphere. A high atmospheric exchange coefficient will bring the vapor pressure deficits of the surface and atmosphere into equilibrium, reducing the gradient driving diffusion of water vapor. As the difference between deficits approaches zero, the atmospheric term of the Penman-Monteith equation loses significance, and ET occurs at a rate proportional to the supply of radiant energy (Slatyer and McIlroy 1961, Munro 1979). Investigations of ET rates from forest ecosystems have supported this theory, referred to as equilibrium ET (ET_{eq}), by obtaining values for α that are close to unity (McNaughton and Black 1973, Munro 1979, Woo and Valverde 1981). As a result, ET_{eq} is calculated by:

$$ET_{eq} = \frac{1}{\rho_w \lambda} \cdot \frac{\Delta Q_A}{\Delta + \gamma} \tag{10}$$

The accuracy of simplifications to the Penman-Monteith ET equation, such as the Priestley-Taylor and equilibrium approaches, have been assessed by using the energy balance method of estimating ET as a comparison. The energy balance model combines measurement of the Bowen ratio (β) and available energy to solve for latent heat flux. This model is attributed a high degree of accuracy in the general literature. According to Monteith and Unsworth (1990), the Bowen ratio is the ratio of sensible heat flux to latent heat flux, $C/\lambda E$. If the transfer coefficients of heat and water vapor are assumed equal, the relation can be estimated by:

$$\beta = \frac{C}{\lambda E} = \frac{\gamma \partial T}{\partial e} \tag{11}$$

which can be substituted in the energy balance equation:

$$R_n - G = C + \lambda E \tag{12}$$

and rewritten as:

$$\lambda E = \frac{(R_n - G)}{1 + \beta} \tag{13}$$

McNaughton and Black (1973) used the energy balance approach to examine diurnal fluctuations in hourly increments of heat fluxes within a Douglas fir forest. After examining sources of possible error, they estimated a 20% uncertainty for hourly ET values, although the consistency of their data indicated less error. The overall accuracy of 24-hour totals of ET was expected to be 15%. A high correlation was found between daily ET measured by the energy balance method and net radiation. A value for α of 1.05 was found when measured daily ET was plotted against daily ET_{eq} which suggests an additional 5% error in the ET_{eq} estimate.

Munro (1979) and Woo and Valverde (1981) verified the equilibrium model against energy balance and water balance calculations for a mid-latitude forested swamp. Munro regressed hourly values of Q_{Eeq} on energy balance estimates of Q_E and found Q_{Eeq} to be a fair approximation of Q_E for any time period which includes small and large ET amounts. He suggested that the equilibrium model offered a simple method to obtain long-term ET estimates based on 24-hour totals. In a 5-month study within the same swamp, Woo and Valverde found that ET_{eq} (572 mm) was about 3% greater than ET estimated by the residual of a water balance (554 mm).

3.0 METHODS

3.1 Site Selection

An underlying goal of this research was to characterize the hydrology of a wetland ecosystem that is well represented in the watersheds of southeastern Virginia. Baseline data and the climatic model gained from this study will be extrapolated to other similar wetlands. The value of long-term, intensive, hydrologic studies on "type localities" was emphasized by the Wetland Hydrology Panel of the Wetlands Value Assessment Workshop (Carter 1986). Towards this end, the selected site includes a common type of poorly drained, seasonally saturated forested wetland with a mixture of deciduous and coniferous tree species found in the coastal plain of Virginia. On a National Wetlands Inventory (NWI) map, the site constitutes a mix of PFO1C and PFO1E wetlands [Palustrine Forested Broad-leaved Deciduous Seasonally Flooded (C) and Seasonally Flooded/Saturated (E)], and uplands. In general, the landscape is made up of flatwoods of varying hydroperiod that are punctuated by sinkholes and upland ridges. The 15-hectare (37 ac) study area is located within the east-central region of the Coastal Plain of Virginia on the York-James Peninsula at 37 12' 0"N and 76 32' 45'' W. Yorktown, Virginia is approximately five kilometers to the southeast. The site elevation ranges from 15 m (50 ft) to 18 m (60 ft) above mean sea level (amsl).

Both hydrophytic and upland vegetation exist in seasonally flooded forested wetlands. Shorter periods of soil anoxia per annum and variation in the degree of flooding between years confers less advantage to the adaptations of hydrophytes and therefore prevents their domination. In the study area, facultative upland (FACU) tree species such as tulip poplar (*Liriodendron tulipifera*), beech (*Fagus grandifolia*), white oak (*Quercus alba*), pignut hickory (*Carya glabra*), and american holly (*Ilex opaca*) are found alongside facultative (FAC) and facultative wetland (FACW) species like sweet gum (*Liquidambar styraciflua*), loblolly pine (*Pinus taeda*), sycamore (*Platanus occidentalis*), and various oaks such as water (*Q. nigra*), laurel (*Q. laurifolia*) and willow (*Q. phellos*).

The soils of the study area formed in fluviomarine deposits, and belong to the Bethera-Izagora-Slagle mapping unit. These soils are deep, and nearly level to gently sloping, and exist on flats and in depressions on uplands. They are clayey or loamy, and are poorly drained and moderately well drained (SCS 1985). Both Bethera silt loam, a clayey, mixed, thermic Typic Paleaquult, and Slagle fine sandy loam, 2% to 6% slopes, a fine-loamy, siliceous, thermic Aquic Hapludult, are mapped by the county soil survey on the study site. The Bethera silt loam consists of a 0.18 m surface layer of dark grayish brown and light brownish gray silt loam, and a subsoil of mottled gray clay loam, silty clay loam, and clay. This Bethera unit has slow permeability and an expected seasonal high water table of 0.3 m above to 0.46 m below the soil surface. The sinkholes and low areas of the study site have this type of soil. The Slagle fine sandy loam consists of a 0.10 m surface layer of dark grayish brown fine sandy loam, a 0.13 m layer of light yellowish brown fine sandy loam, and a subsoil of mottled yellowish brown clay loam grading into a mottled clay loam and sandy clay loam. This Slagle unit has moderate permeability in the upper part of the subsoil and moderately slow or slow in the lower part. In the study area, the flatwoods and ridges are characterized by Slagle soils.

The geology of the Yorktown quadrangle has been described by Johnson (1972). The study area lies on the Grafton plain adjacent to the western extent of the Lee Hall

Scarp. The Grafton plain is a level, poorly drained area sloping eastward at 0.2 m per kilometer (1 ft/mi) in the western part and relatively flat at 16.75 m (55 ft) towards the eastern part. The surficial stratigraphic unit is the Windsor Formation with an approximate thickness of 7.6 m (25 ft) in the study area. The Formation has been divided into two informal members, a "lower cross-bedded sand and bedded silt member and an upper silty-clay, sandy-silt, and clayey sand member" with "major vertical and lateral variations in lithology" (Johnson 1972). The lower Windsor grades upward from medium to coarse sand and gravel to fine sand and clayey silt. The upper Windsor is a mixture of sand, silt, and clay. Deposits of iron oxide appear surrounding decayed roots, and along fracture planes in more clayey sediments.

The Windsor Formation is underlain by the Yorktown Formation which Johnson (1972) subdivided into six facies based on texture, composition, and bedding features. In the study area, the Yorktown Formation is reported to be composed of an upper weathered zone, a possible middle coquina facies, and a lower facies of sandy silt. The composition and structure of the weathered zone varies with the characteristics of the specific site and in general is a clayey sand. The coquina facies is composed of shell material infilled with a fine to coarse-grained biofragmental sand, and exhibits a carbonate composition of 47 to 89 percent by weight (Johnson 1972). A ferricrete zone may exist above the coquina facies where soluble iron in groundwater is precipitated due to the increase of pH from the carbonate shells. Leaching of carbonate from the Yorktown Formation has caused localized subsidence of Windsor sediments, forming depressions, called "sinkholes," that contain standing water for part of the year. The sandy silt facies consists of medium bluish-gray sandy silt with narrow layers of shell and fine to medium quartz sand.

3.2 Hydrologic Measurements

A comprehensive water balance requires the measurement or estimation of all water flows to and from the study volume: precipitation, evapotranspiration, inflow and outflow of surface and groundwater, and changes in water storage. Under steady-state conditions and in the absence of surface flows or of net surface flow (i.e., $S_i - S_o = 0$), the water balance equation reduces to:

$$0 = P_n - ET \pm G_n \pm b \tag{14}$$

where:

G_n = net groundwater flow

b = errors of measurement

The climatic water balance requires the measurement of water table level, P_n, and ET. The water table was monitored by a grid of water table observation wells at approximately 100 m intervals with additional wells located to monitor topographic features. A total of 17 wells were used for this study. Well depths range from 0.71 m to 3.10 m with the majority being 1 m to 2 m in depth. The depth of each well and length of screen were determined during installation based on different soil profiles and expected depth to water table.

Wells were constructed from schedule 40 PVC pipe with an inner diameter of 5.1 cm (2.0 in) and a screen slot of 0.25 mm (0.010 in). Boreholes were advanced by bucket auger with a diameter of 8.26 cm (3.25 in). The screen was packed with #2 well gravel, a filter sand with predominantly 1.5 mm to 2 mm grain size. Most wells were screened the length of the borehole to within 11 cm to 29 cm of the soil surface and completed with a bentonite plug. Four wells were constructed differently, because, due to difficulties in well installation, the gravel pack extended further above the screen than intended. Well 6 was screened from 1.59 m to 2.38 m in a sinkhole, but the well gravel backfill came to 0.80 m depth. Well 7 was screened from 1.85 m to 3.05 m on a ridge where a deeper water table level was expected. The borehole was filled to 1.00 m with well gravel. Well 9 was screened from 1.12 m to 1.75 m in a sinkhole and had the borehole filled to 0.59 m with gravel. Well 11 was screened from 1.29 m to 2.04 m in wet flatwoods with gravel placed up to 1.05 m depth.

Water table levels were measured with a Solinst flat tape meter graduated in 3 mm (0.01 ft) intervals. Water table levels were almost exclusively measured in late afternoon between the times of 1430 to 1700 EST with the most frequent sampling occurring around 1600 EST. To maintain the integrity of the time series data, sampling at a consistent time of day ensured that the short-term signal of daily water table fluctuations was not incorporated into the longer term signal for the balance periods. Daytime latent heat exchange of forests follows the distribution of net radiation. After an approximate one hour time lag in the morning, ET increases rapidly with the flux of net radiation, peaks shortly after solar noon, and then declines evenly with the magnitude of net radiation. In the evening, latent heat flux remains for a short period of time at a level greater than that supported by the energy flux due to net radiation (McNaughton and Black 1973). Given this daily fluctuation in latent heat flux, the water table level of late afternoon was assumed to reflect the water loss from ET that day. Sampling began June 1994 at weekly intervals in some wells with other wells included as they were constructed. Daily sampling occurred during higher water table levels from March to May 1995. Since many wells were almost dry in the summer and showed little response to storm infiltration, water levels were read weekly unless a significant storm raised the water table.

Gross precipitation (P_g) was measured by a recording, tipping bucket rain gage located approximately one kilometer from the center of the site. A radius of 1.3 km (0.81 mi) from the gage outlines a circle of 5.3 km^2 (2.0 mi^2) area, and encompasses the research area. The gage is located in a square, 4 ha field which is mowed periodically and surrounded by trees that function to minimize measurement errors due to wind. The field is maintained for the operation of two commercial radio towers, and thus the gage had to be positioned away from guy wires and towers. The towers were presumed to have no effect on the measurement of rainfall. The tipping bucket gage reduces or eliminates errors from evaporation, the use of dip stick or volumetric container, and splash. However, this gage is susceptible to errors from lost catch as the bucket tips, unmeasured catch when the bucket partially fills, and adhesion. The errors due to partial fill of bucket and adhesion will be compensated for by adding 0.25 mm (0.01 in) (i.e., the precipitation depth that fills one bucket), which is the sum of 0.13 mm (0.005 in). for adhesion to the funnel surface and 0.13 mm (0.005 in) for the mean amount of water remaining in an untipped bucket and lost to evaporation, to each 24-hour period in which rainfall occurred and that was preceded by two days of no rainfall.

For this study, the total error in the measurement of P_g was estimated to be 6%, the sum of 1% for gage error and 5% for areal averaging. The minimum gage error was used since the tipping bucket rain gage is one of the most accurate methods of rainfall measurement, and, when calibrated, is accurate to 0.5% at a rainfall rate of 13 mm/hr (Model 6010 Manual, WEATHERtronics Division, Qualimetrics, Inc.). Error due to exposure was assumed to be negligible due to optimum conditions for the location of the gage. The error due to areal averaging was calculated from equation (2) given the area of a circle centered upon the gage and encompassing the study area. It was recognized that the regression coefficients for equation (2) were calculated for a geographic area that may differ from southeast Virginia in climatic characteristics, such as the spatial and temporal variability of rainfall. The short-term water balances vary in duration from weeks to months, and include single to many storm events. Without a well-defined relation between longer sampling times and increased accuracy in estimating P_g, a measurement error of 6% was used for the purposes of this study.

Net precipitation (P_n) inputs to the water balance models were equated with throughfall and calculated from the literature equations for predicting T from measurements of P_g. The canopy type within a 50-meter radius of the well site was categorized as either pine or hardwood if either type had greater than 75% cover otherwise the canopy was designated as mixed pine and hardwood. Based on these canopy assessments, three equations were used to predict P_n (mm) from the sum of daily P_g (mm) for each balance period with the number of days of rainfall (N):

1) pine canopy $$P_n = 0.80\ P_g - 0.25N \tag{15}$$

2) mixed canopy $$P_n = 0.85\ P_g - 0.52N \tag{16}$$

3) hardwood canopy $$P_n = 0.901\ P_g - 0.787N \tag{17}$$

The equation for the pine canopy was obtained from a review of studies on interception by loblolly pine (Pinus taeda L.) by Helvey (1971). Loblolly pine is the predominant pine species of the study area. Both growing and dormant season equations for the prediction of T in hardwood forests were available from Helvey and Patric (1965). Since the difference between these equations was small relative to the errors contained in other components of the water balance, the growing season equation was used for all balances. For mixed canopy, P_n was modeled as an average of the linear regressions for pine and hardwood canopies. The uncertainty in predicting P_n, the actual precipitation input for the water balances, is estimated at 15%, considering: 1) the standard errors associated with source studies of interception; 2) the greater uncertainty in the weighted average equations used in this study; and, 3) an additional error from applying these empirical equations to a different location.

Net radiation (Q_N), air temperature, and wind speed and direction were measured every 20 seconds, and stored as 15-minute averages by a Campbell CR10 datalogger. The sensors were located within the perimeter of the forested wetland, and were 27 m above the soil surface and approximately 5 m above the nearest treetops. Q_N was measured by a REBS Q6 net radiometer placed to the south of the tower to avoid shadow error. The study used a non-guyed, telescoping tower designed by Tri-Ex Tower Corp., which required a minimum of disturbance to the radiation signature of the ecosystem. Air temperature was provided by a shielded Vaisala HMP35C. Wind speed and direction sensors were located at the opposite ends of a horizontal mast oriented perpendicular to the other sensors to reduce interference between the sensors. This study assumes the greater uncertainty of the equilibrium model compared to the energy balance model is offset by integration over longer time periods as suggested by Munro (1979). Therefore, a total measurement error of 20% is used in calculation of ET for this study.

Net radiation measurements at the research site were not available on two dates during the study period. The weather tower was serviced on 2/21/95 between the hours of 1145 and 1500 EST and on 4/9/95 between 1330 and 1715. At a distance of 6.4 km (4 mi) from the site, the Virginia Institute of Marine Science (VIMS) monitors several instruments which provide local weather data. An Eppley pyranometer measures global solar radiation and records the observations in 6 minute averages. The VIMS pyranometer and the net radiometer at the site measure different quantities of radiant energy flux (Figure 3). The pyranometer measures the short-wave radiation (i.e., less than 4.0 μm) received on a horizontal surface from sun and sky while the net radiometer measures total (short-wave and long-wave) net radiative flux through a horizontal plane (Rassmusson et al. 1993). A strong correlation between these two quantities would be expected since global solar radiation is a principal component of net radiation.

Linear regression relationships between site net radiation and VIMS global solar radiation were used to estimate the missing on-site radiation measurements for calculating ET. The correlation used data for periods of positive net radiation that was recorded simultaneously by the two dataloggers in the form of a 6-minute average for VIMS and a 15-minute average for the site. For example, a noon-time reading at VIMS represents an average radiation flux from 1154 to 1200 while the simultaneous reading at the site is an average for 1145 to 1200. This disparity in time averaging would weaken a correlation between the two radiometers on days of large short-term fluctuations in radiation flux. Given the seasonal variation in forest albedo and fluctuations in atmospheric attenuation of solar radiation, two 1-week periods centered on each date with missing data were used to find a relation for each respective afternoon of site inactivity. When site net radiation (SITE) was plotted against VIMS global solar radiation (VIMS) for the period 2/18/95 to 2/24/95 (Figure 4), linear regression analysis showed that SITE was related to VIMS by the equation:

$$\mathrm{SITE} = -2.598 + 0.7223\ \mathrm{VIMS},\ r^2 = 0.91 \tag{18}$$

Upon examination of a plot of the residuals in Figure 5, the linear model provided a satisfactory description of the data. Likewise for the period of 4/6/95 to 4/12/95 (Figure 6), SITE can be estimated by the equation:

Figure 3. Comparison of global solar radiation measured at the Virginia Institute of Marine Science and net radiation measured above tree canopy on site on February 22, 1995.

VIMS Pyranometer & Site Net Radiometer

2/22/95

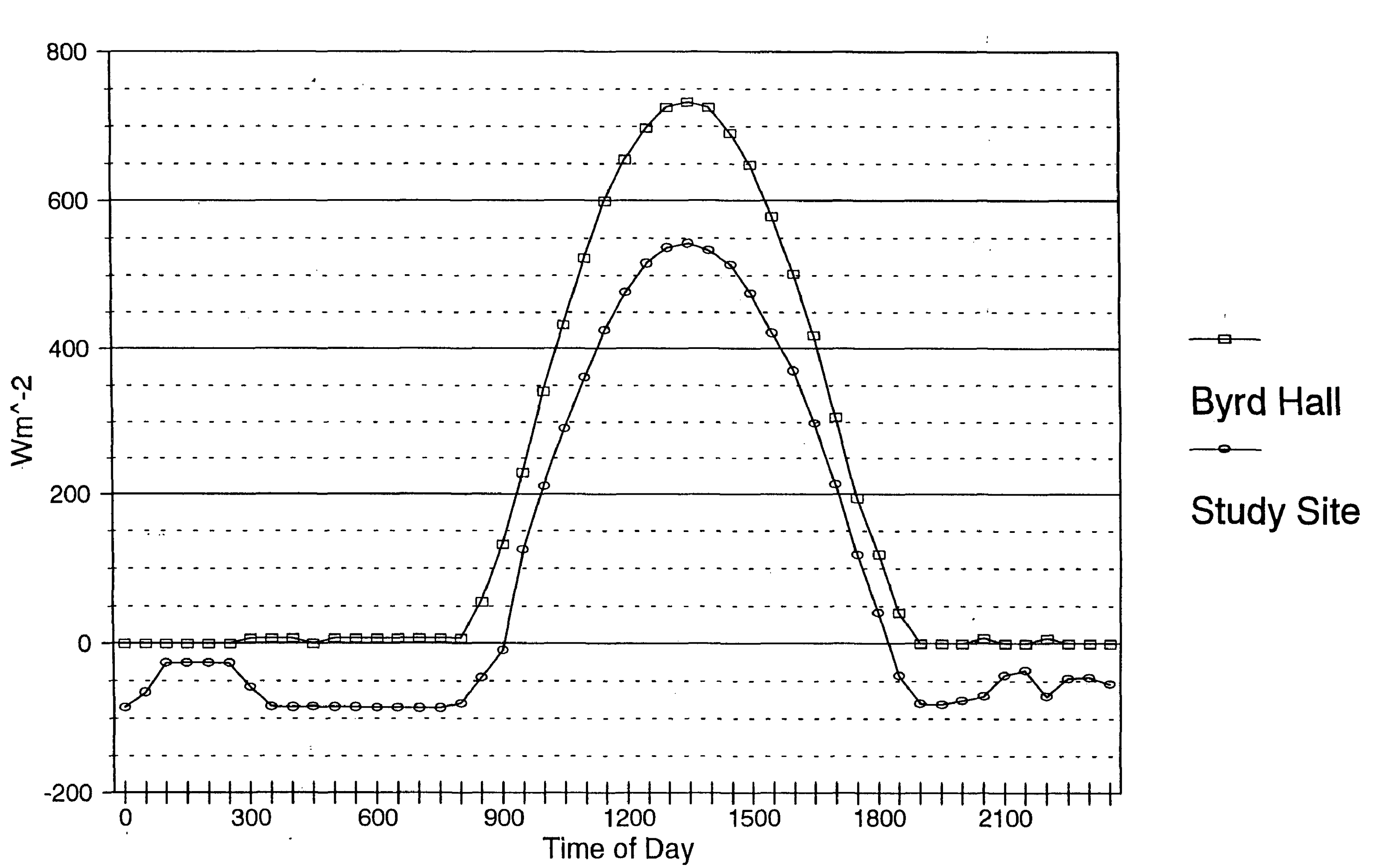

Figure 4. Linear regression of site net radiation versus VIMS global solar radiation for time periods of positive net radiation between February 18, 1995 and February 24, 1995.

Linear Regression of Site Net Radiation vs VIMS Global Radiation

Time Periods of Positive Net Radiation from 2/18/95 to 2/24/95

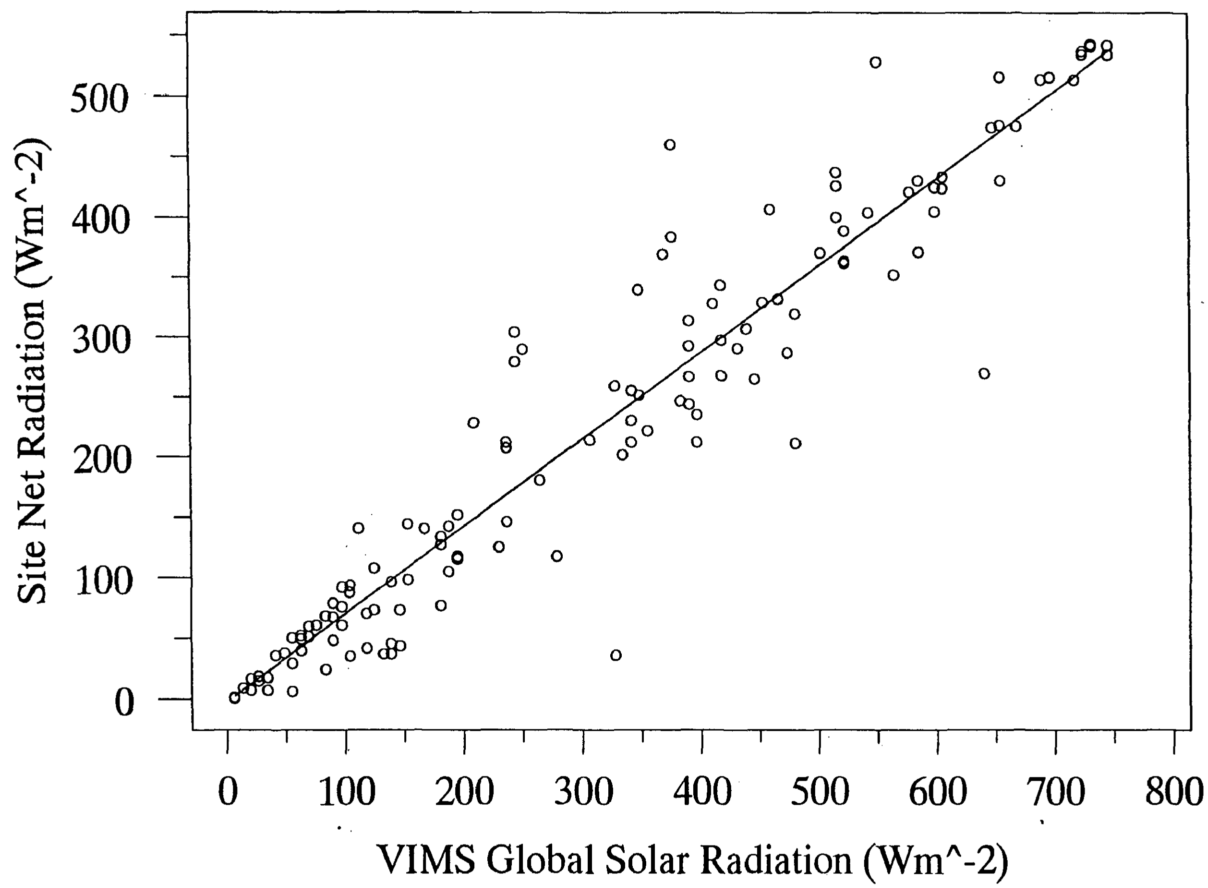

Figure 5. Plot of residuals from regression of site net radiation for the period of February 18, 1995 to February 24, 1995.

Plot of Residuals from Regression of Site Net Radiation

2/18/95 to 2/24/95

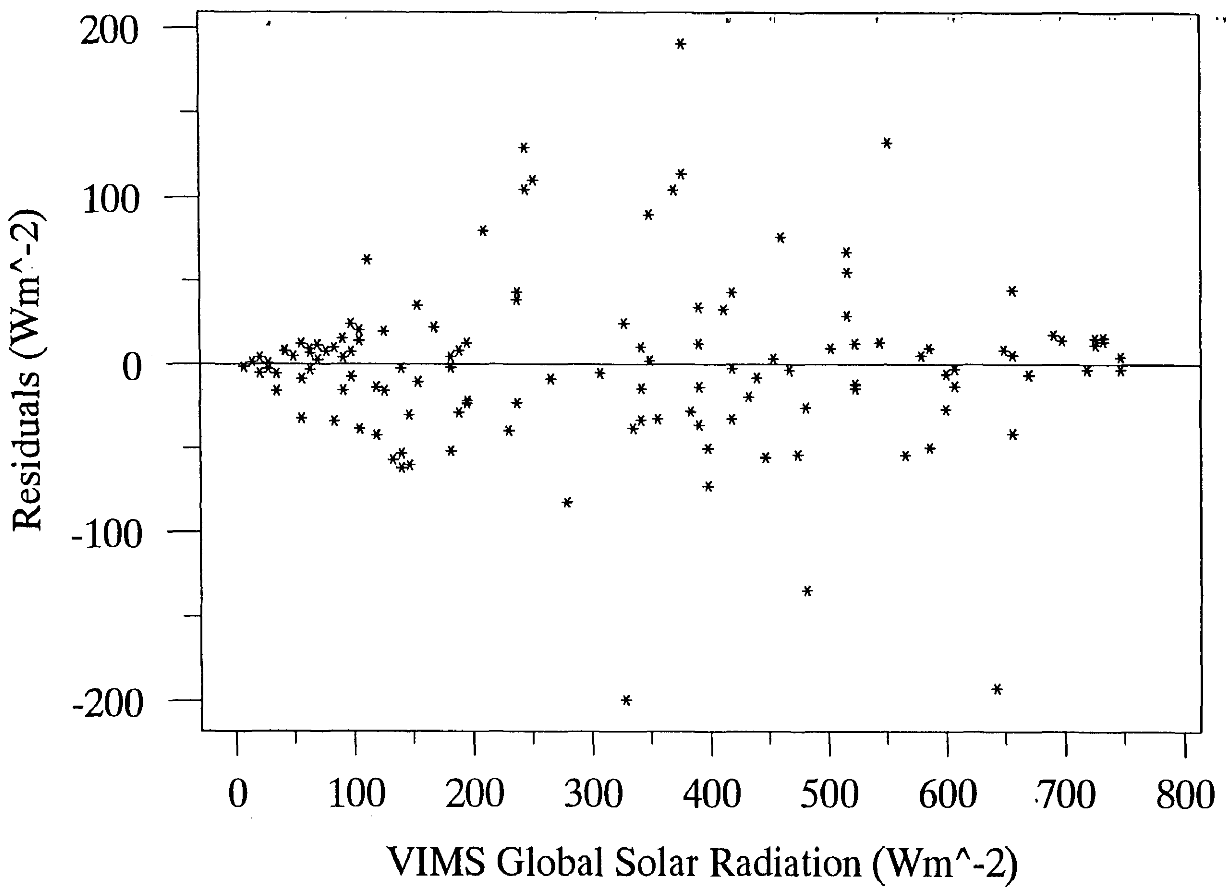

$$SITE = -10.33 + 0.7382\ VIMS,\ r^2 = 0.94 \qquad (19)$$

As earlier, a plot of the residuals shows the linear relation is adequate (Figure 7). Daily estimates of ET for 2/21/95 and 4/9/95 used the VIMS data adjusted by the respective regression equation and substituted for the missing site data. On 11/10/94 and 1/15/95, negative net radiation was recorded on site, resulting in daily ET values of -0.18 mm/day and -0.02 mm/day, respectively. Both occasions involved days of rainfall during the winter season. It is likely that these were instances where a very small value for daily net radiation was influenced by the measurement error of the instrument. For the purpose of this study, these days were assumed to have zero ET based on the use of the equilibrium ET model which is driven by net radiation.

3.3 Error Analysis for Water Balance Residual

To summarize the importance of error analysis with respect to the water balances for this study, the relative error associated with each measured component of the climatic water balance is 15% for throughfall which is the net precipitation (P_n) input for the water balance, and 20% for ET which is modeled using the equilibrium approach discussed earlier. If the standard errors of estimate of P_n and ET are assumed to be independent and are symbolized by α and β, respectively, then the standard error of the difference (γ) between P_n and ET is given by:

$$\gamma = \sqrt{\alpha^2 + \beta^2} \qquad (20)$$

The short-term balances for this study varied in duration, and P_n and ET did not always maintain their normal proportions based on 30-year averages. As a result, it is not possible to predict an exact residual that would be significant. However, the following

Figure 6. Linear regression of site net radiation versus VIMS global solar radiation for time periods of positive net radiation between April 6, 1995 and April 12, 1995.

Linear Regression of Site Net Radiation vs VIMS Global Radiation

Time Periods of Positive Net Radiation from 4/6/95 to 4/12/95

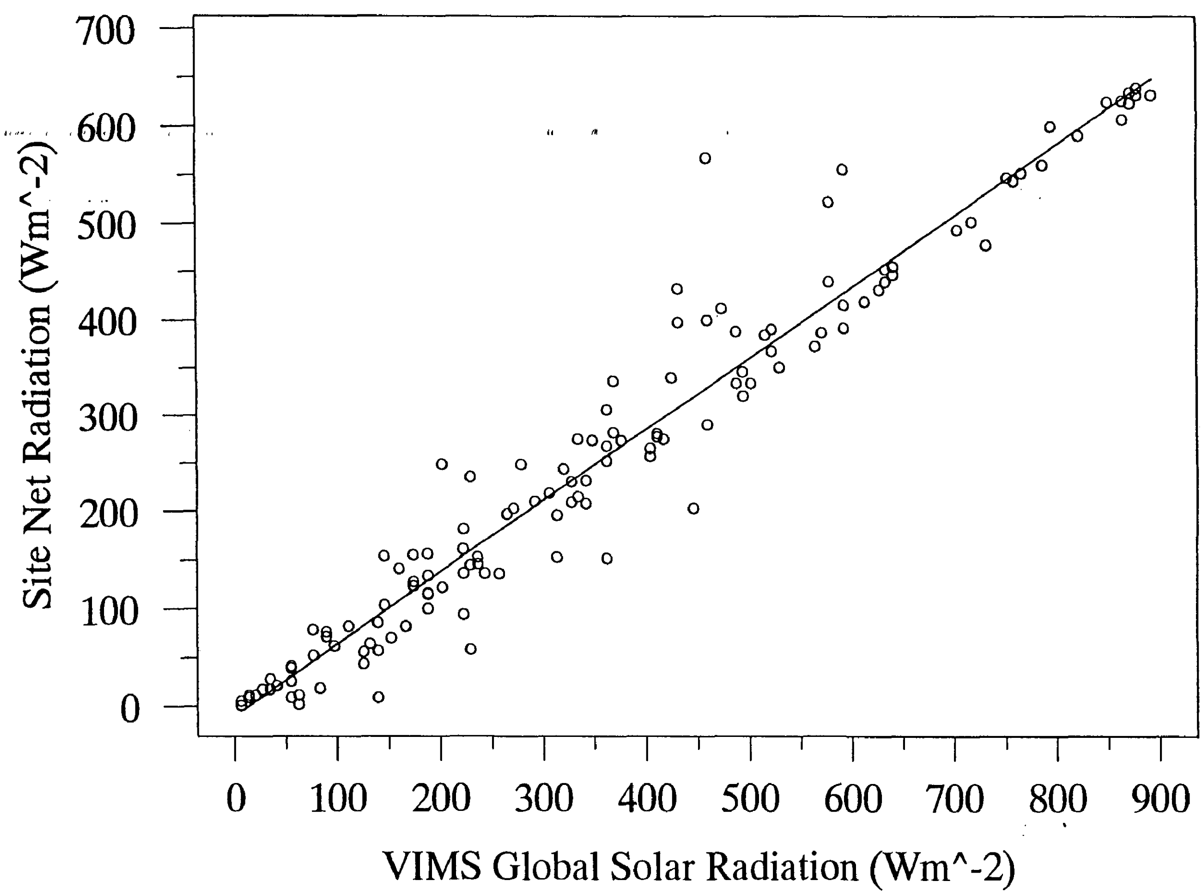

Figure 7. Plot of residuals from regression of site net radiation for the period of April 6, 1995 and April 12, 1995.

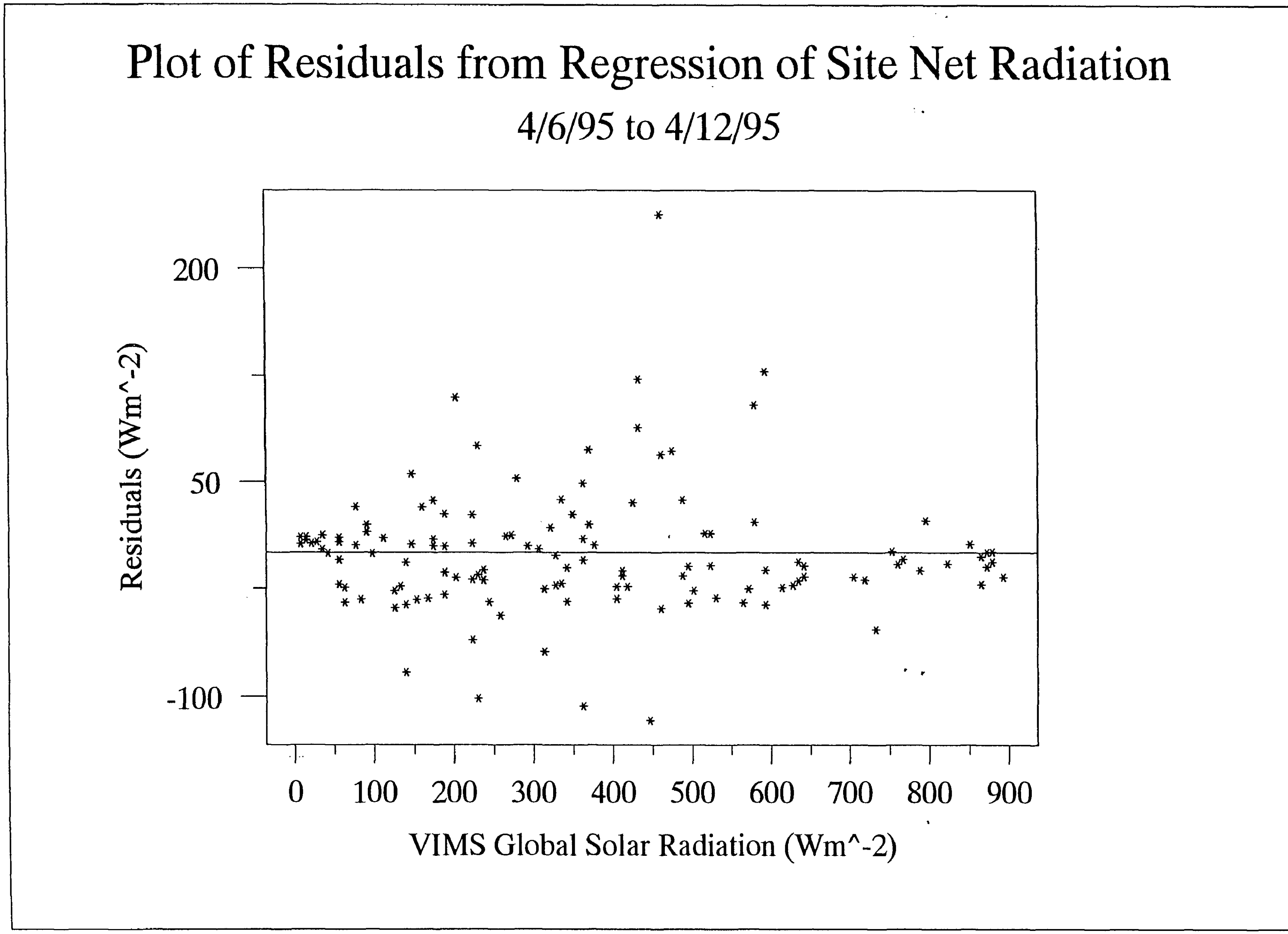
Plot of Residuals from Regression of Site Net Radiation
4/6/95 to 4/12/95
Residuals (Wm^-2)
200
50
-100
0
100
200
300
400
500
600
700
800
900
VIMS Global Solar Radiation (Wm^-2)

examples provide some insight of the interplay between the relative magnitudes of P_n and ET and the pooled standard error of the resulting difference. The relative magnitude of the pooled standard error of the residual with respect to its value can be shown for different months of the year. A typical monthly rainfall during the season of soil moisture recharge is 94 mm (3.7 in) of which approximately 20% may be intercepted, resulting in a P_n of 75 mm (3.0 in). One of the higher monthly estimates of ET for the recharge season as found during this study is approximately 50 mm (2.0 in). The standard errors for P_n and ET are 11 mm (0.44 in) and 10 mm (0.40 in), respectively. Therefore, the difference in P_n and ET is 25 mm (1.0 in) with standard error of the residual equal to 15 mm (0.58 in) or a relative error equal to 60%. At this time of year, the pooled standard error of the residual is not larger than the residual itself, and P_n is significantly greater than ET which corresponds to the expected recharge for this season. For the month of July, the normal rainfall is 129 mm (5.06 in) and P_n would be 103 mm (4.05 in) with a standard error of 15 mm (0.61 in). Monthly ET is approximately 120 mm (4.72 in) with a standard error of 24 mm (0.94 in). Therefore, the residual is -17 ± 28 mm. At this time, the standard error of the residual is larger than the residual itself and it is uncertain whether the month has a positive or negative vertical balance given the measurement errors associated with P_n and ET. It is known from observation that this is a season of soil moisture loss and water table decline. However, the uncertainty in the P and ET balance prevents drawing conclusions on the potential role of groundwater flow in the ecosystem and on adjacent land features. It is for this reason that this study and other ongoing and future research on ecosystem hydrodynamics where new hypotheses are being formed regarding intra-feature and inter-feature interaction must explicitly account for sources and magnitudes of error in the results.

4.0 RESULTS AND DISCUSSION

4.1 Precipitation

Hourly gross precipitation (P_g) totals were stored in dBase IV (Ashton-Tate, 1990) which was used to summarize hourly data into 24-hour totals by Julian day (Figure 8). For the 248-day period from 10/17/94 to 6/21/95, 694 ± 42 mm of rainfall occurred over 80 days with no incidence of snowfall. Of the days when rainfall occurred, mean daily P_g was 8.68 mm (s.d. = 10.79 mm, n = 80) with a minimum of 0.51 mm and a maximum of 63.25 mm. A frequency distribution of daily P_g data grouped into 2.5 mm (0.1 in) intervals shows values skewed towards the smallest two size classes (Figure 9). The cumulative distribution of P_g by size class shows 55% of the daily values were less than 5 mm (0.2 in) and 6.25% were greater than 25 mm (1 in)(Figure 10).

The size and frequency of rainfall events has a significant effect on canopy interception processes. The proportion of P_g intercepted by the canopy varies with the magnitude of daily P_g according to the linear equations for predicting P_n. Figure 11 shows the increasing effect of the line intercept of the throughfall equations at low daily P_g values. At higher daily P_g values, the ratio of gross to net rainfall dominates the relationship. Figure 12 shows the sum of daily P_g values within each respective size class. The largest share of total P_g fell at rates of 15 to 20 mm/day (0.6 to 0.8 in/day), and no P_g occurred at a rate of 42.5 to 62.5 mm/day (1.7 to 2.5 in/day). Interception was calculated as the difference between P_g and P_n where P_g was measured and P_n was predicted for three canopy types by equations (14), (15), and (16). Figure 13 shows the

Figure 8. Gross precipitation for the study period: October 17, 1994 to June 21, 1995.

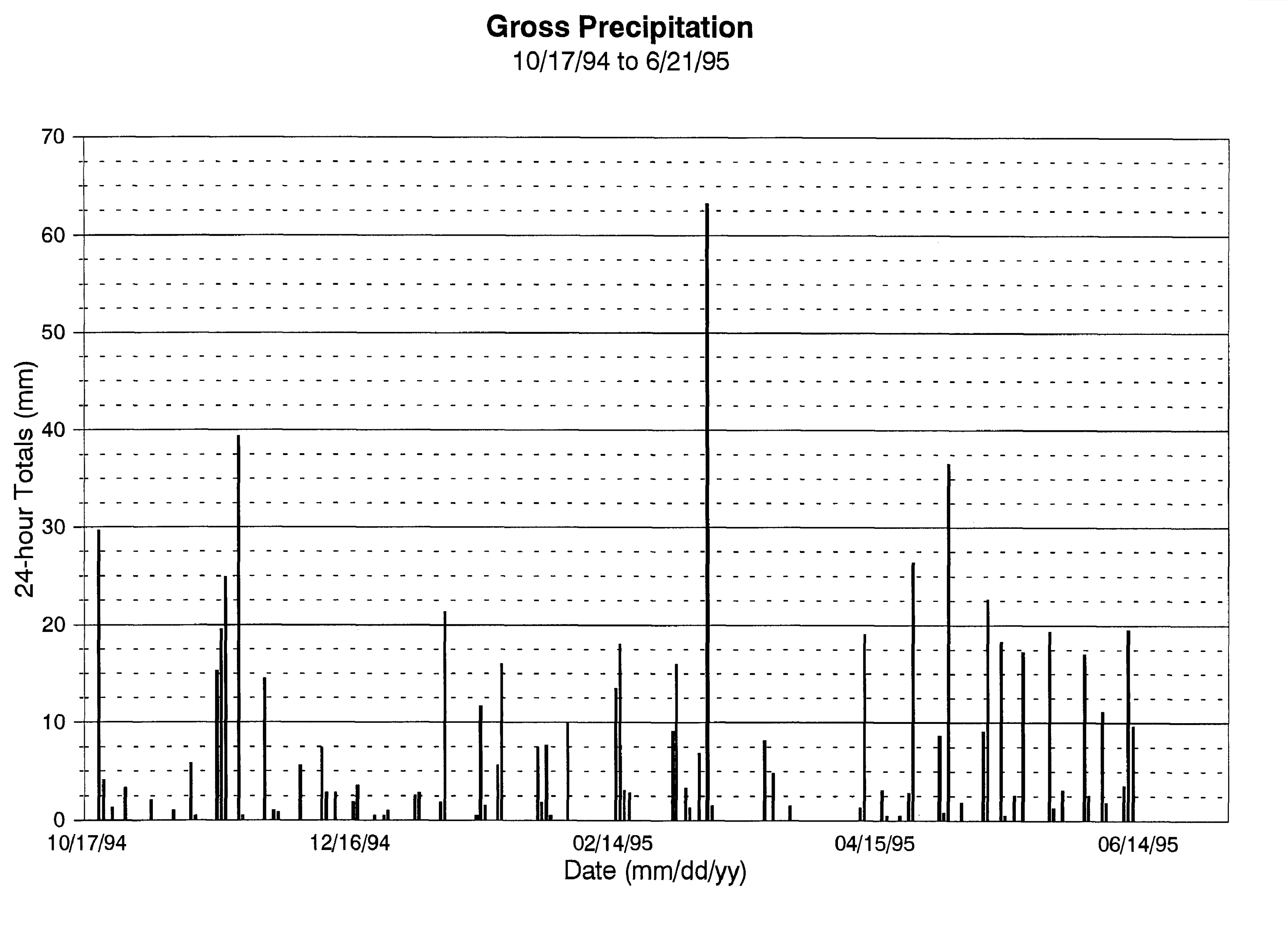
Gross Precipitation
10/17/94 to 6/21/95
24-hour Totals (mm)
70
60
50
40
30
20
10
0
10/17/94
12/16/94
02/14/95
04/15/95
06/14/95
Date (mm/dd/yy)

Figure 9. Frequency distribution of gross precipitation where P_g in 24-hour totals is distributed in 2.5 mm size classes.

Frequency Distribution of Gross P

10/17/94 to 6/21/95

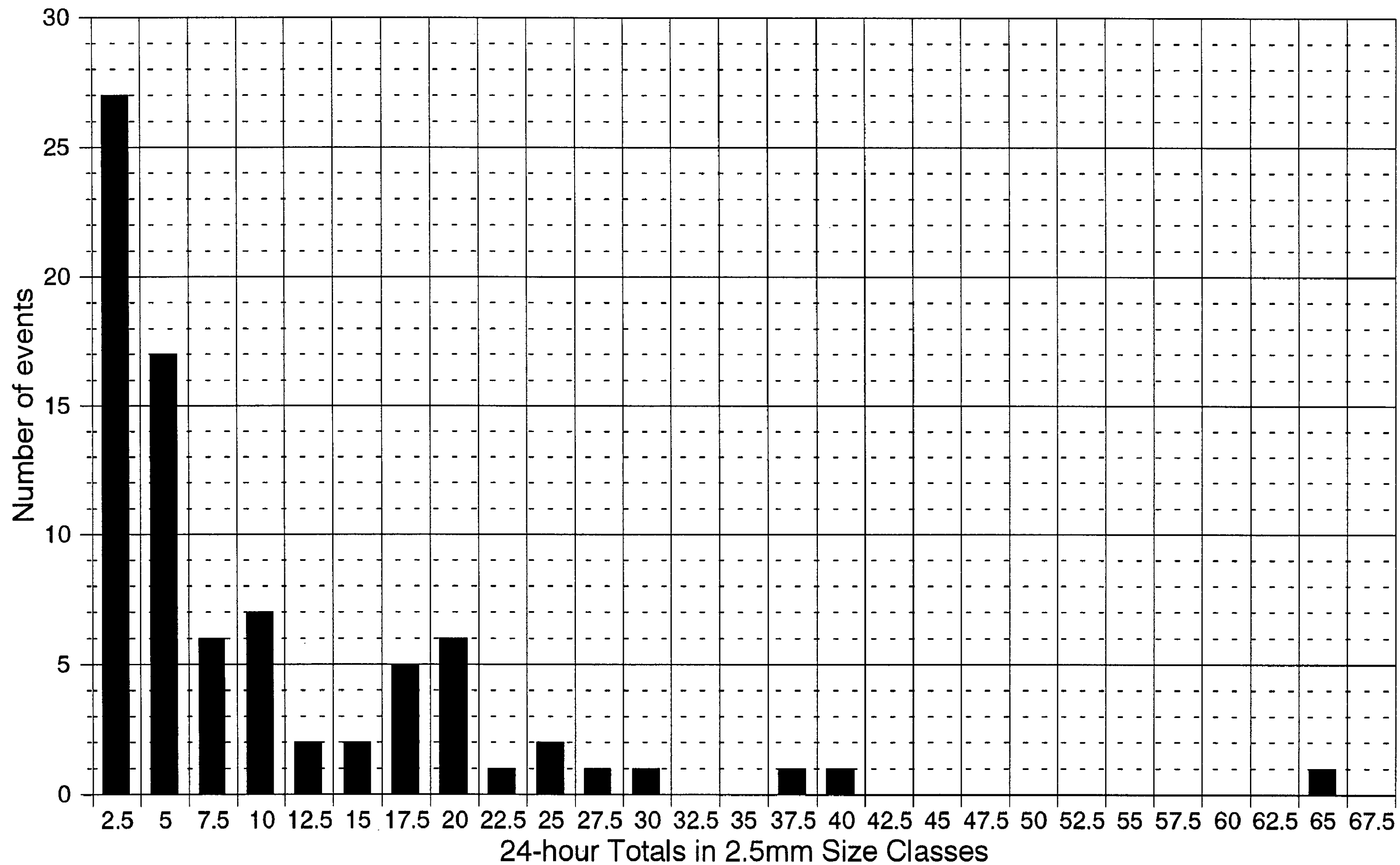

Figure 10. Cumulative frequency distribution of gross precipitation by 2.5 mm size class.

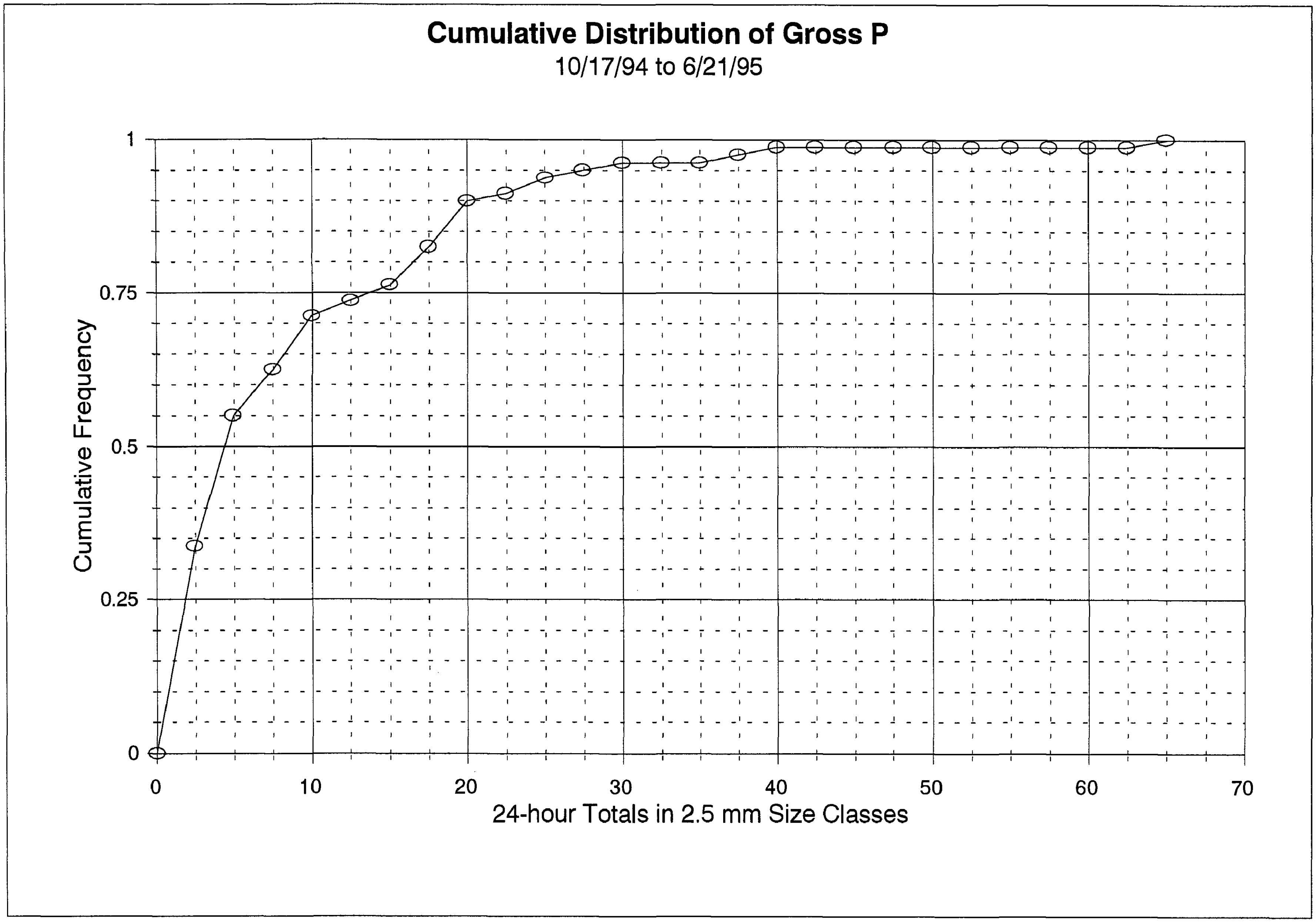
Cumulative Distribution of Gross P
10/17/94 to 6/21/95
Cumulative Frequency
0
0.25
0.5
0.75
1
0
10
20
30
40
50
60
70
24-hour Totals in 2.5 mm Size Classes

Figure 11. Interception by hardwood, mixed, and pine canopies by 2.5-mm size class of P_g and expressed as a percent of P_g.

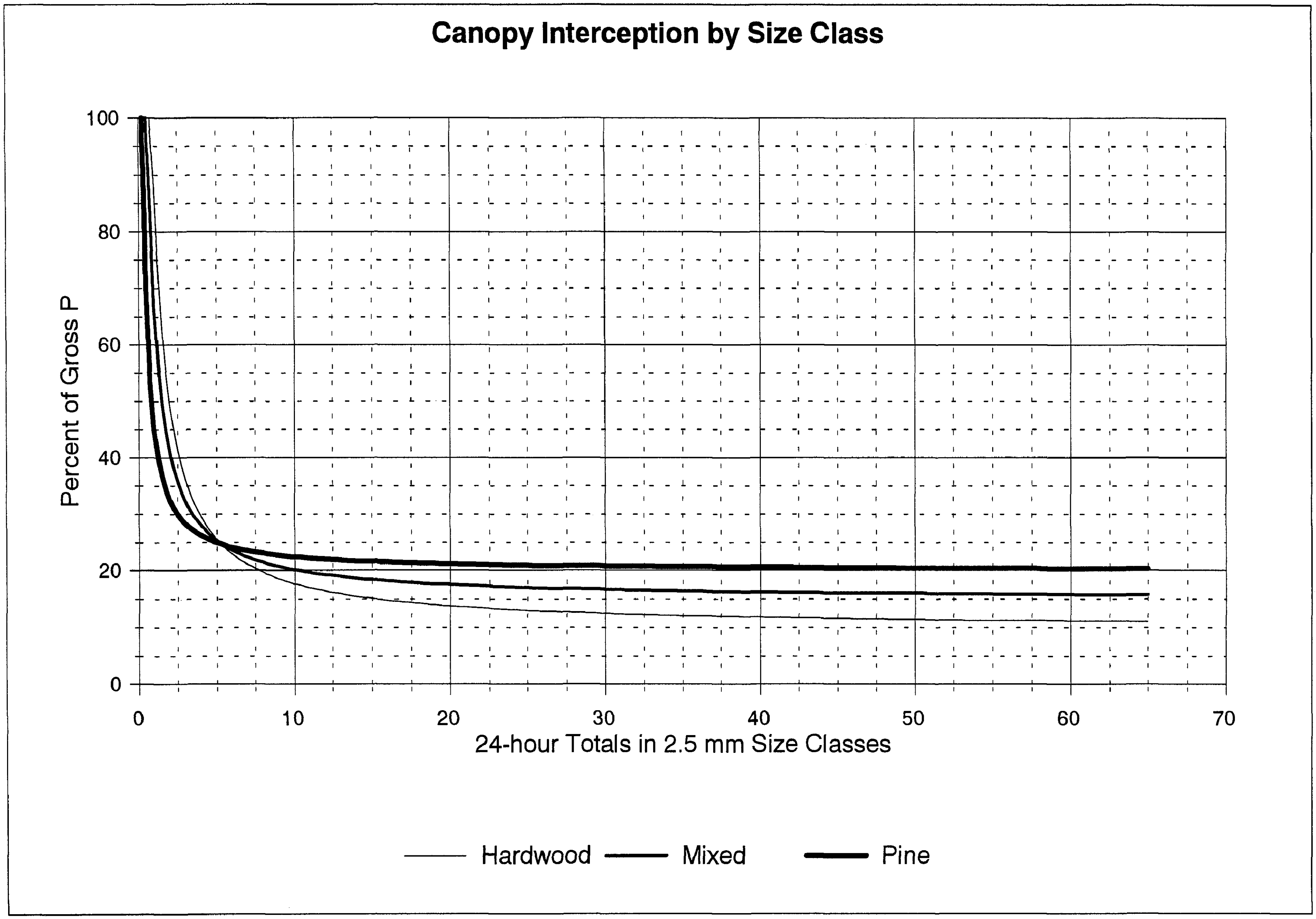
Canopy Interception by Size Class
Percent of Gross P
100
80
60
40
20
0
0
10
20
30
40
50
60
70
24-hour Totals in 2.5 mm Size Classes
Hardwood
Mixed
Pine

Figure 12. Total P_g for the study period distributed by size class.

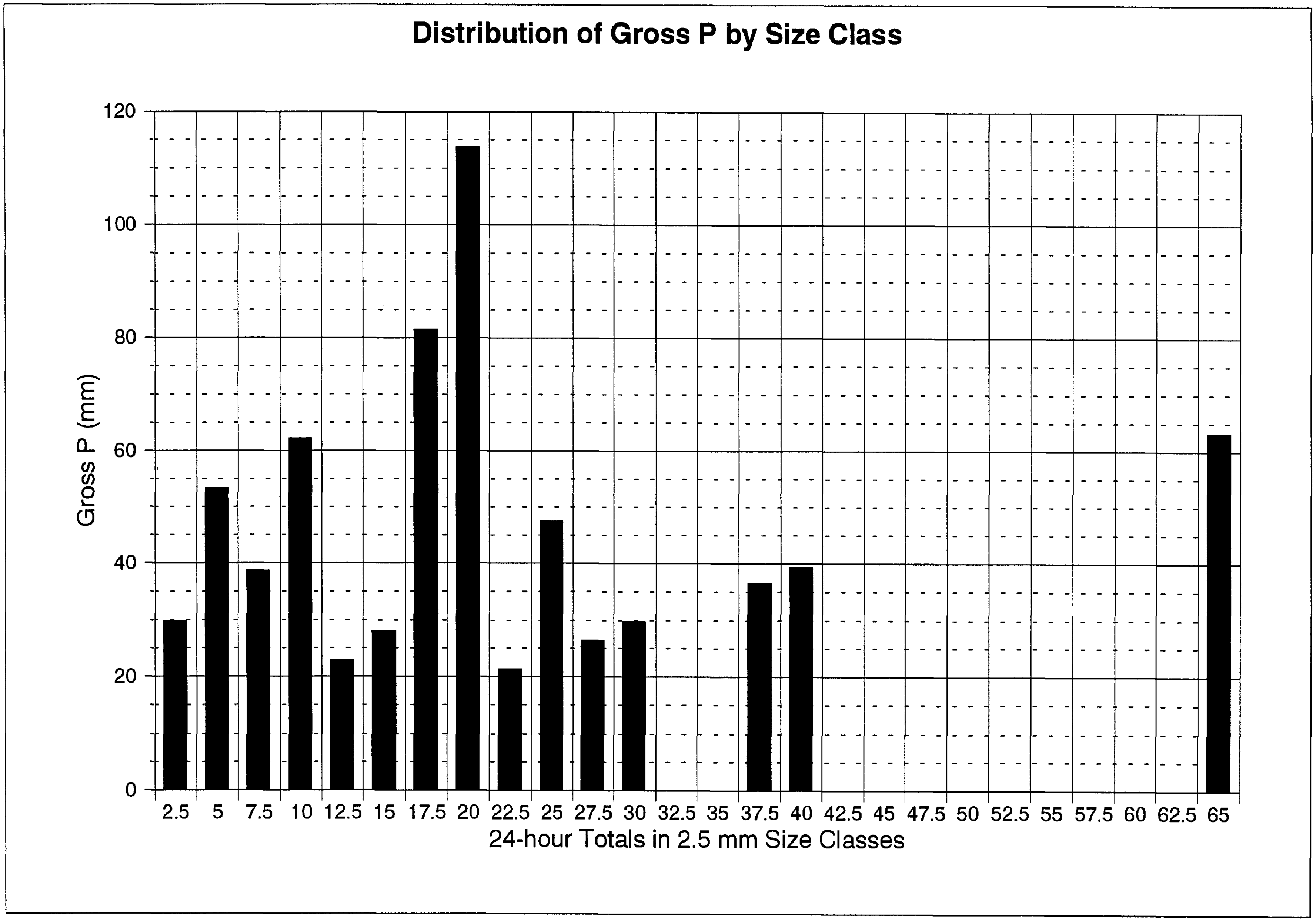
Distribution of Gross P by Size Class
Gross P (mm)
120
100
80
60
40
20
0
2.5 5 7.5 10 12.5 15 17.5 20 22.5 25 27.5 30 32.5 35 37.5 40 42.5 45 47.5 50 52.5 55 57.5 60 62.5 65
24-hour Totals in 2.5 mm Size Classes

size class totals partitioned into I and P_n based on mixed canopy conditions. The proportion of interception losses increases at lower size classes, and, conversely, larger daily P_g events contribute a greater proportion of their rainfall to the water balance. A comparison of the magnitude of I for the three canopy types, hardwood, mixed and pine shows the hardwood canopy intercepting the least and pine the greatest for size classes greater than 5 mm (Figure 14). For daily P_g events less than 5 mm, the order of interception by species is reversed such that the hardwood canopy intercepts the greater proportion and the pine canopy the least. It is uncertain whether the throughfall model accurately predicts canopy interception at low rainfall or whether the reversal in relative magnitude is an artifact of using a linear, least squares regression to generate the relationship. Given a conceptual model where throughfall is inversely proportional to a parameter expressing the amount of leaf area in a canopy (e.g., leaf area index), then the pine canopy would be expected to have the highest capacity for interception. Thus, the x-axis intercept of the throughfall equations should reflect the initial storage capacity of the canopy with pine canopies having the greater value. Instead, the solutions of the throughfall equations used in this study for $P_n = 0$ are 0.87 mm for hardwood, 0.61 mm for mixed, and 0.31 mm for pine. This discrepancy from the conceptual throughfall model may have been caused by the use of a generalized or summary equation for hardwood canopy versus an observed relation between P_g and throughfall in a pine canopy. However, without onsite measurements of throughfall, it was decided to keep the throughfall equations in their original form and examine the magnitude of potential error that may result from the use of the original equations.

If the reversal in the magnitude of interception at low P_g for hardwood and pine canopy types is inaccurate, then the effect of the throughfall model on the uncertainty of the water balance residual needs to be considered. For daily P_g events less than approximately 7.5 mm, P_n would be overestimated for balances involving a pine canopy

Figure 13. Interception of P_g by size class under mixed canopy conditions.

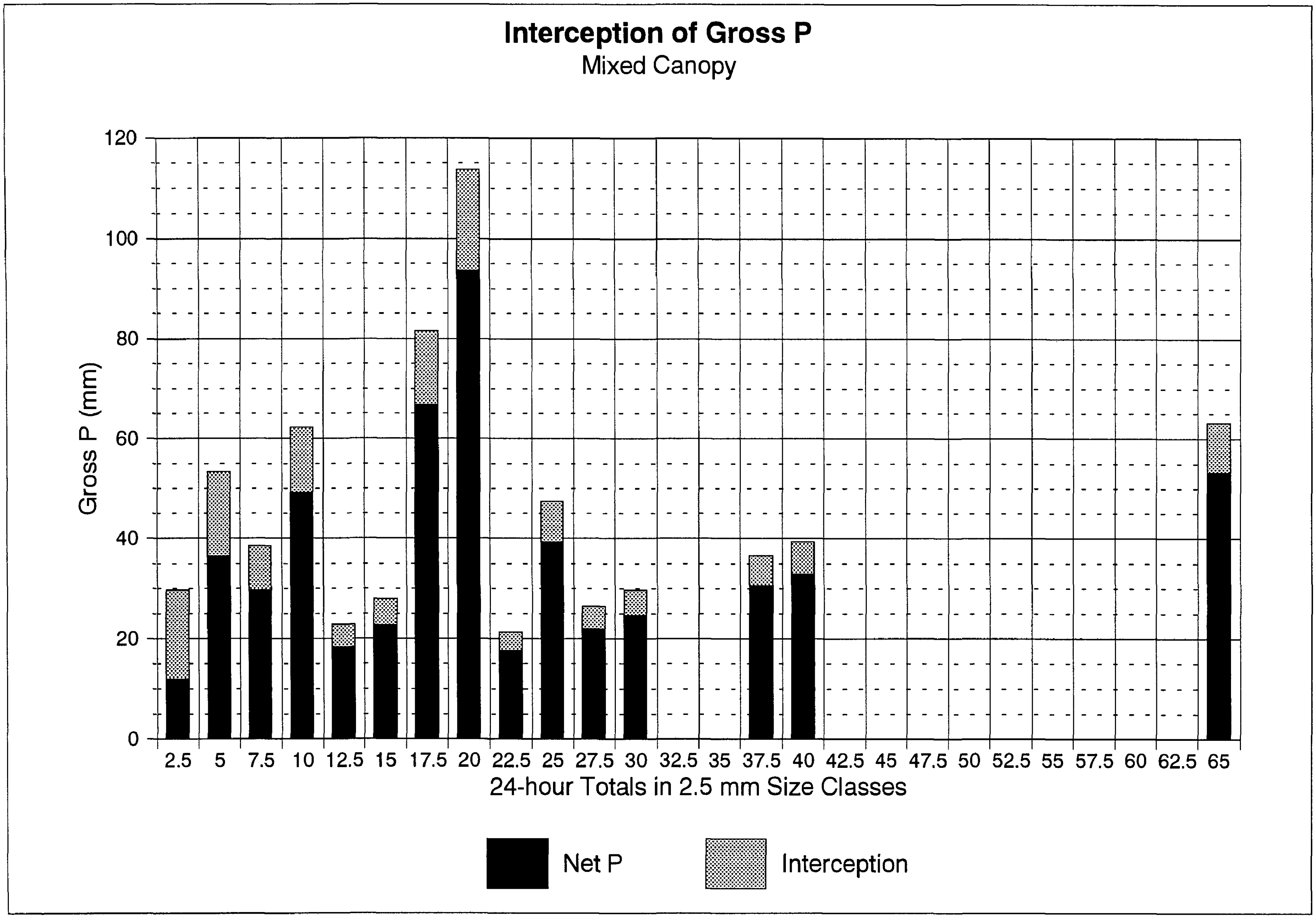
Interception of Gross P
Mixed Canopy
Gross P (mm)
0
20
40
60
80
100
120
2.5
5
7.5
10
12.5
15
17.5
20
22.5
25
27.5
30
32.5
35
37.5
40
42.5
45
47.5
50
52.5
55
57.5
60
62.5
65
24-hour Totals in 2.5 mm Size Classes
Net P
Interception

Figure 14. Comparison of interception between hardwood, mixed, and pine canopies by size class.

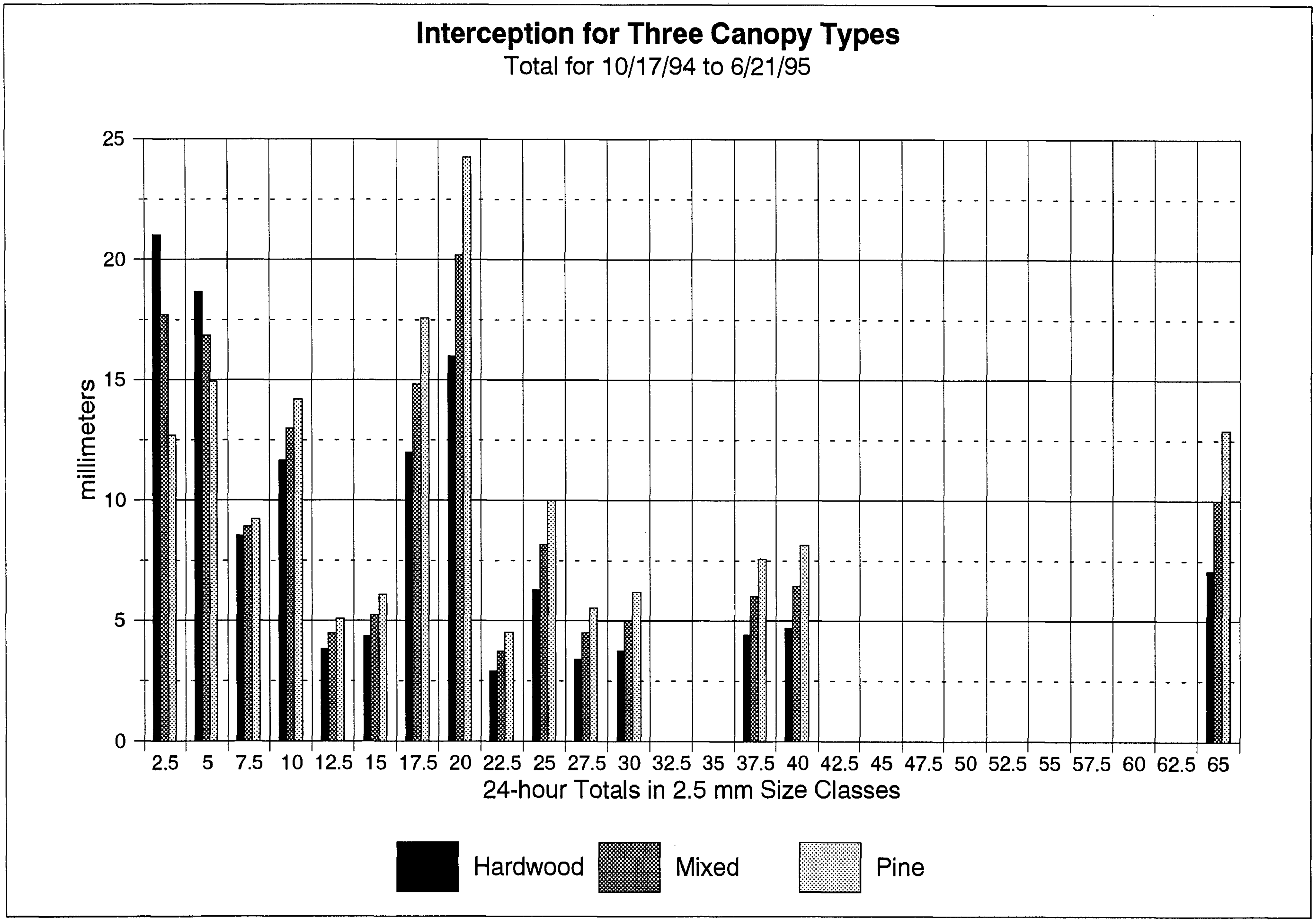

Interception for Three Canopy Types
Total for 10/17/94 to 6/21/95
millimeters
25
20
15
10
5
0
2.5 5 7.5 10 12.5 15 17.5 20 22.5 25 27.5 30 32.5 35 37.5 40 42.5 45 47.5 50 52.5 55 57.5 60 62.5 65
24-hour Totals in 2.5 mm Size Classes
Hardwood
Mixed
Pine

and underestimated for hardwood site balances. About 18% (122 mm) of the total P_g for the study period fell at rates less than 7.5 mm/day (Figure 15). The hardwood and pine canopies intercepted 40% and 30% of this category, respectively. As an approximate estimate of the error, we may assume that these proportions are reversed (i.e., hardwood interception is 30% and pine interception is 40%), thus the difference in interception of 10% which equals 12 mm (i.e., 10% of the total 122 mm for size classes less than 7.5 mm) for the 248-day study period is an estimate of the error. The short-term water balances calculated in this study extended an average of 42 days and ranged between 8 days and 103 days. If we assume that P_g and frequency of storm size are equally distributed over the study period, then the duration of the average water balance, 42 days (17%) of the 248-day study period, can be used to calculate the average expected total P_g and amount of daily P_g less than 7.5 mm for an average balance. By this method, a 42-day balance would be expected to have 14 days of rainfall for a total P_g of 118 mm of which 21 mm (18% of P_g) would be expected at a rate less than 7.5 mm/day. If there is a 10% error in I for daily P_g less than 7.5 mm, then the average additional error in the P_n estimate is 2 mm. The expected P_n for pine and hardwood canopies according to equations (14) and (16) are 91 mm and 95 mm, respectively. Therefore, if the reversal in relative interception between pine and hardwood canopies is incorrect, then on average this inaccuracy would add a relative error of 2.2% and 2.1%, respectively, to the residual of any water balances for these canopy types. There would not be a significant contribution to the error of the residual for balances of mixed canopy type since the equation for P_n is an average of the other equations and the errors would cancel.

Total cumulative P_g for the study period was 694 ± 42 mm, using the selected 6% measurement error, and was close to the expected 714 mm for Norfolk, VA (ORF) according to average monthly precipitation for the 1961 to 1990 period of record (NOAA 1994). The winter and spring months of 1995 were drier than normal as shown in Figure

Figure 15. Cumulative percent of total P_g for the study period by size class.

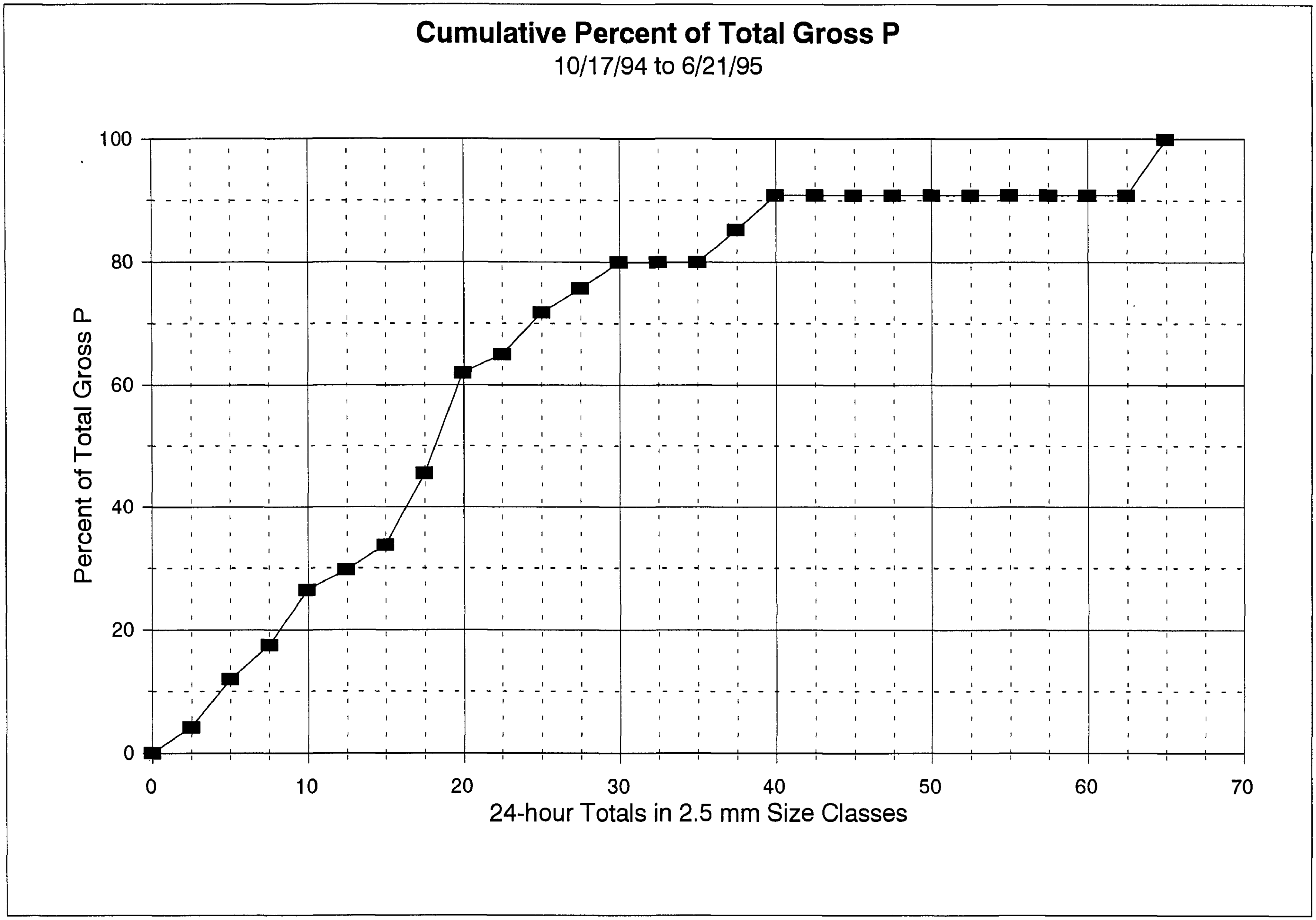
Cumulative Percent of Total Gross P
10/17/94 to 6/21/95
Percent of Total Gross P
100
80
60
40
20
0
0
10
20
30
40
50
60
70
24-hour Totals in 2.5 mm Size Classes

16 where the observed cumulative P_g remains less than expected from January 1995 through mid-June 1995. Expected cumulative P_g was generated by distributing average monthly precipitation equally over the days of each respective month and calculating a running total for each day of the study period. On March 8, 1995, the dry period was punctuated by one large rainfall of 63.25 mm, the maximum daily P_g for the study, which ended the precipitation deficit, only to be followed by more than a month of little rainfall. Slow surface water flow through the leaf litter was observed at well 27 located beside a shallow (approximately 7 cm) drainage feature that serves the study area. This flow went unmeasured, but was on the order of 1500 cm^3/sec for one day, or approximately 130 m^3. The additional error in the water balance residual resulting from this surface flow is a function of the dimensions of the source area. For example, for one well site representing 100m^2, this volume of water represents 13.6 mm, a large error compared to the residual of the water balance. In reality, it is estimated that the surface flow drained from a larger area of approximately 12 well sites which reduces depth per unit surface area to 1.1 mm. Even this outflow was offset by unmeasured water inflow from a smaller, intermittent drainage feature that enters the well field from higher elevations to the northwest, and accounts for a portion of the questioned surface outflow. Therefore, if this is a close approximation of the temporary surface outflow, then the unit area loss of water is on the order of a few millimeters. The error associated with the surface outflow on the residual of a balance is related to the magnitude of the residual. Other than this single event, the dry period prevented surface water flows during the study period and therefore allowed that flow to be excluded from steady-state water balances.

Evapotranspiration

The daily equilibrium ET time series for the period of 10/18/94 to 6/21/95 is shown in Figure 17. Analysis of ET values began on the second day of the study period following the convention of measuring well water levels in the late afternoon. Daily ET

Figure 16. Observed cumulative P_g versus expected cumulative P_g for Norfolk, Virginia for the study period.

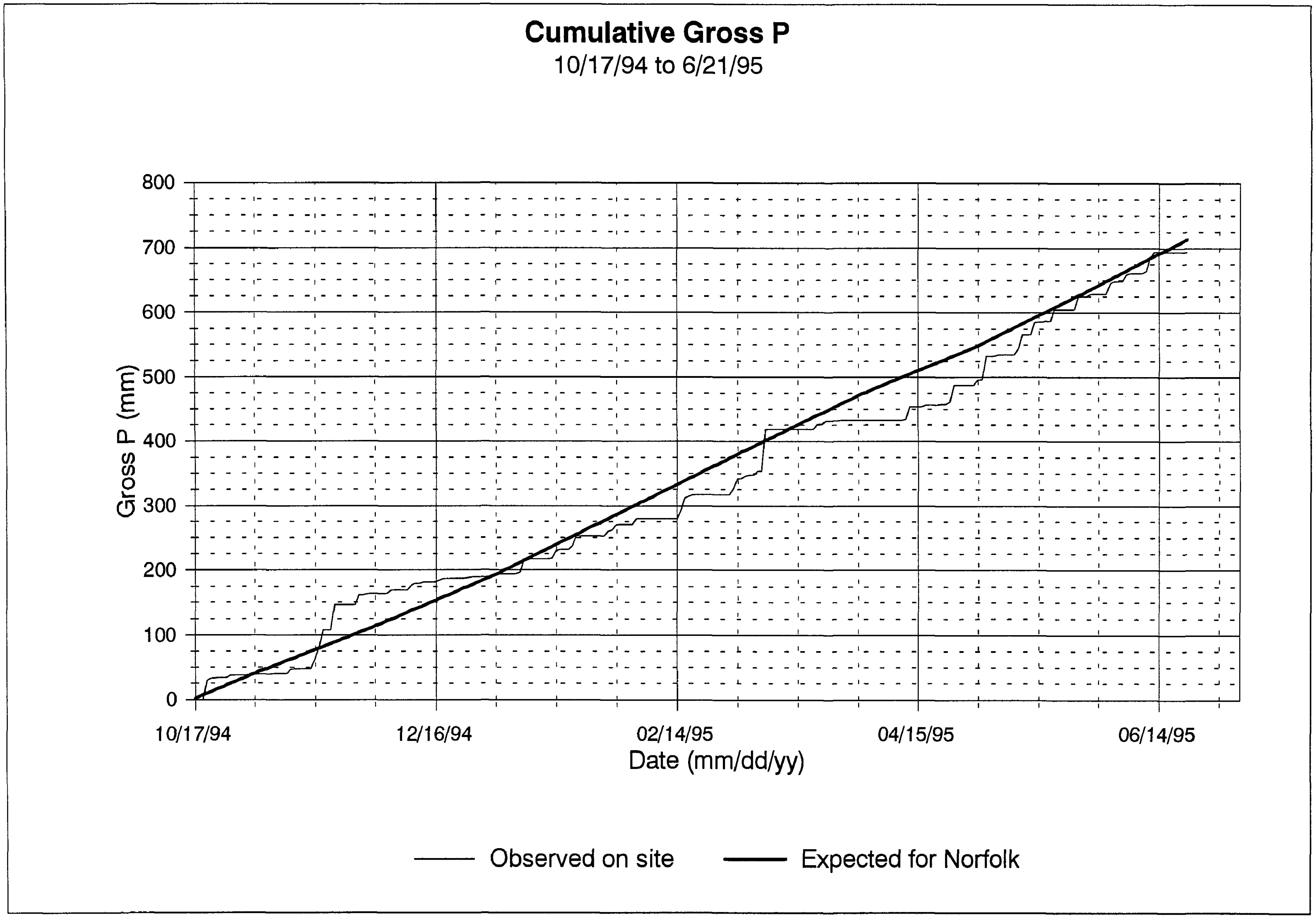
Cumulative Gross P
10/17/94 to 6/21/95
Gross P (mm)
800
700
600
500
400
300
200
100
0
10/17/94
12/16/94
02/14/95
04/15/95
06/14/95
Date (mm/dd/yy)
Observed on site
Expected for Norfolk

Figure 17. Daily equilibrium ET along with weekly averages for the study period.

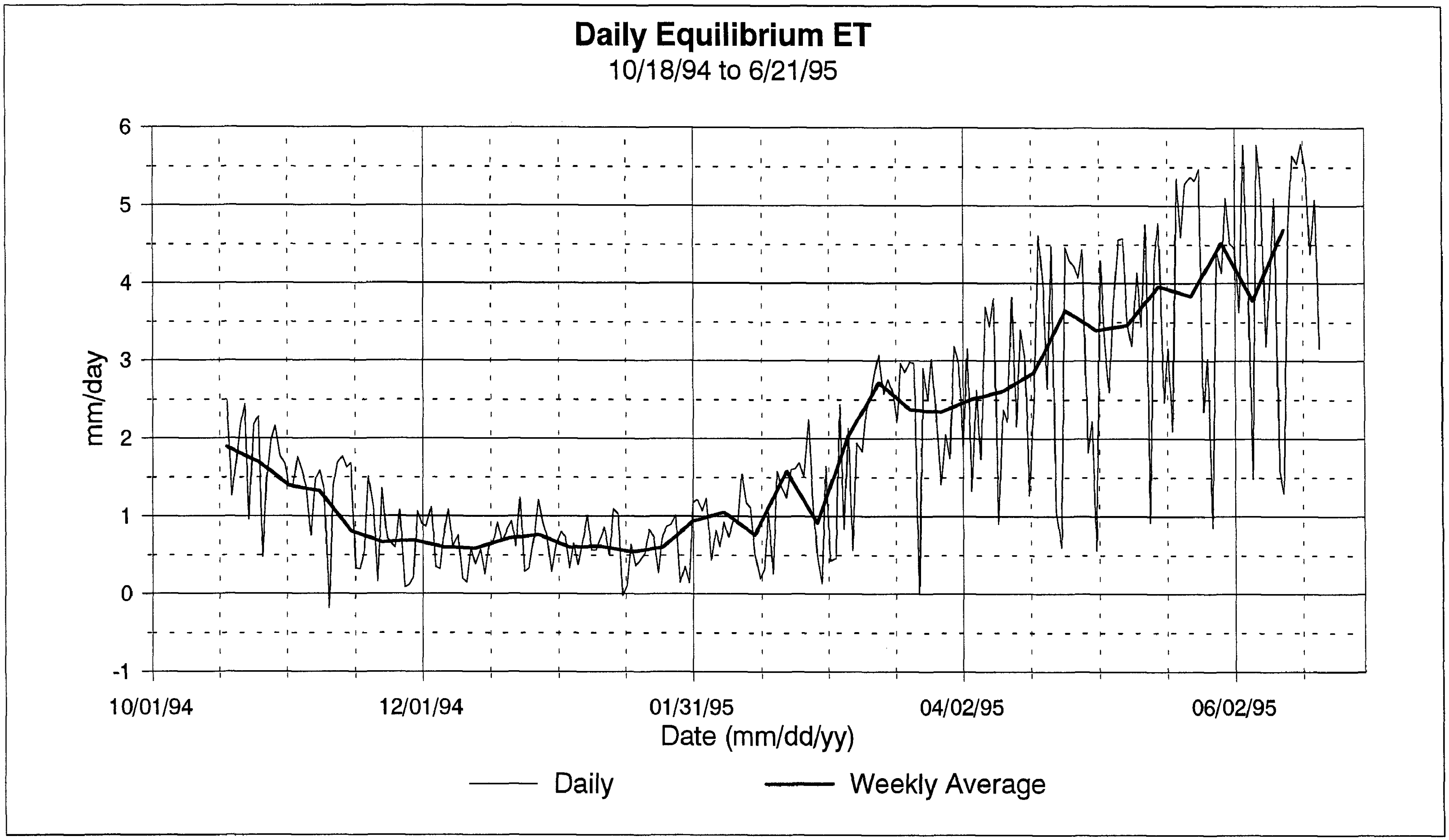
Daily Equilibrium ET
10/18/94 to 6/21/95
mm/day
6
5
4
3
2
1
0
-1
10/01/94
12/01/94
01/31/95
04/02/95
06/02/95
Date (mm/dd/yy)
Daily
Weekly Average

values ranged from 0 mm/day to 5.8 mm/day on 6/17/95. The seasonal low of the annual ET cycle occurred in December and January when daily ET averaged 0.6 mm/day and rarely exceeded 1 mm/day. Beginning in February, the daily ET rate increased by approximately 1 mm for each month, such that daily ET fluctuated around 4 to 5 mm/day by June when this study was concluded. As ET rates increased in the spring, daily variability increased as well. By separating the different terms of the equilibrium ET equation and plotting their relative values together, it is obvious that seasonal variability in the magnitude of fluctuations in daily ET was predominantly due to the net radiation term (Figure 18). The weighting factor containing Δ and γ exhibited a relatively constant seasonal variance over the study period. Although, a longer period of monitoring might show that the variance of the weighting factor is slightly greater in the winter than the summer. This pattern can be discerned in Figure 18, but comparisons are needed with additional years to test its validity. In general, the seasonal fluctuation of the weighting factor was between approximately 0.40 in January and February and 0.70 in May and June. The annual low of the weighting factor occurs about a month after the net radiation annual low. In Figure 18, daily net radiation is expressed as its water equivalent derived from the energy flux in MJ day^{-1} m^{-2} divided by the latent heat of vaporization ($\lambda \approx 2.5$ MJ kg^{-1}) and the density of water ($\rho_w \approx 1000$ kg m^{-3}). The pronounced daily fluctuations result primarily from the scattering of solar radiation by cloud cover. By this model, the magnitude of the daily net radiation term represents the meteorological upper limit to the rate of daily ET if all energy flux was dedicated to latent heat exchange. Under certain site conditions, latent heat flux leaving the site can be in excess of net radiation influx as a result of additional energy supplied by advected sensible heat influx. Commonly, this added energy for ET is supplied by air masses of higher temperature and lower relative humidity than exist in the microclimate of the site, resulting in an "oasis effect" where the observed ET rate is higher than expected by measurements of net radiation. This phenomena underlies the importance of selecting a site with adequate fetch. The greater

Figure 18. Separation of daily equilibrium ET values into component terms of daily net radiation and weighting factor.

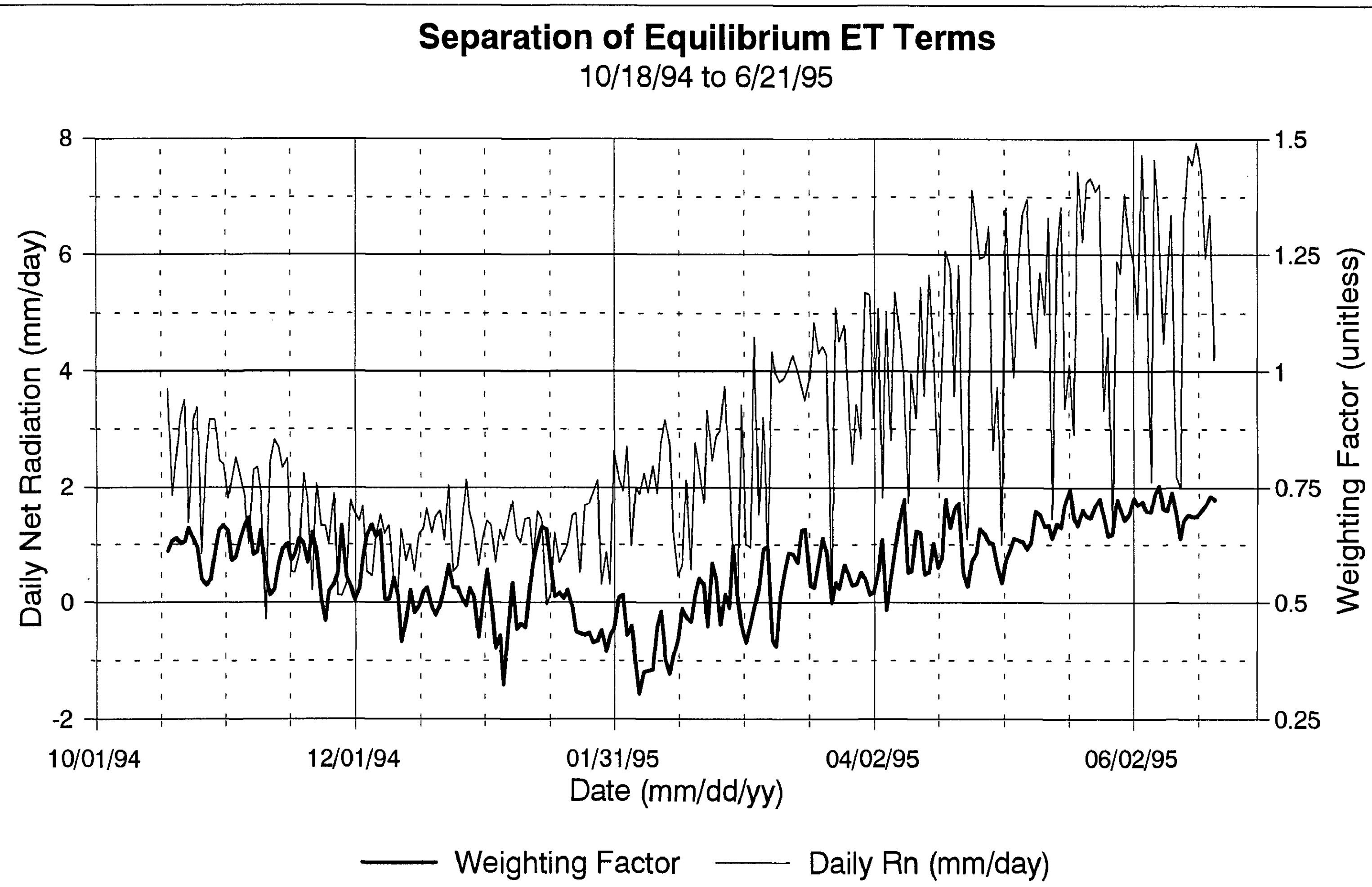

Separation of Equilibrium ET Terms
10/18/94 to 6/21/95
Daily Net Radiation (mm/day)
8
6
4
2
0
-2
Weighting Factor (unitless)
1.5
1.25
1
0.75
0.5
0.25
10/01/94
12/01/94
01/31/95
04/02/95
06/02/95
Date (mm/dd/yy)
Weighting Factor
Daily Rn (mm/day)

the fetch surrounding the site the more likely the wind profile has equilibrated between the site microclimate and the overlying air mass.

Total ET was 480 ± 96 mm for the study period according to the equilibrium ET model, accounting for 69 ± 14% of P_g and 87 ± 17% of P_n for the mixed canopy type (Figure 19). This result agrees closely with the 75% of $P_{g,}$, or 520 mm, predicted by the Thornthwaite method. However, the Thornthwaite estimate is an annual proportion, and the results of this study do not include the summer season when the P:ET ratio is low. Extrapolating through the remainder of the year, I would expect the annual proportion of P_g lost by equilibrium ET to be greater than 69%. It is difficult to speculate how much of an increase in percentage would occur, because the higher ET rate of the summer is partially accommodated by a small peak in the rate of P_g. Although the results of past investigations do not agree consistently, there is evidence that well-watered forests transpire at 80 ± 10% the rate of crop PET (Shuttleworth 1993). In this regard, forested wetlands on the study site would be expected to evapotranspire 416 ± 52 mm (i.e., 80 ± 10% of 520 mm) or from 52.5% to 67.5% of P_g for this study period according to the crop PET predicted by the Thornthwaite method.

The change of slope in the cumulative P and ET plots in Figure 19 signifies seasonal variations in the rates of P and ET. The initial low ET rate is followed by a steepening, and thereby increasing, ET rate as expected for the October to June period of study. At the same time, seasonal deviations from the normal rate of P were observed, although total P for the study was close to normal. The period of less than normal rate of P in the two months beginning in early January was compensated for by a greater than normal rate of P during the two month period beginning in mid-April. According to the Norfolk records of normal monthly P, these two time periods usually accumulate similar amounts of P (NOAA 1994, see Figure 1). These deviations from seasonal normal rates

Figure 19. Cumulative P_g, P_n for hardwood, mixed and pine canopies, and ET for the study period.

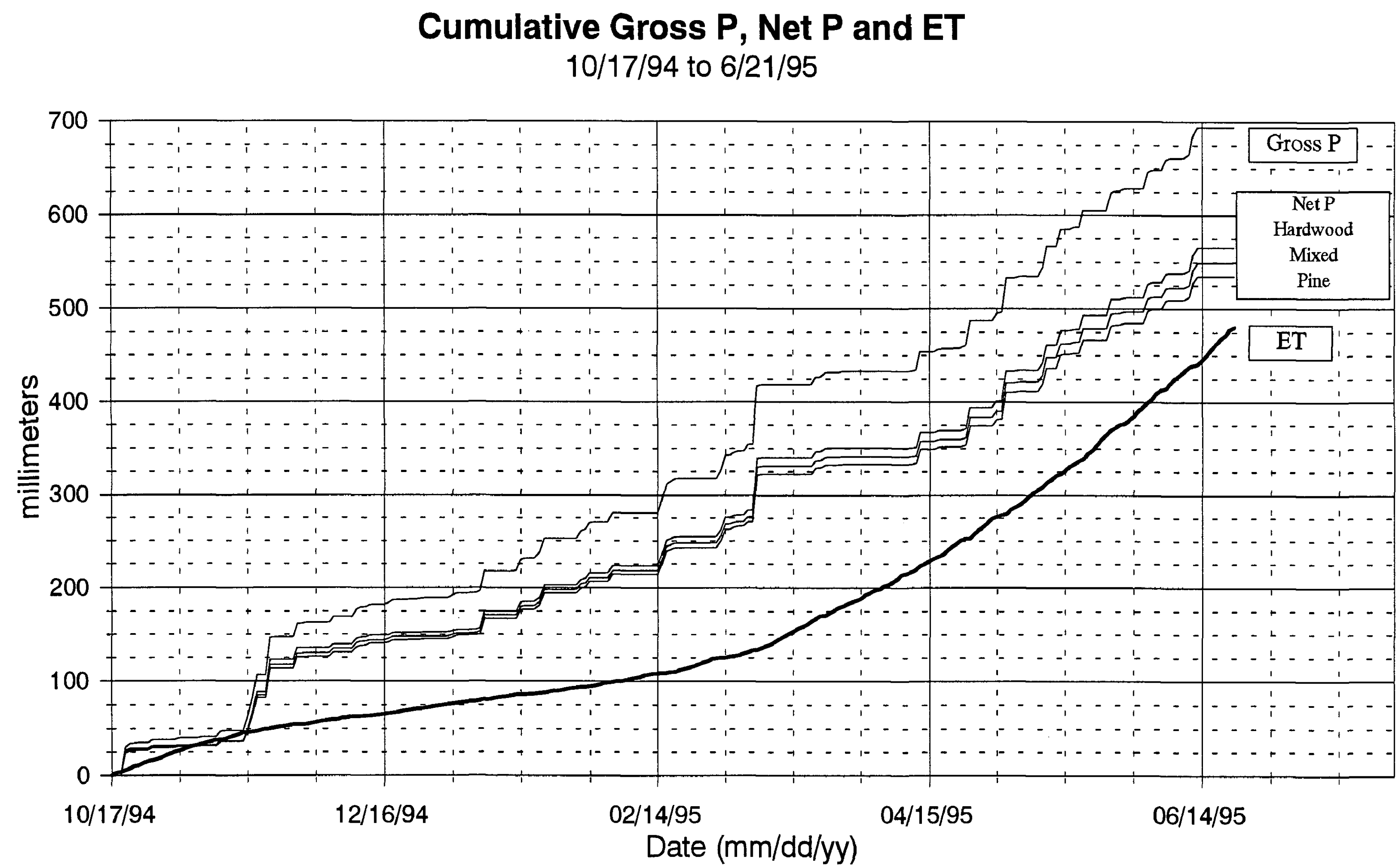

Cumulative Gross P, Net P and ET
10/17/94 to 6/21/95
millimeters
700
600
500
400
300
200
100
0
10/17/94
12/16/94
02/14/95
04/15/95
06/14/95
Date (mm/dd/yy)
Gross P
Net P
Hardwood
Mixed
Pine
ET

of P are reflected in Figure 16 where cumulative P_g decreases below expected amounts in January 1995 and recovers in May and June 1995.

The divergence and convergence of the P and ET plots in Figure 19 are the basis for the unique hydrodynamics of wet flatwoods, and are the reason for conducting short-term steady-state water balances of these ecosystems. An annual water budget can not present data in a way that reveals the seasonal dynamics of climate and soil moisture. A divergence of the P_g or P_n plot from the plot of ET occurs when the rate of P is greater than the rate of ET. If this surplus is greater than the rate of net groundwater loss, then soil moisture recharge will occur and water table levels will rise. A convergence of the P and ET plots indicates a more rapid loss to ET than can be replaced through P, resulting in decreased soil moisture and decreasing water table levels. It is this fluctuation of the two dominant vertical fluxes with respect to each other that affects the amount of water available for changes in soil storage, as well as the amount and direction of groundwater flow. Unlike wetlands whose hydroperiod is buffered by a constant surface or groundwater inflow, wet flatwoods can possess unique, oscillating, groundwater flow regimes due to significant vertical fluctuations in water table level over a year. The complexity of these flow regimes is strongly influenced by vertical and lateral variability in hydraulic conductivity (K) of soil layers, and specific yield (S_y) of the surficial aquifer. Unless water balances are performed on a shorter time scale, these opposing groundwater flows will yield a lesser sum over the time period of the balance.

As found by Crownover et al. (1995) in a cypress swamp and pine flatwood landscape in Florida, the topography of the water table and the resultant groundwater flow directions in landscapes with soils of relatively homogeneous K distribution are closely related to the topography of the land surface. Under these conditions, large fluctuations in water table elevation are likely to affect rates of groundwater flow more than direction of flow. As the water table increases in elevation, the water table topography mimics the surface topography to a greater degree, thus increasing gradients in hydraulic head and rate of flow. With decreasing water table elevation, water table topography flattens with respect to the land surface topography, and differences in hydraulic gradients, and therefore rate of groundwater flow, decrease. On the other hand, landscapes where areas of higher and lower K are juxtaposed can experience significant reversals in groundwater flow direction. Phillips and Shedlock (1993) studied relations between ground water and surface water in a landscape of small seasonal ponds and broad upland ridges on a forested Coastal Plain drainage basin. They found that the low K soils beneath the ponds were the location of higher water table elevations than adjacent, high K sandy ridges during summer and fall, and, subsequently, this gradient was reversed in winter and spring.

The seasonal pattern of water availability is illustrated by a graph of the difference in the cumulative distributions of P_g versus ET, and mixed canopy P_n versus ET (Figure 20). If we ignore the short-term perturbations of large rainfall events and dry periods, the residuals of both climatic balances increase through the fall, winter and spring. The residual of P_g - ET increases to a high of approximately 250 mm in mid-May whereas the residual of P_n - ET approaches an approximate high of 150 mm in mid-March. The dry period in March and April obscures the trend of the P_n - ET residual. The peak in the seasonal pattern of the residuals occurs when P and ET rates are equal. When interception loss is considered, a reduction in net input by P shifts the peak of the residual of the climatic balance earlier in the year. A discussion of the residual must be qualified by a consideration of the accumulation of measurement errors. The measurement errors I have adopted for P_g, P_n and ET are 6%, 15% and 20%, respectively. At the time of the peak in the residual of P_g - ET, approximate estimates for total P_g and ET are 585 mm and 335 mm, respectively. Assuming the errors are independent, the residual of the P_g - ET

Figure 20. Cumulative daily residual plots of P_g - ET and P_n - ET for the study period.

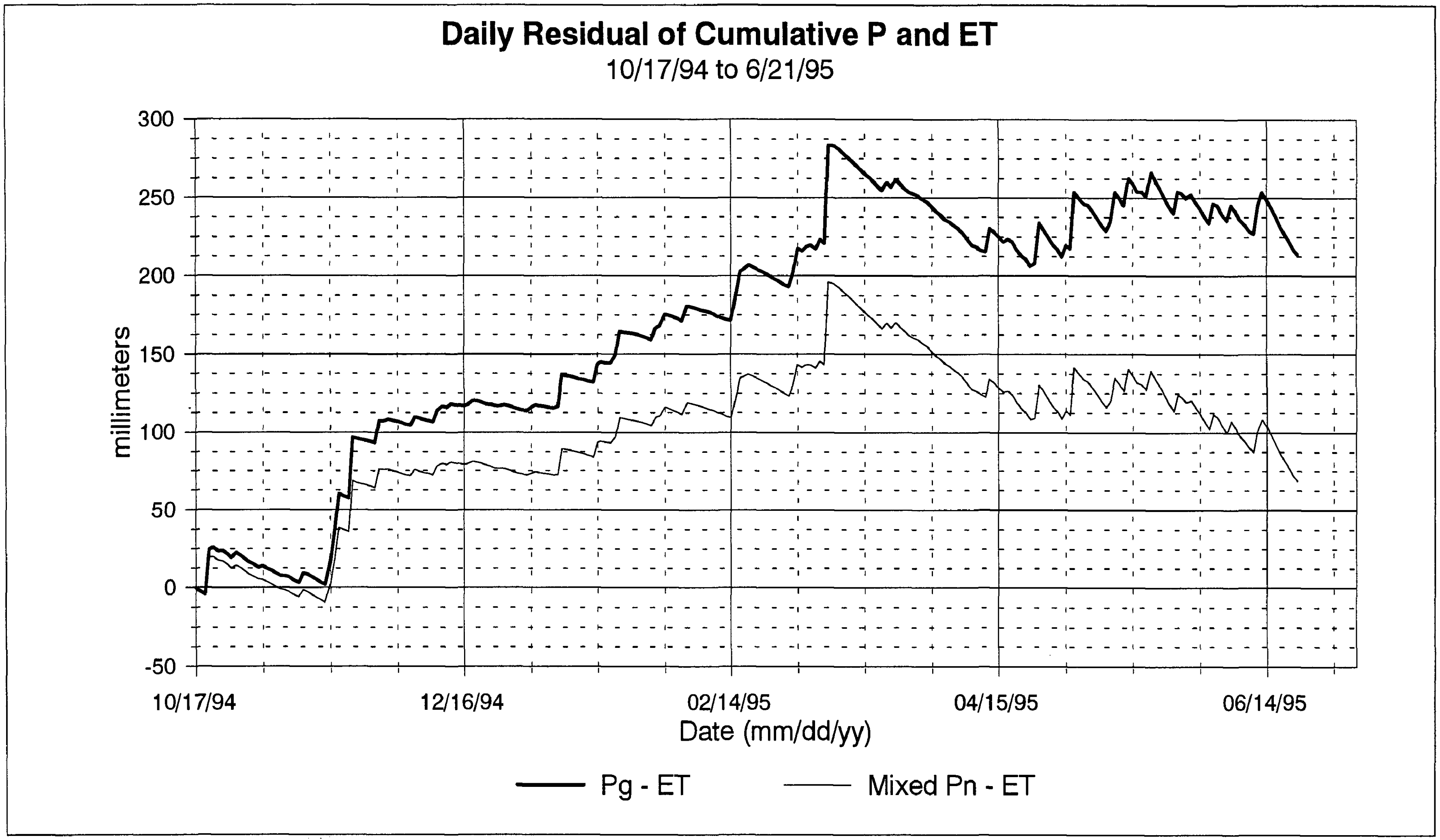
Daily Residual of Cumulative P and ET
10/17/94 to 6/21/95
millimeters
300
250
200
150
100
50
0
-50
10/17/94
12/16/94
02/14/95
04/15/95
06/14/95
Date (mm/dd/yy)
Pg - ET
Mixed Pn - ET

balance has a standard error of $(35^2 + 67^2)^{0.5}$ or 76 mm, and equals 250 ± 76 mm. The peak in the P_n - ET balance occurred when P_n was about 300 mm, and ET was 150 mm. The residual of the P_n - ET balance has a standard error of $(45^2 + 30^2) = 54$ mm, and therefore equals 150 ± 54 mm.

The climatic balance between P and ET is clearly reflected in both the seasonal and total variation in water table levels observed for this study. Seasonally, the time period of positive slope in the residual plot is concurrent with rising water table levels in the well hydrographs of all three land features, flatwoods, sinkhole and ridge, in the study area (Appendix 1). The ensuing dry period between mid-March and mid-April results in a water table drawdown. From mid-April to mid-May, the water table levels fluctuate greatly as a result of the increasing ET rate which rapidly depletes soil water storage in between storm events. The water table levels of the flatwoods and the sinkhole tend to fluctuate about a constant or slightly decreasing depth. After mid-May, the flatwoods and sinkhole water table levels show a general decline. The ridge water table levels fluctuate less in response to storms, and, in general, decline from a high after the storm of March 8.

The total range of the residual of the climatic balance is useful for checking the hypothesis concerning the availability of water for groundwater outflow. In that, if there is little groundwater outflow from this site and water surplus from the climatic balance is being sequestered for the most part as soil water storage, then the rise in water table level during the recharge season should be a function of the specific yield of the soils and the balance residual. For example, the residual of P_n - ET was zero at the start of the study period and peaked at approximately 150 mm in mid-March. The specific yield (S_y) of the silt loam, fine sandy loam, and silty clay soils present on the study site may range between 0.125 and 0.25, but this property can vary significantly (M. Focazio, personal comm.). S_y of the water table aquifer can be estimated from the ratio of climatic balance residual to change in water table level. Sinkhole well #3 experienced a 680 mm increase in water table level between the start of the study on October 17, 1994 and February 22, 1995 before ponding occurred after the high rainfall of mid-March. In this same period of time, P_n for a mixed canopy was 248 ± 37 mm, and ET was 117 ± 23 mm, resulting in 131 ± 44 mm of free water depth. Therefore, an estimate of S_y at well #3 is 0.19 ± 0.06. Significant losses to net groundwater outflow would force the S_y estimate to a higher than expected value, and significant gains would have the opposite effect. Since the S_y estimate is within the expected range, it is probable that large net groundwater gains or losses did not occur in the vicinity of the well in this sinkhole. In the wet flatwood, Well #16 experienced a 1090 mm rise in water table level between 1/18/95 and 3/1/95 in response to a surplus of 50 ± 20 mm of P_n over ET, resulting in an estimated S_y of 0.05 ± 0.02. Well #7 located on a ridge increased its water table level by 960 mm between 1/25/95 and 3/8/95. During this time period, P_n - ET equaled 37 ± 19 mm, resulting in an estimate of S_y of 0.04 ± 0.02. Lower values for estimated S_y indicate the possibility of net groundwater inflow to these areas. Preliminary results of work succeeding this study indicate seasonal reversals in water table gradients and therefore groundwater flow between sinkholes and flatwoods, similar to earlier discussion of research by Phillips and Shedlock (1993). The water table level in the flatwoods decreases below that of the sinkholes during the summer and into the fall. During the winter, the flatwoods water table rises above the level in the sinkhole. In this way, a significant amount of ground water may have flowed from sinkhole to flatwood during the late winter and early spring period used to estimate S_y. However, this phenomena would not explain the low S_y of the ridge since groundwater outflow from a higher water table elevation in the ridge would cause an overestimation of S_y. Further study is planned where the well network will be registered to a common datum, making analysis of spatial and temporal groundwater flow possible.

Steady-state Water Balances

A total of 45 balances were calculated using the water level data from 17 wells located in 3 different landscape features: wet flatwood, ridge, and sinkhole. Table 1 presents the results of the water balances organized by the three landscape features and sorted within landscape feature by ascending balance beginning date. Each individual water balance has a unique balance number (#1 to #45) which is used in the following discussion to facilitate identification. The balance periods do not necessarily correspond in time between features since the end points of the balance rely on recurring water levels and date of well completion. In general, the earliest flatwood balances began on 1/25/95, ridge balances on 2/1/95, and sinkhole balances on 10/17/94, with all landscape features having balances extending through 6/21/95. Balance durations varied from 8 days to 103 days, with an average length of 42 days (s.d. = 23). Components of the climatic water balance, P_n, ET, and G_n, are given in units of depth per unit area (mm) and proportion of P_n (%). For the purpose of comparison, discussion of results uses components expressed as a percentage of P_n. In this way, seasonal variation in the fate of precipitation inputs as ET or G_n outputs can be compared easily.

P_n was a relatively constant proportion of P_g with an average of 80% for all balances. Despite differences in duration, number and intensity of rain events, and canopy types, the throughfall model estimated similar amounts of interception within a few percentage points for all balances. P_n averaged 77%, 80% and 82% of P_g for steady-state balances for wells with pine, mixed and hardwood canopy, respectively. For all balances, the results show percentage of P_n lost to ET varied from 30% to 500%. In general, the lowest ET losses occurred in balances that included or were within the first five months of the study period. Six balances for the wet flatwood (1, 2, 4), ridge (27), and sinkhole (35, 36) occurred between October 1994 and mid-March 1995 for which

Table 1. Short-term, steady-state water balances (#1 to #45) by landscape feature.

Water Balance Number	Well Number	Landscape Feature	Vegetation Canopy	Balance Beginning Date (mm/dd/yy)	Balance Ending Date (mm/dd/yy)	Duration of Balance (days)	Pg (mm)	Standard Error of Pg (mm)	Pn (mm)	Standard Error of Pn (mm)	Pn/Pg %	EqET (mm)	Standard Error of EqET (mm)	EqET/Pn %	Pn-EqET (Gn) (mm)	Standard Error of Gn (mm)	Gn/Pn %
1	14	Flatwood	Pine	1/25/95	2/1/95	8	17	1	13	2	76	5	1	38	8	2	62
2	11	Flatwood	Hardwood	1/25/95	3/15/95	50	166	10	137	21	83	59	12	43	78	24	57
3	16	Flatwood	Mixed	1/25/95	4/14/95	80	201	12	160	24	80	134	27	84	26	36	16
4	14	Flatwood	Pine	2/8/95	3/18/95	39	139	8	108	16	78	56	11	52	52	20	48
5	18	Flatwood	Pine	2/8/95	3/30/95	51	153	9	119	18	78	84	17	71	35	25	29
6	21	Flatwood	Mixed	2/15/95	4/12/95	57	154	9	123	18	80	111	22	90	12	29	10
7	16	Flatwood	Mixed	2/22/95	3/23/95	30	114	7	92	14	81	54	11	59	38	18	41
8	22	Flatwood	Mixed	2/22/95	5/9/95	77	217	13	174	26	80	189	38	109	-15	46	9
9	11	Flatwood	Hardwood	3/23/95	5/18/95	57	161	10	131	20	81	167	33	127	-36	39	27
10	22	Flatwood	Mixed	3/30/95	5/2/95	34	100	6	79	12	79	93	19	118	-14	22	18
11	18	Flatwood	Pine	4/5/95	5/8/95	34	101	6	78	12	77	101	20	129	-23	23	29
12	11	Flatwood	Hardwood	4/12/95	5/24/95	43	172	10	141	21	82	146	29	104	-5	36	4
13	23	Flatwood	Pine	4/14/95	5/17/95	34	134	8	104	16	78	108	22	104	-4	27	4
14	27	Flatwood	Mixed	4/14/95	5/18/95	35	134	8	107	16	80	112	22	105	-5	28	5
15	14	Flatwood	Pine	4/14/95	5/31/95	48	175	11	136	20	78	165	33	121	-29	39	21
16	16	Flatwood	Mixed	4/19/95	5/10/95	22	87	5	69	10	79	69	14	100	0	17	0
17	25	Flatwood	Pine	4/19/95	5/22/95	34	148	9	115	17	78	114	23	99	1	29	1
18	21	Flatwood	Mixed	4/19/95	6/12/95	55	227	14	182	27	80	199	40	109	-17	48	9
19	22	Flatwood	Mixed	4/24/95	5/26/95	33	165	10	134	20	81	120	24	90	14	31	10
20	16	Flatwood	Mixed	5/6/95	5/16/95	11	51	3	41	6	80	38	8	93	3	10	7
21	18	Flatwood	Pine	5/10/95	5/22/95	13	70	4	55	8	79	45	9	82	10	12	18
22	23	Flatwood	Pine	5/14/95	6/13/95	31	128	8	99	15	77	118	24	119	-19	28	19
23	21	Flatwood	Mixed	5/31/95	6/21/95	22	65	4	52	8	80	90	18	173	-38	20	73
24	16	Flatwood	Mixed	6/13/95	6/21/95	9	10	1	8	1	80	40	8	500	-32	8	400
25	20	Ridge	Mixed	2/1/95	5/14/95	103	314	19	252	38	80	226	45	90	26	59	10
26	19	Ridge	Mixed	2/8/95	3/30/95	51	153	9	123	18	80	84	17	68	39	25	32
27	7	Ridge	Mixed	2/22/95	3/15/95	22	101	6	83	12	82	34	7	41	49	14	59
28	20	Ridge	Mixed	3/14/95	5/2/95	50	114	7	90	14	79	131	26	146	-41	29	46
29	19	Ridge	Mixed	3/30/95	5/15/95	47	152	9	121	18	80	140	28	116	-19	33	16
30	7	Ridge	Mixed	4/5/95	5/22/95	48	172	10	137	21	80	153	31	112	-16	37	12
31	7	Ridge	Mixed	4/19/95	6/1/95	44	171	10	137	21	80	155	31	113	-18	37	13
32	19	Ridge	Mixed	4/24/95	6/21/95	59	233	14	187	28	80	227	45	121	-40	53	21
33	28	Ridge	Mixed	5/2/95	5/19/95	18	109	7	88	13	81	60	12	68	28	18	32
34	20	Ridge	Mixed	5/6/95	5/16/95	11	51	3	41	6	80	38	8	93	3	10	7
35	3	Sinkhole	Mixed	10/17/94	1/5/95	81	195	12	152	23	78	79	16	52	73	28	48
36	9	Sinkhole	Mixed	1/18/95	2/1/95	15	39	2	30	5	77	9	2	30	21	5	70
37	3	Sinkhole	Mixed	1/18/95	4/5/95	78	202	12	161	24	80	114	23	71	47	33	29
38	6	Sinkhole	Mixed	1/25/95	4/24/95	90	234	14	185	28	79	161	32	87	24	43	13
39	9	Sinkhole	Mixed	2/15/95	4/5/95	50	153	9	123	18	80	92	18	75	31	26	25
40	3	Sinkhole	Mixed	3/30/95	5/19/95	51	172	10	137	21	80	153	31	112	-16	37	12
41	6	Sinkhole	Mixed	4/12/95	5/22/95	41	172	10	137	21	80	135	27	99	2	34	1
42	9	Sinkhole	Mixed	4/12/95	5/26/95	45	192	12	154	23	80	153	31	99	1	38	1
43	24	Sinkhole	Mixed	4/14/95	6/21/95	69	240	14	191	29	80	255	51	134	-64	58	34
44	9	Sinkhole	Mixed	6/7/95	6/21/95	15	35	2	27	4	77	60	12	222	-33	13	122
45	6	Sinkhole	Mixed	6/12/95	6/21/95	10	29	2	24	4	83	41	8	171	-17	9	71

ratios of $ET:P_n$ expressed as a percent are 38%, 43%, 52%, 41%, 52%, and 30%, respectively. There are no obvious differences in these ratios that correspond to different land features. The mean ratio of $ET:P_n$ for these six balances is 43%, thus leaving an average of 57% of P_n for groundwater recharge. In fact, all features showed net groundwater outflow, which is expressed as a positive residual ($+G_n$) in Table 1, in excess of the pooled standard error of the residual. These results demonstrate that the residual of the climatic balances for fall and winter can not be accounted for by the change in storage alone (i.e., a rise in water table level), and that more than half of P_n exited the site as groundwater outflow.

The expected cumulative P_n for a mixed canopy forest between mid-October and mid-March is approximately 340 ± 51 mm based on normal monthly P_g and degree of interception. Based on the net recharge rate of 57% found in this study, approximately 194 ± 59 mm of free water depth on a unit area basis would be expected to recharge ground water during this October to March time period for an average of 39 ± 12 mm per month. This is a general estimate based on expected rainfall for Norfolk and the average seasonal net recharge for late fall to early spring found in this study. However, the 1994/1995 period of winter recharge was characterized by a unique distribution of storm sizes and rates of rainfall, and relative amount of actual to normal P over time. Given typical climatic variation in seasonal water availability between years, seasonal soil moisture dynamics and by extension wetland hydrodynamics can differ significantly. In this way, if an early dry period in October and November did not occur as in the 1994/1995 recharge period or if more large storm events occurred, it is likely that some proportion of P_n would be lost to surface outflows due to saturation to soil surface.

A dry period occurred from mid-March to mid-April when only 14 ± 1 mm of an expected 89 mm of rainfall occurred. Balances that are dominated by this dry period showed ET losses greater than P_n inputs, yielding ET:P_n ratios of 127%, 118%, and 129% for the flatwoods (9, 10, 11), 146%, 116% for ridges (28, 29), and 112% for the sinkholes (40). These values indicate some form of water input to the steady-state, climatic balance either as water flow into the system or as an overestimation of outflow from the system. Although the ridge balance (28) with an ET:P_n ratio of 146% is the only balance where G_n is significantly greater than zero when the standard error of the residual is considered. Preliminary findings from nested piezometers do not support groundwater inputs from deeper, regional groundwater flows. It is not likely that net subsurface exchanges between land features provided the surplus water since the residuals (G_n) for all land features are positive. A possible explanation for the source of the water input is an overestimation of losses to ET. During the dry period, plant transpiration may have been reduced by water stress, as a result of an inadequate supply of soil moisture to maintain PET rates. In addition, equilibrium ET will likely overestimate the rate of ET from hardwood or mixed species forests during winter dormancy. Although evaporation from the vegetative structure and transpiration from the evergreen species still proceeds, the equilibrium ET model does not account for changes in surface resistance to vapor transfer. A large reduction in transpiring surfaces may cause an increase in the surface resistance to aerodynamic transfer. If ET was overestimated during the dormant season, then a larger proportion of P_n may have contributed to net groundwater outflow in the balances before mid-March. The balances encompassing both the winter months and dry period of March and April have ET:P_n ratios of intermediate value compared to the ratios of either period.

From late April through May, more normal rainfall patterns resumed and ET increased, resulting in a close parity between P_n and ET. A partial list of the ET:P_n ratios for balances of this time period are 104%, 105%, 121%, 99%, 90%, 93%, and 82% for flatwoods (12 and 13, 14, 15, 17, 19, 20, 21), 113%, 68%, and 93% for ridges (31, 33, 34), and 99% for sinkholes (41 and 42). The well hydrographs show the water table level fluctuating in response to storm events and an increasing ET rate (see Appendix). If a period of time is selected where steady-state conditions are met, short-term surpluses and deficits of water compensate for each other, leaving no water for groundwater outflow.

The rate of ET increased above P_n to a maximum for the study period during the third week in June 1995. The balances that include June are characterized by ET:P_n ratios above 100%. The ratios for the flatwood balances (22, 23, 24) are 119%, 173%, and 500%; the ridge balance (32) was 121%; and, the sinkhole balances (43, 44, 45) are 134%, 222%, and 171%. As before during the dry period in March and April, the steady-state water balances predict an additional source of water to account for the water lost to ET. Since the water table levels were similar between the two time periods for most wells, plant water stress and reduced ET relative to predicted equilibrium ET may have caused ET to be overestimated. Another explanation may be that steady-state conditions were violated by changes in the volume of soil moisture storage. As seen by the rapid rate of water level decline in the flatwood and sinkhole wells, ET removed a significant portion of water in the root zone. If deeper portions of the soil profile had a large part of the plant-available soil moisture removed by ET, the entire profile may not have saturated again completely in response to a storm event. In this way, a higher water table level would have been recorded than actually existed, and the volume of water in storage would have been less.

The results of the steady-state water balances show seasonal variation in net groundwater flows as calculated by the residual of the difference between P_n and ET. The study area, which included wet flatwoods, sinkholes and ridges, experienced net groundwater outflow on the order of 57% of P_n for a forest of mixed, hardwood and evergreen canopy between October 1994 and March 1995. Therefore, the wet flatwoods of the study area were not "hydrologically neutral" land features as hypothesized. The marked water table fluctuations in wet flatwoods over a year did not represent a balance between changes in volume of soil moisture storage and seasonal water surplus or deficit. Several balances exhibited ET:P_n ratios greater than 100%, indicating an additional water source beside rainfall. Preliminary results from nested piezometers show no discharge of regional groundwater flow in the study area, and no significant surface inflows or outflows occurred. Possible explanations for the apparent source of water are: 1) a dry period from mid-March to mid-April may have caused plant water stress and a reduction in ET rate; 2) equilibrium ET may overestimate for deciduous forests during winter dormancy; and, 3) well water levels may not have reflected deeper, unsaturated layers in the soil profile after storm events, thus overestimating the volume of storage.

The residual of the climatic balance exhibited a fairly uniform response between the land features of the site for the different seasons of the study period. If significant differences in the partitionment of P_n into vertical and lateral flows exist between the wet flatwoods, sinkholes and ridges or if measurable exchanges occur between these features, the model used in this study did not detect them. This information could be obtained by performing water balances where direction and magnitude of groundwater flow are measured as well as on site estimates of canopy interception.

APPENDIX Water Level Hydrographs

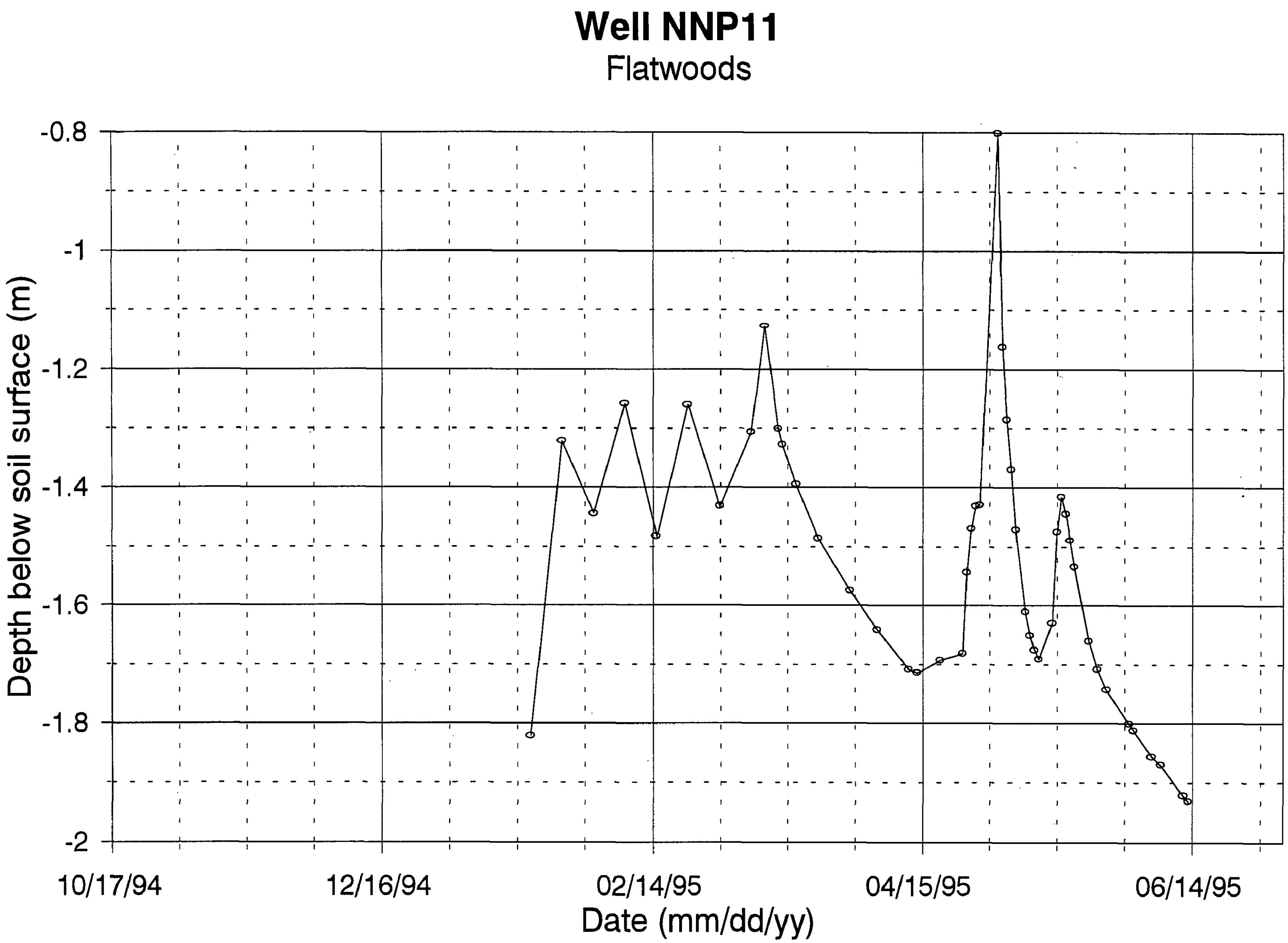
Well NNP11
Flatwoods
-0.8
-1
-1.2
-1.4
-1.6
-1.8
-2
Depth below soil surface (m)
10/17/94
12/16/94
02/14/95
04/15/95
06/14/95
Date (mm/dd/yy)

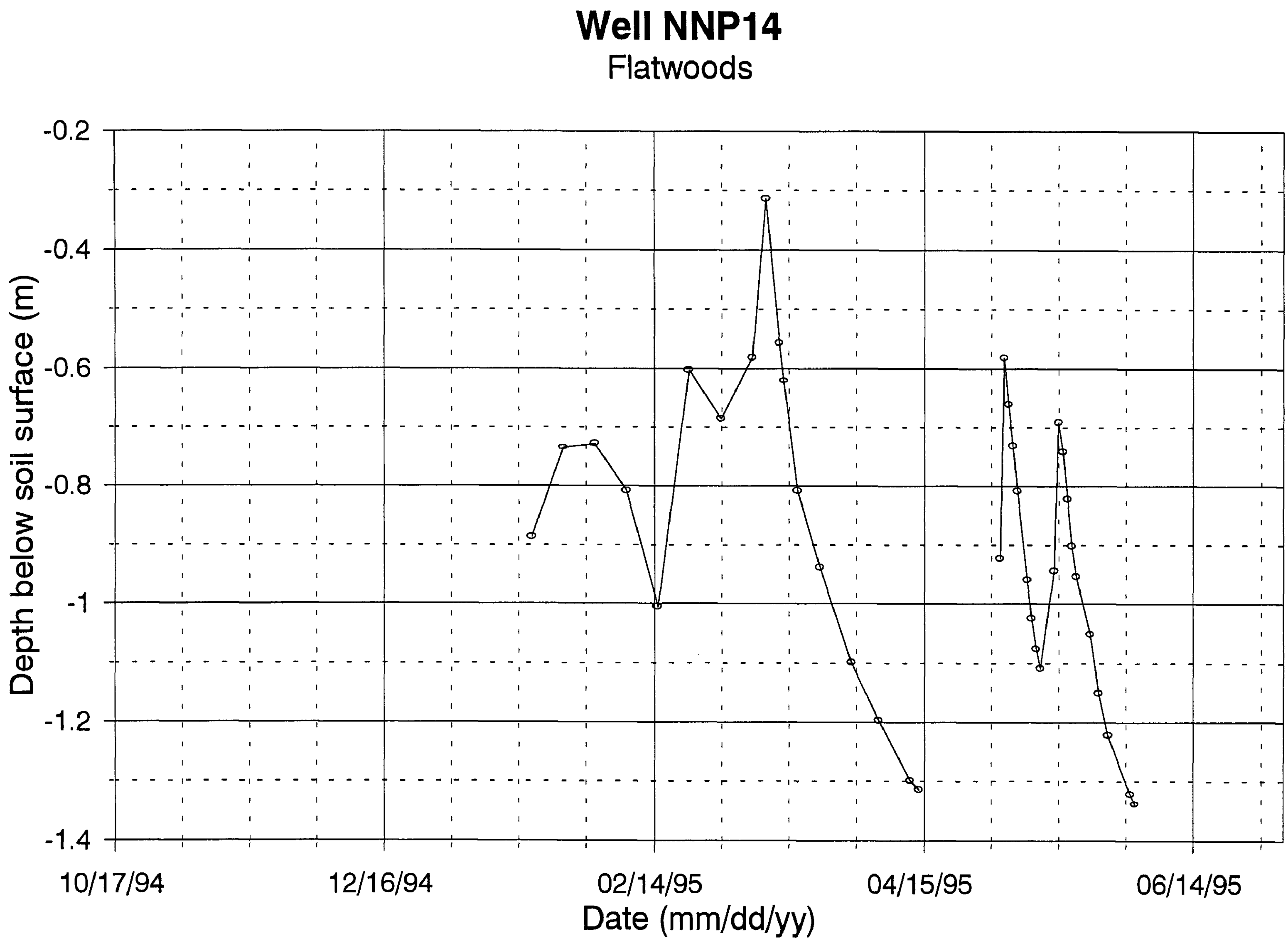
Well NNP14
Flatwoods
-0.2
-0.4
-0.6
-0.8
-1
-1.2
-1.4
Depth below soil surface (m)
10/17/94
12/16/94
02/14/95
04/15/95
06/14/95
Date (mm/dd/yy)

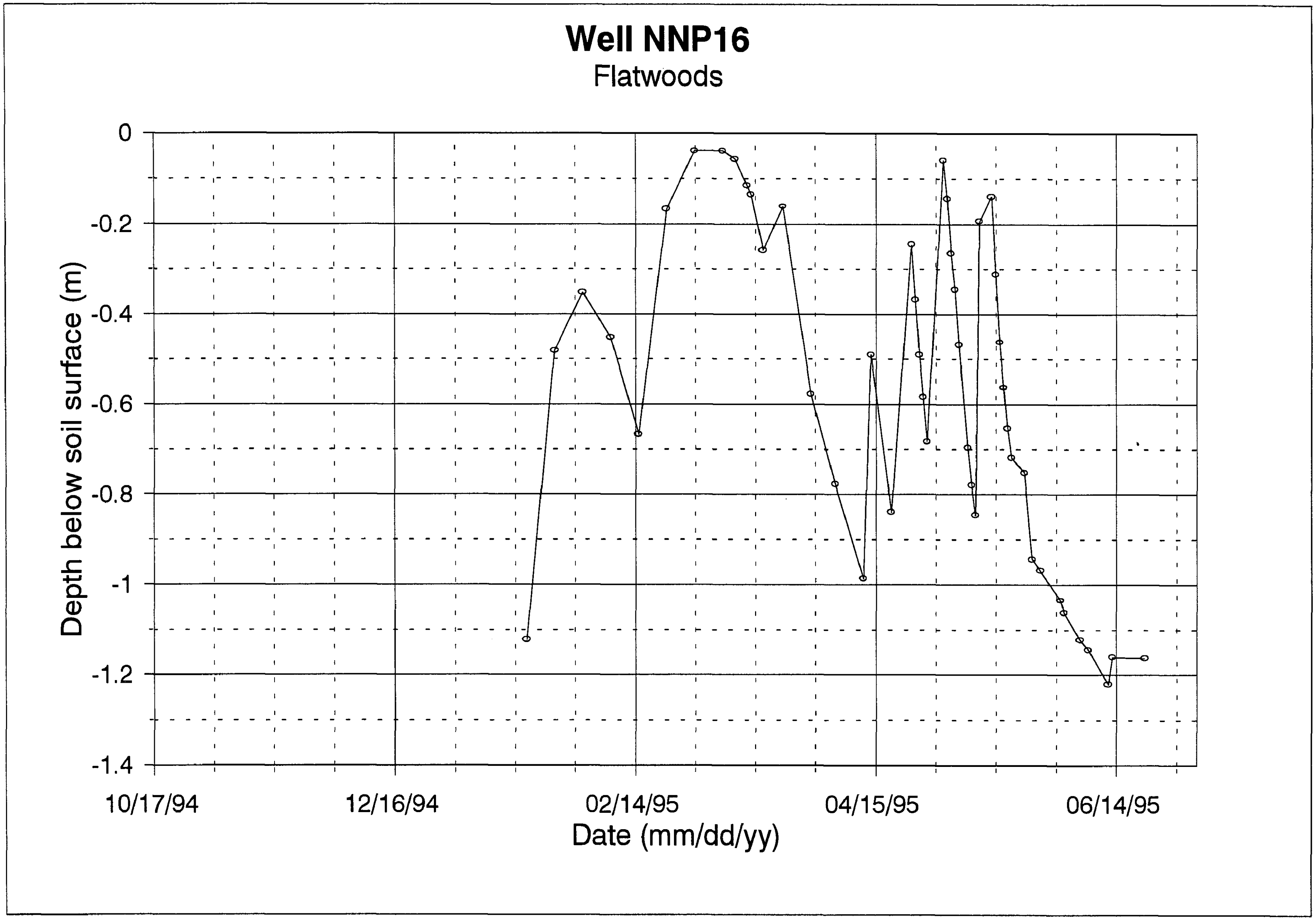

Well NNP16
Flatwoods
Depth below soil surface (m)
0
-0.2
-0.4
-0.6
-0.8
-1
-1.2
-1.4
10/17/94
12/16/94
02/14/95
04/15/95
06/14/95
Date (mm/dd/yy)

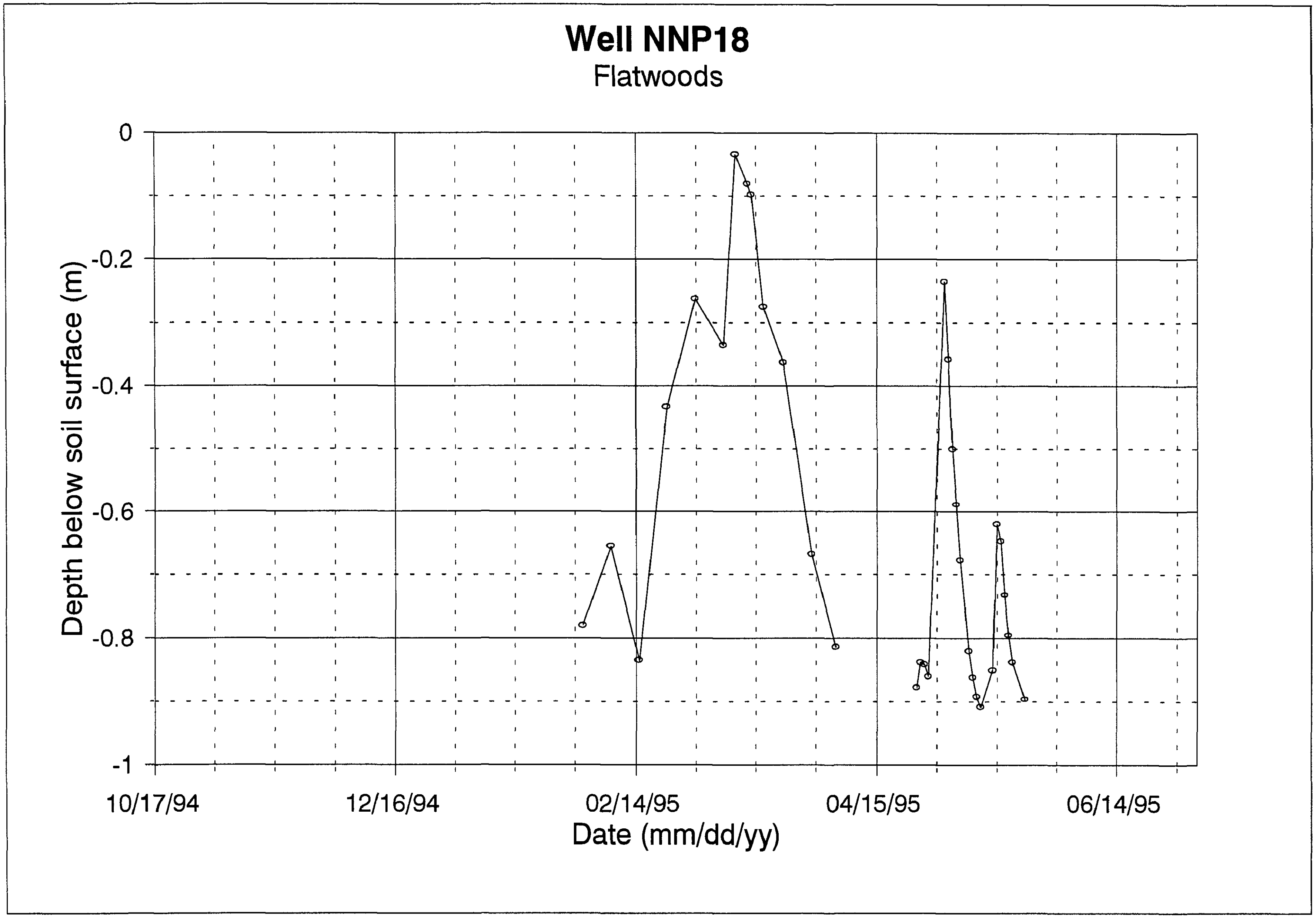

Well NNP18
Flatwoods
0
-0.2
-0.4
-0.6
-0.8
-1
Depth below soil surface (m)
10/17/94
12/16/94
02/14/95
04/15/95
06/14/95
Date (mm/dd/yy)

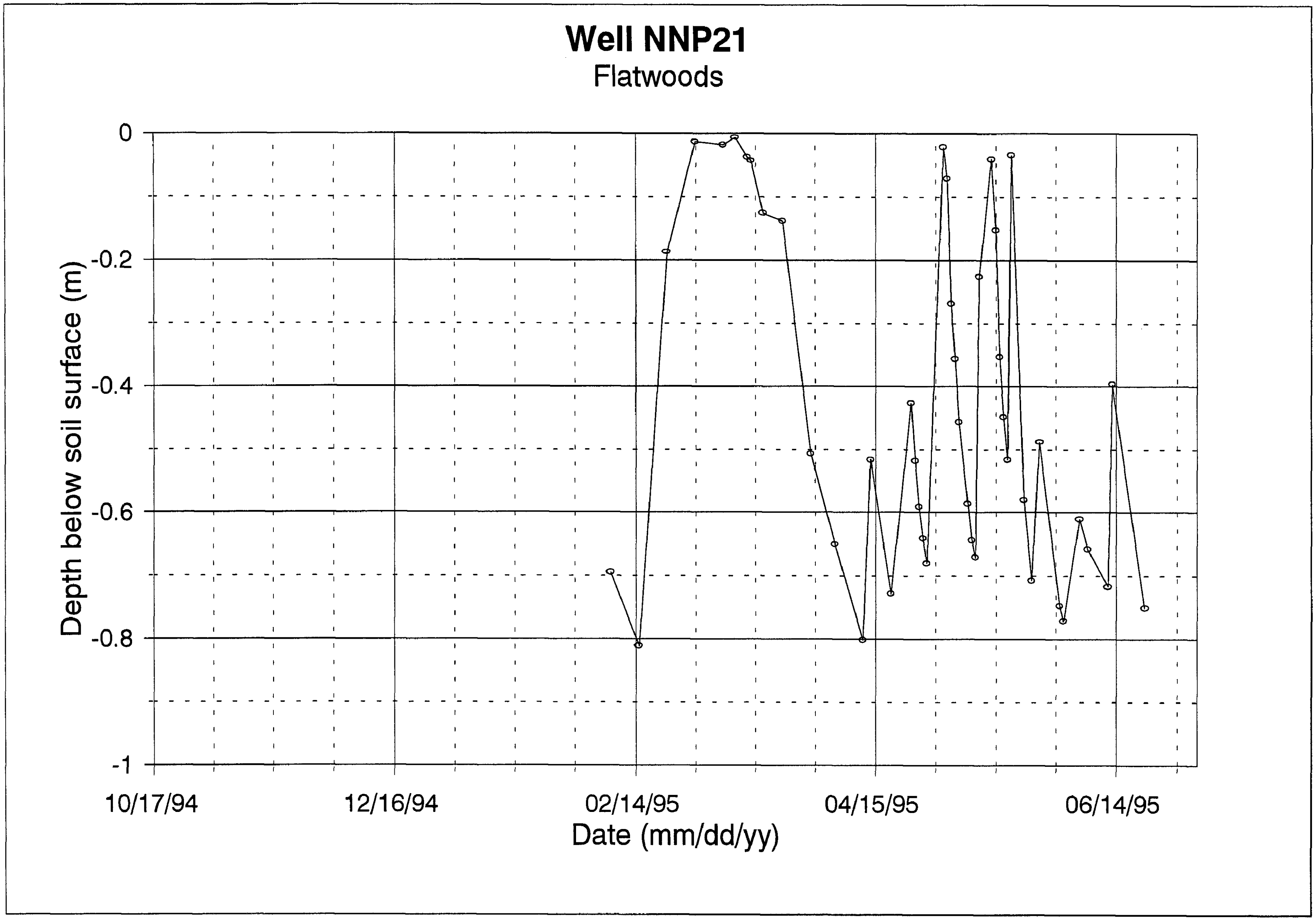
Well NNP21
Flatwoods
0
-0.2
-0.4
-0.6
-0.8
-1
Depth below soil surface (m)
10/17/94
12/16/94
02/14/95
04/15/95
06/14/95
Date (mm/dd/yy)

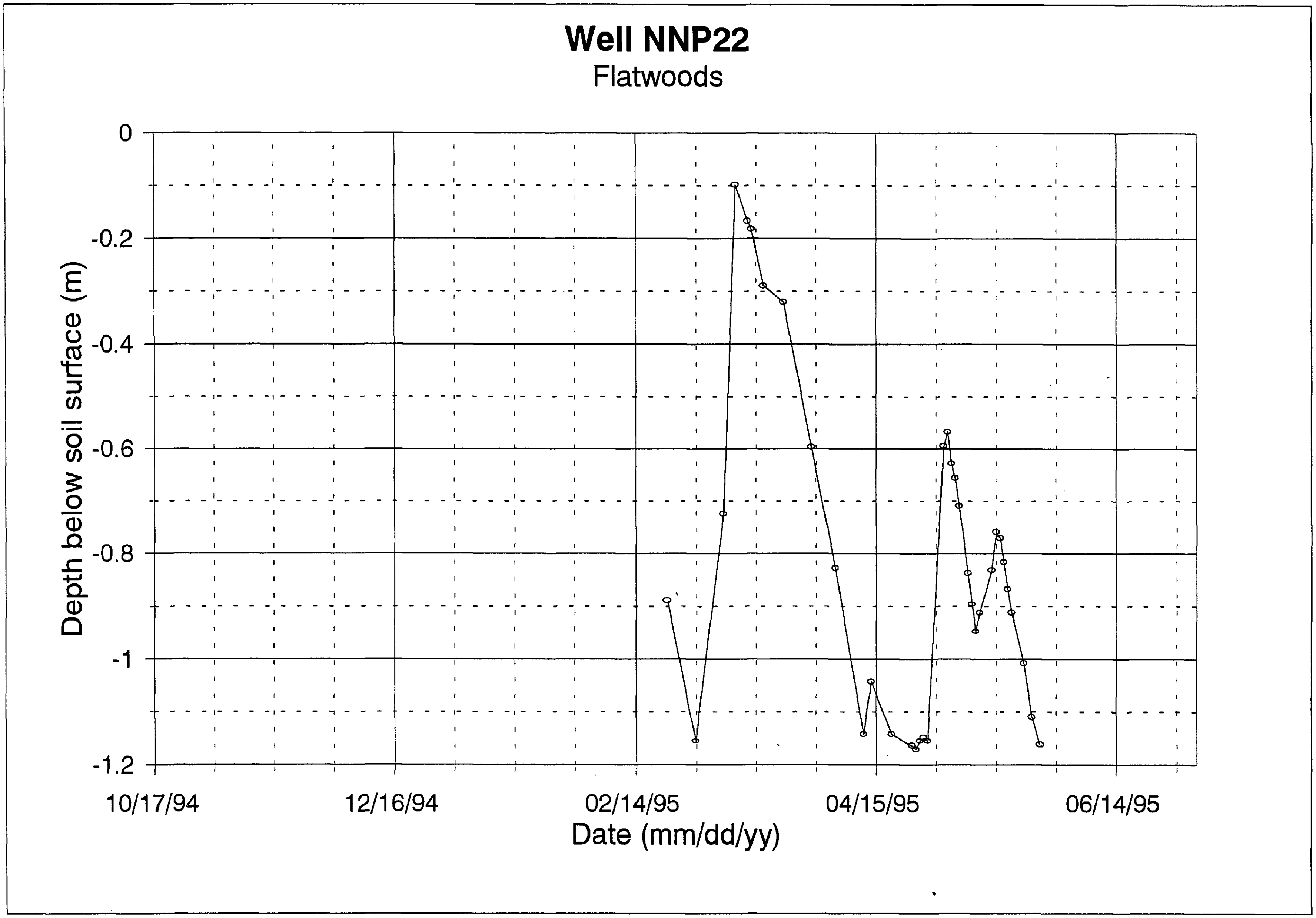
Well NNP22
Flatwoods
0
-0.2
-0.4
-0.6
-0.8
-1
-1.2
Depth below soil surface (m)
10/17/94
12/16/94
02/14/95
04/15/95
06/14/95
Date (mm/dd/yy)

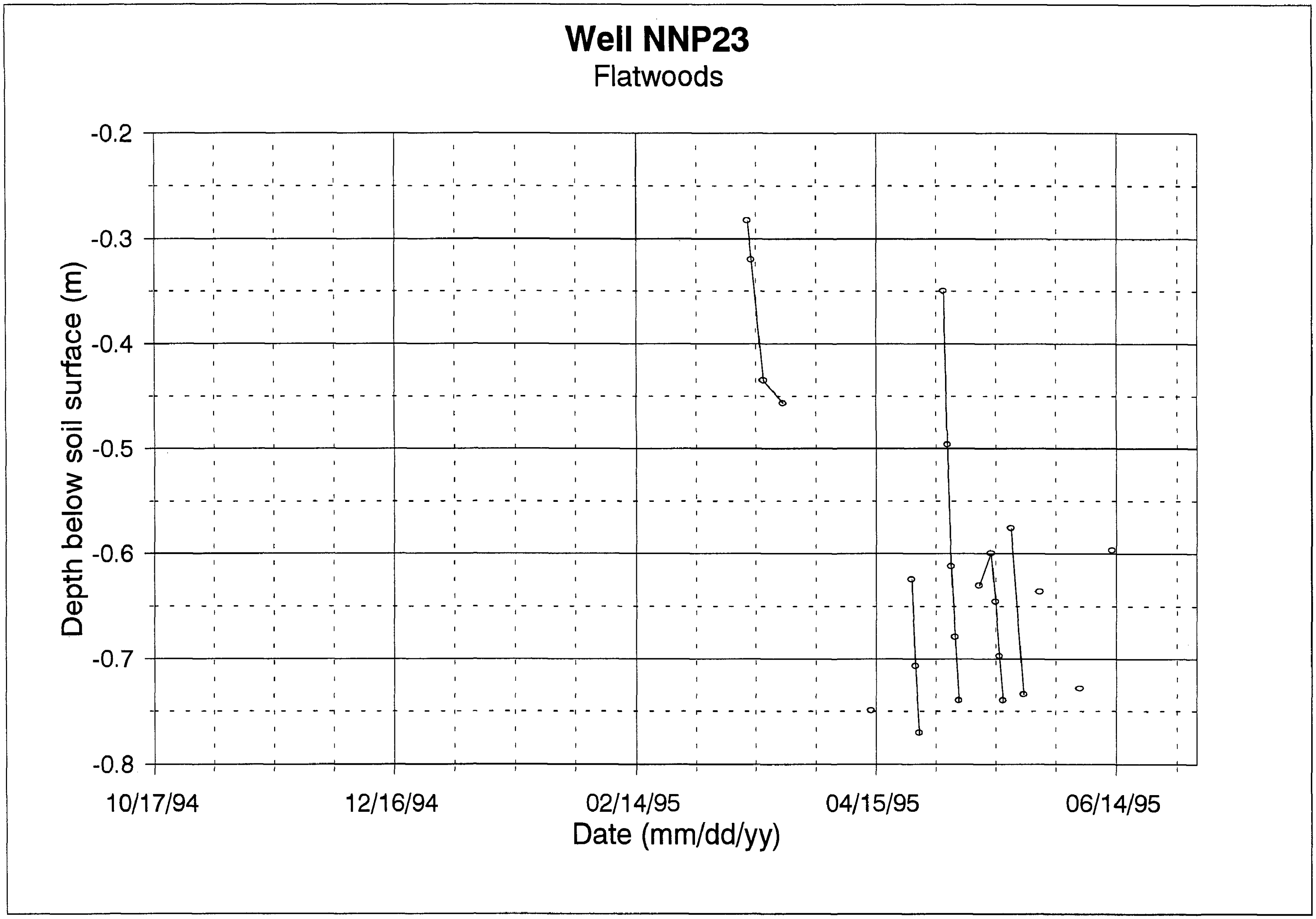

Well NNP23
Flatwoods
-0.2
-0.3
-0.4
-0.5
-0.6
-0.7
-0.8
Depth below soil surface (m)
10/17/94
12/16/94
02/14/95
04/15/95
06/14/95
Date (mm/dd/yy)

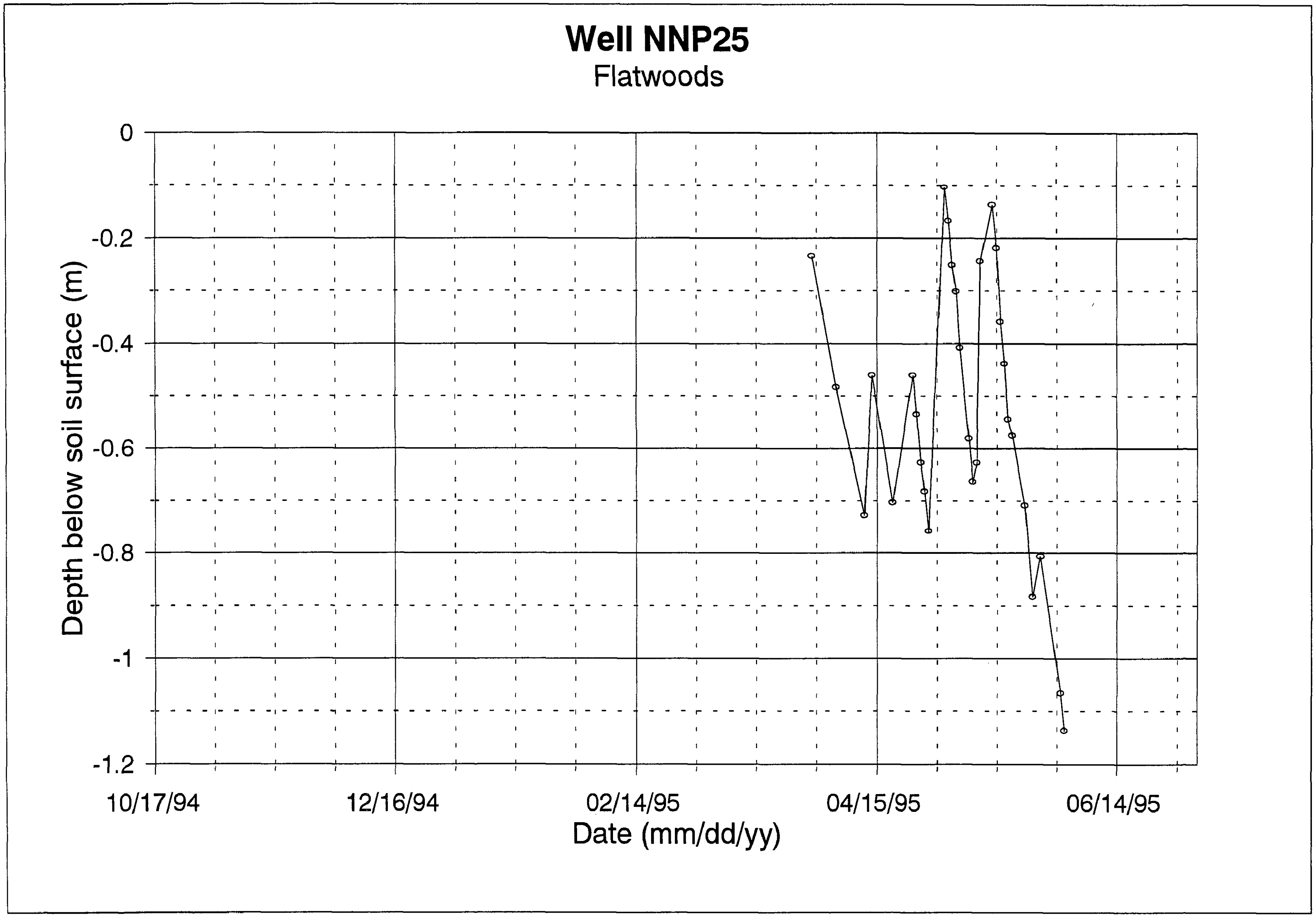
Well NNP25
Flatwoods
Depth below soil surface (m)
0
-0.2
-0.4
-0.6
-0.8
-1
-1.2
10/17/94
12/16/94
02/14/95
04/15/95
06/14/95
Date (mm/dd/yy)

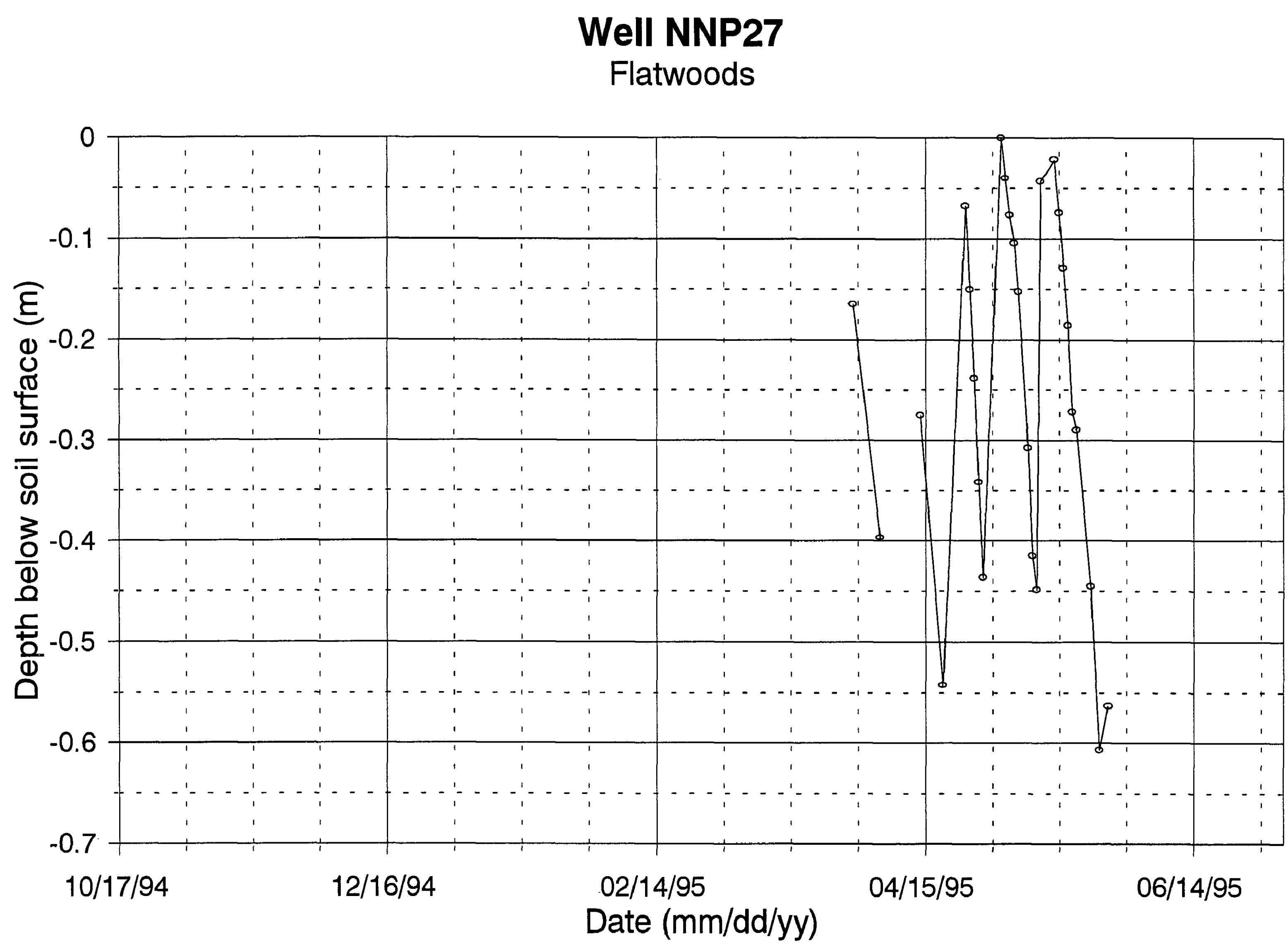
Well NNP27
Flatwoods
0
-0.1
-0.2
-0.3
-0.4
-0.5
-0.6
-0.7
Depth below soil surface (m)
10/17/94
12/16/94
02/14/95
04/15/95
06/14/95
Date (mm/dd/yy)

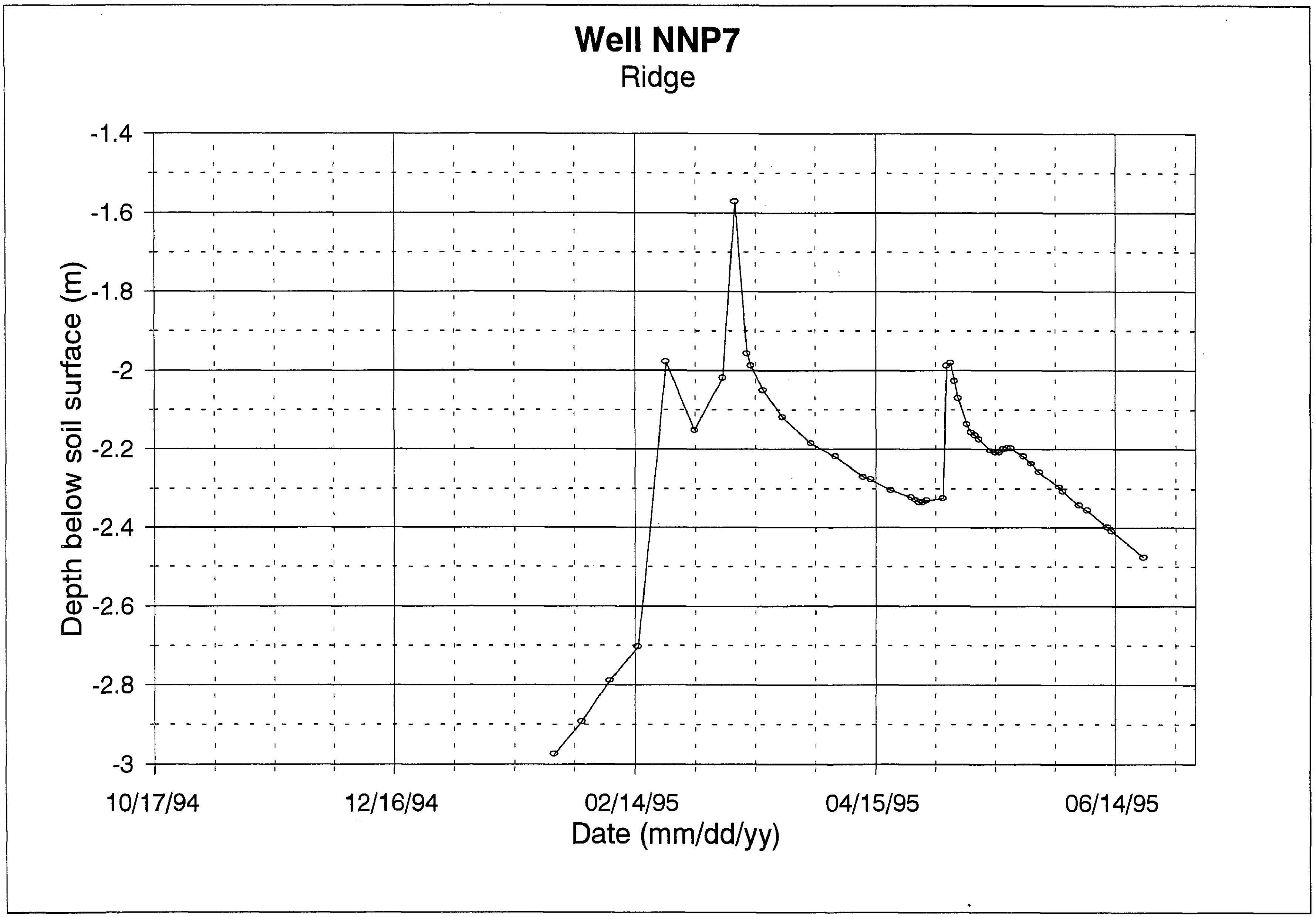
Well NNP7
Ridge
Depth below soil surface (m)
-1.4
-1.6
-1.8
-2
-2.2
-2.4
-2.6
-2.8
-3
10/17/94
12/16/94
02/14/95
04/15/95
06/14/95
Date (mm/dd/yy)

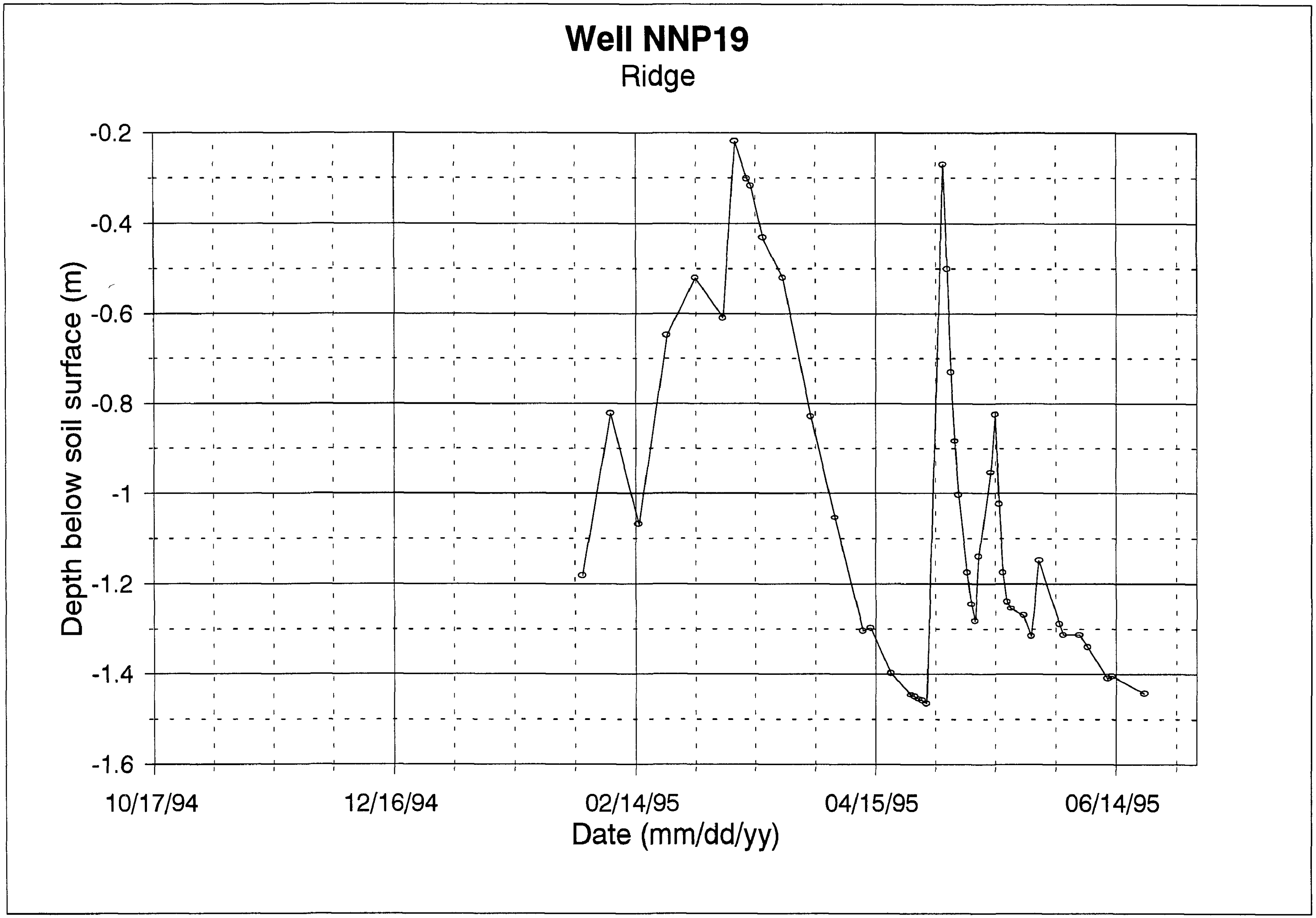
Well NNP19
Ridge
-0.2
-0.4
-0.6
-0.8
-1
-1.2
-1.4
-1.6
Depth below soil surface (m)
10/17/94
12/16/94
02/14/95
04/15/95
06/14/95
Date (mm/dd/yy)

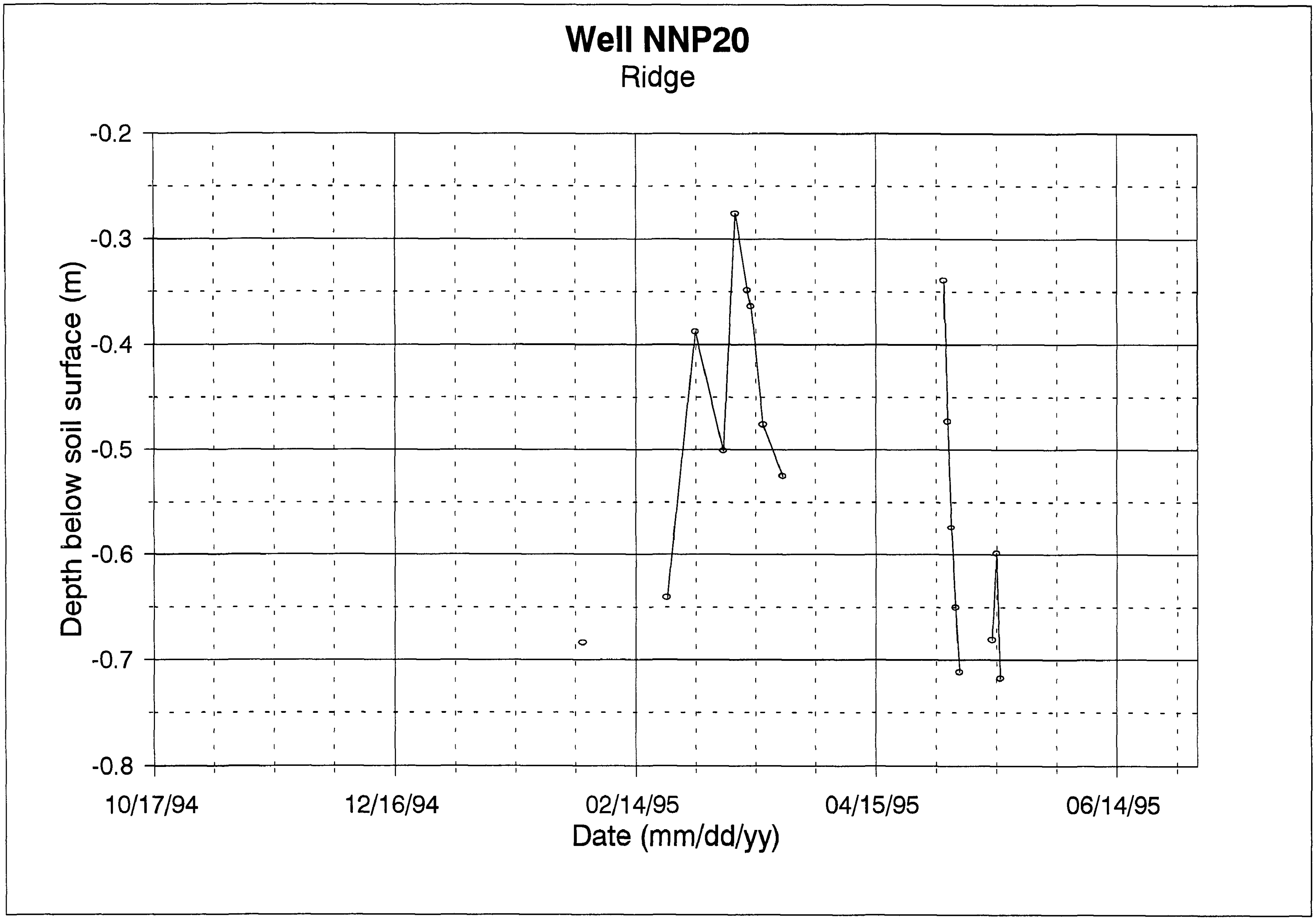
Well NNP20
Ridge
Depth below soil surface (m)
-0.2
-0.3
-0.4
-0.5
-0.6
-0.7
-0.8
10/17/94
12/16/94
02/14/95
04/15/95
06/14/95
Date (mm/dd/yy)

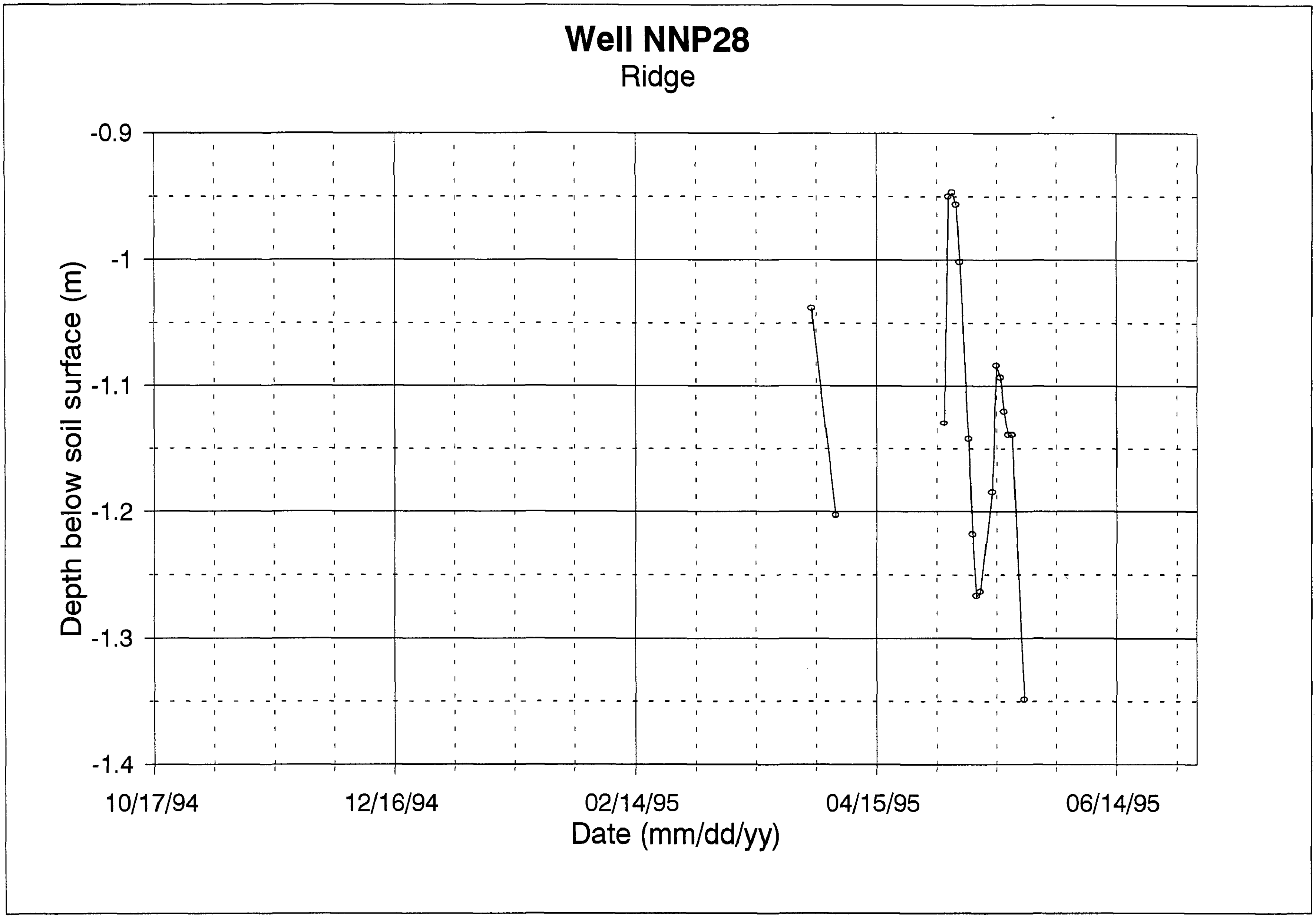
Well NNP28
Ridge
Depth below soil surface (m)
-0.9
-1
-1.1
-1.2
-1.3
-1.4
10/17/94
12/16/94
02/14/95
04/15/95
06/14/95
Date (mm/dd/yy)

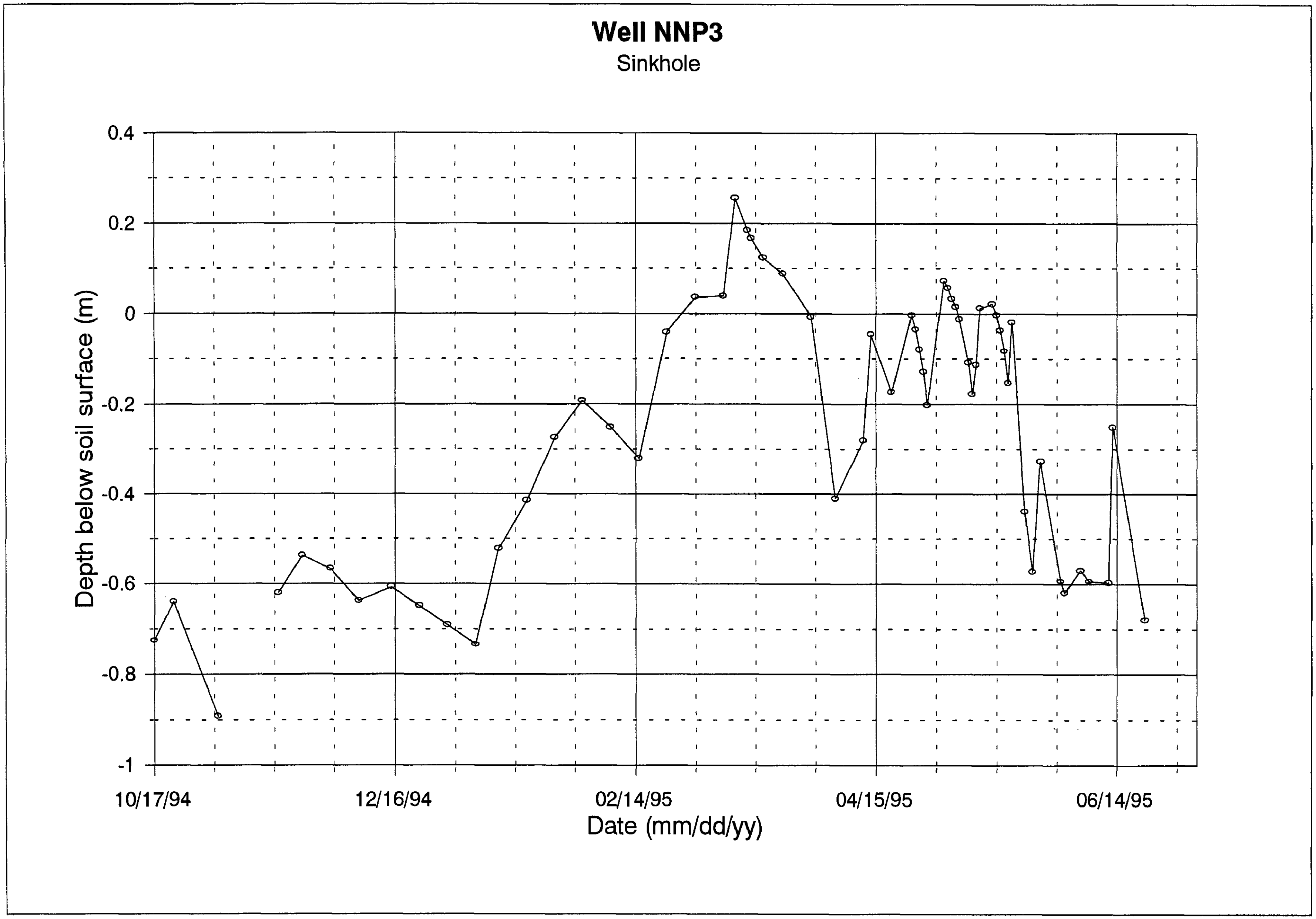

Well NNP3
Sinkhole
0.4
0.2
0
-0.2
-0.4
-0.6
-0.8
-1
Depth below soil surface (m)
10/17/94
12/16/94
02/14/95
04/15/95
06/14/95
Date (mm/dd/yy)

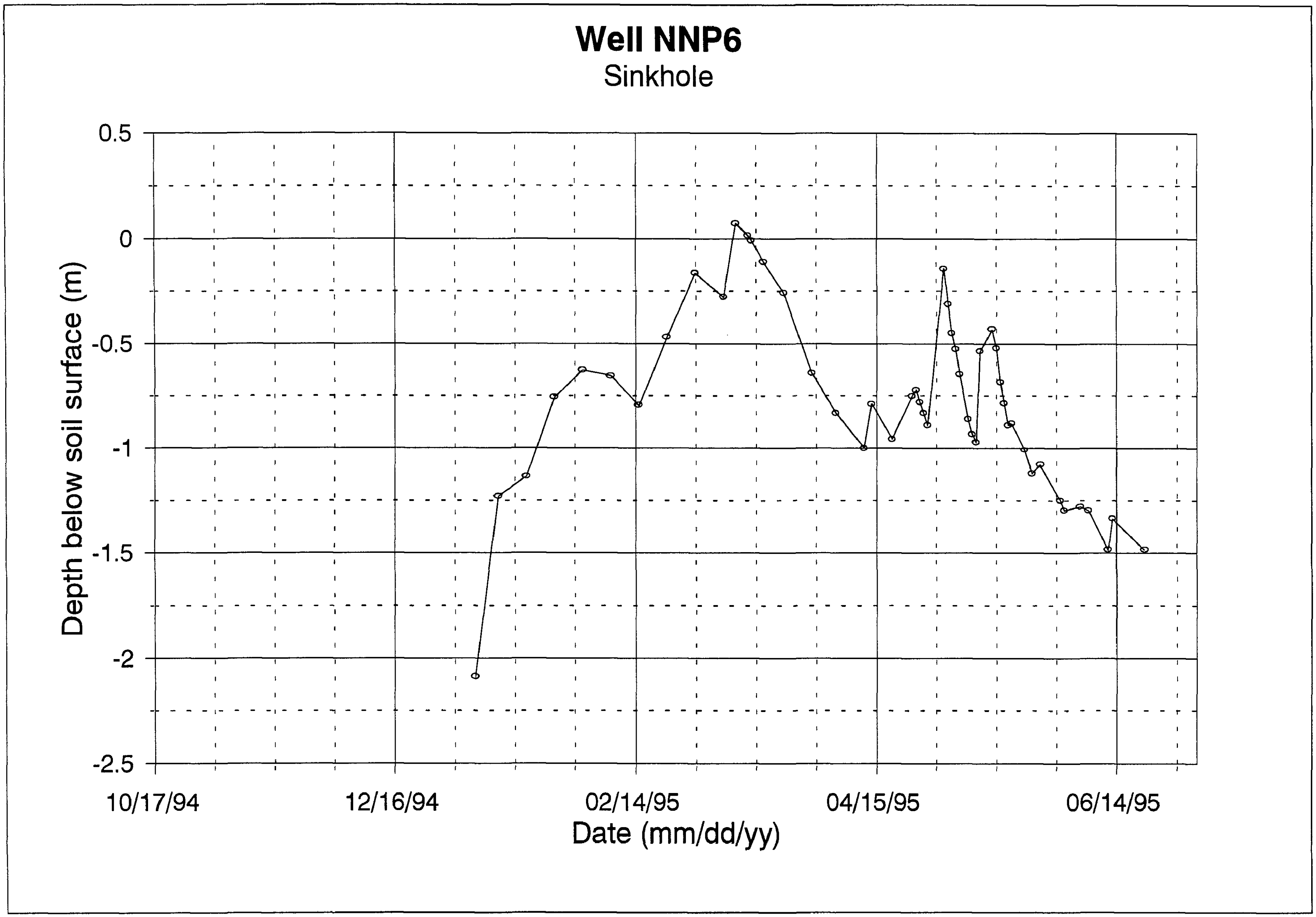
Well NNP6
Sinkhole
Depth below soil surface (m)
0.5
0
-0.5
-1
-1.5
-2
-2.5
10/17/94
12/16/94
02/14/95
04/15/95
06/14/95
Date (mm/dd/yy)

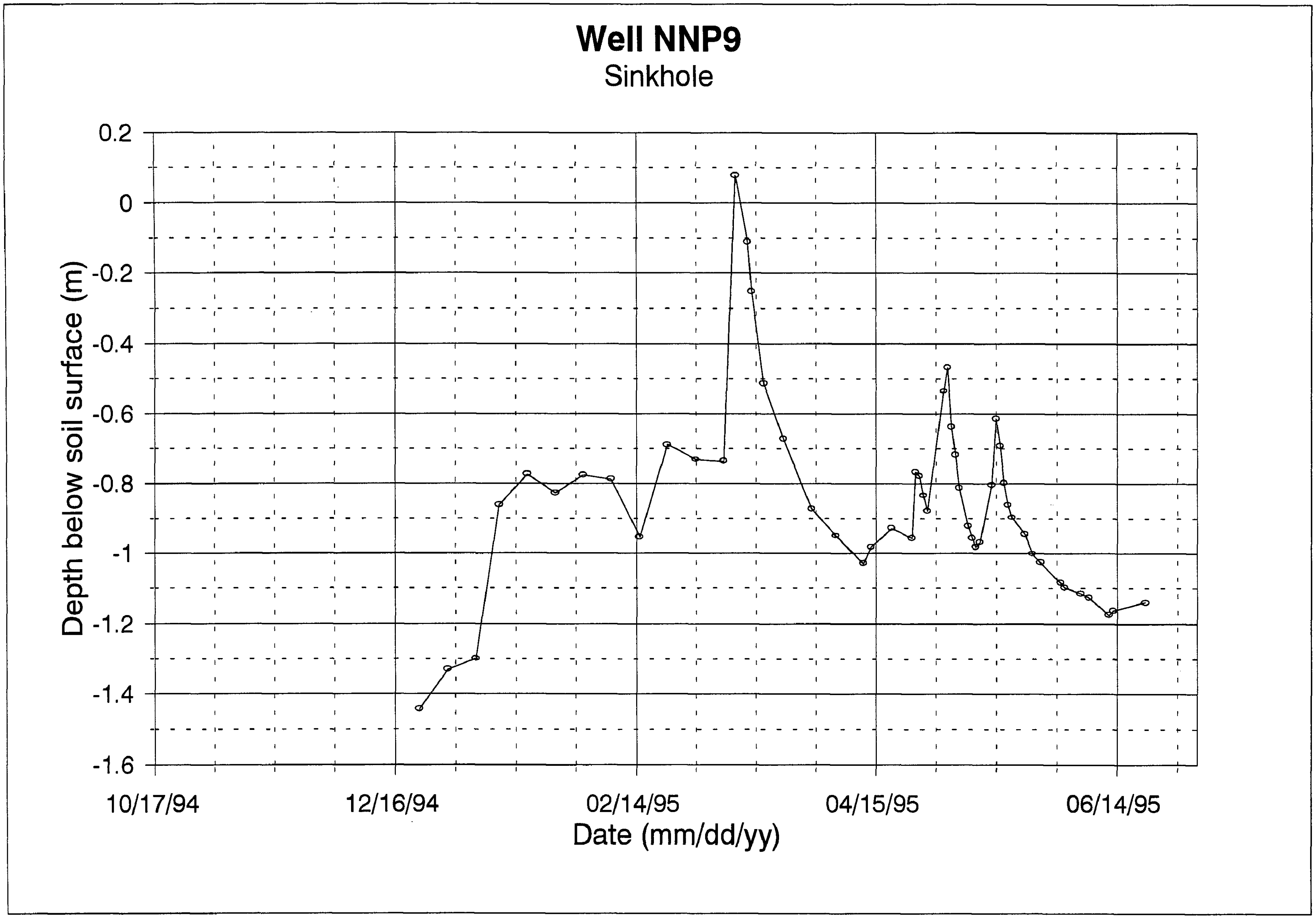
Well NNP9
Sinkhole
Depth below soil surface (m)
0.2
0
-0.2
-0.4
-0.6
-0.8
-1
-1.2
-1.4
-1.6
10/17/94
12/16/94
02/14/95
04/15/95
06/14/95
Date (mm/dd/yy)

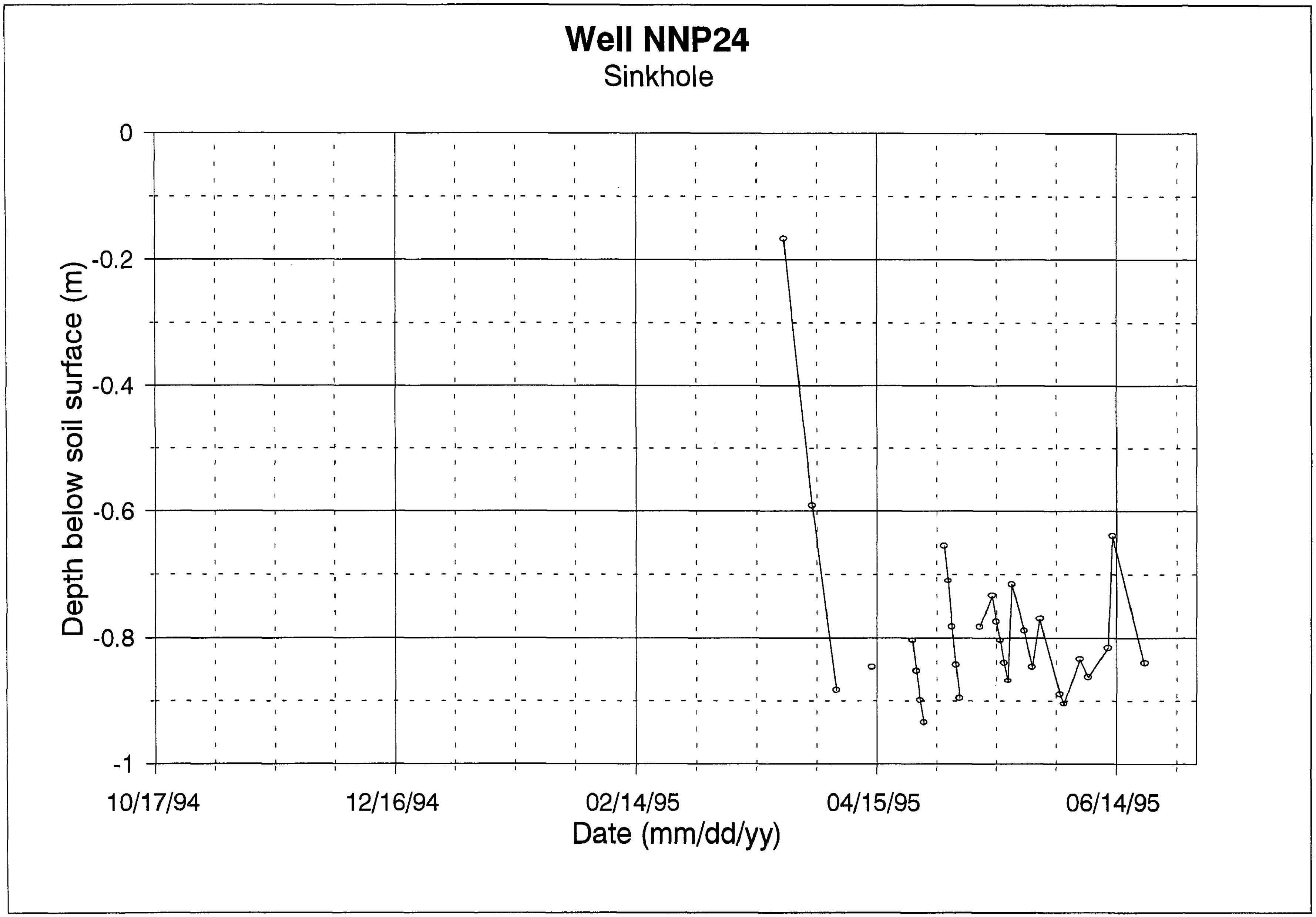
Well NNP24
Sinkhole
Depth below soil surface (m)
0
-0.2
-0.4
-0.6
-0.8
-1
10/17/94
12/16/94
02/14/95
04/15/95
06/14/95
Date (mm/dd/yy)

LITERATURE CITED

Blaney, H.F. and W.D. Criddle. 1950. Determining water requirements in irrigated areas from climatological and irrigation data. USDA SCS TP-96, p. 48.

Carter, V. 1986. An overview of hydrologic concerns related to wetlands in the United States. Can. J. Bot. 64:364-374.

Corbett, E. S. 1967. Measurement and estimation of precipitation on experimental watersheds. In *International Symposium on Forest Hydrology*, W. E. Sopper and H. W. Lull, eds., Pergamon Press, New York, NY, pp. 107-127.

Crownover, S.H., N.B. Comerford, D.G. Neary, and J. Montgomery. 1995. Horizontal groundwater flow patterns through a Cypress swamp-Pine flatwoods landscape. Soil Sci. Soc. Am. J. 59:1199-1206.

Duever, M.J. 1988. Hydrologic processes for models of freshwater wetlands. In *Wetland Modelling*, W.J. Mitsch, M. Straskraba, and S.E. Jorgensen, eds., Elsevier, New York, NY, pp. 9-39.

Hargreaves, G.H. 1975. Moisture availability and crop production. Trans. Am. Soc. Agric. Eng. 18(5):980-984.

Helvey, J. D. 1971. A summary of rainfall interception by certain conifers of North America. In *Biological Effects in the Hydrogeological Cycle.* Proceedings of the 3rd International Seminar for Hydrology Professors, Purdue University, p. 103 - 113.

Helvey, J. D. and J. H. Patric. 1965. Canopy and litter interception of rainfall by hardwoods of eastern United States. Water Resources Res. 1(2):193-206.

Johnson, G. H. 1972. *Geology of the Yorktown, Poquoson West, and Poquoson East quadrangles, Virginia*: Virginia Division of Mineral Resources Rept. Inv. 30, 57p.

LaBaugh, J. W. 1986. Wetland ecosystem studies from a hydrologic perspective. Water Resources Bull. 22(1):1-10.

Lide, R. F., V. G. Meentemeyer, J. E. Pinder, III, and L. M. Beatty. 1995. Hydrology of a Carolina bay located on the Upper Coastal Plain of western South Carolina. Wetlands 15(1):47-57.

McNaughton, K. G. and T. A. Black. A study of evapotranspiration from a Douglas fir forest using the energy balance approach. Water Resour. Res. 9(6):1579-1590.

Monteith, J. L. and M. H. Unsworth. 1990. *Principles of Environmental Physics, 2nd ed.*, Edward Arnold, New York, NY, 291p.

Munro, D.S. 1979. Daytime energy exchange and evaporation from a wooded swamp. Water Resourc. Res. 15(5):1259-1265.

National Oceanic and Atmospheric Administration. 1994. Local Climatological Data, Annual Summary with Comparative Data, Norfolk, Virginia (ORF). Asheville, NC.

Phillips, P.J. and R.J. Shedlock. 1993. Hydrology and chemistry of groundwater and seasonal ponds in the Atlantic Coastal Plain in Delaware, USA. Journal of Hydrology 141:157-178.

Priestley, C. H. B. and R. J. Taylor. 1972. On the assessment of surface heat flux and evaporation using large-scale parameters. Mon. Weather Rev. 100(2):81-92.

Rassmusson, E. M., R. E. Dickinson, J. E. Kutzbach, and M. K. Cleaveland. 1993. Climatology. In *Handbook of Hydrology*, D. R. Maidment, ed., McGraw-Hill, Inc., New York, NY, pp. 2.1-2.44.

Richardson, C. J. and E. J. McCarthy. 1994. Effect of land development and forest management on hydrologic response in southeastern coastal wetlands: A review. Wetlands 14(1):56-71.

Rykiel, E. J., Jr. 1984. General hydrology and mineral budgets for Okefenokee Swamp: Ecological significance. In *The Okefenokee Swamp*, Cohen, A.D., Casagrande, D.J., Andrejko, M.J., and G.R. Best, eds., Wetland Surveys, Los Alamos, NM, pp. 212-228.

Shuttleworth, W. J. 1991. Evaporation models in hydrology. In *Land Surface Evaporation: Measurement and Parameterization*, T. J. Schmugge and J. C. Andre, eds., Springer-Verlag.

Shuttleworth, W. J. 1993. Evaporation. In *Handbook of Hydrology*, D. R. Maidment, ed., McGraw-Hill, Inc., New York, NY, pp. 4.1-4.53.

Slatyer, R. D. and I. C. McIlroy. 1961. *Practical Microclimatology.* UNESCO, Paris, 310 p.

Smith, J. A. 1993. Precipitation. In *Handbook of Hydrology*, D. R. Maidment, ed., McGraw-Hill, Inc., New York, NY, pp. 3.1-3.47.

Thornthwaite, C. W. 1948. An approach toward a rational classification of climate. Geogr. Rev. 38:55-94.

Tiner, R.W., I. Kenenski, T. Nuerminger, J. Eaton, D.B. Foulis, G.S. Smith, and W.E. Frayer. 1994. Wetlands of the Chesapeake Watershed: Status and trends from 1982 to 1989. Technical Report R5ES. U.S. Fish and Wildlife Service, Region 5, Ecological Services, Hadley, MA.

Virginia Institute of Marine Science. January, 1995. York River Ambient Monitoring Data. **VIMS Scientific Data Archive** (*http://www.vims.edu/data_archive*). Virginia Institute of Marine Science, School of Marine Science, College of William & Mary. Gloucester Point, VA 23062.

Waring, R. H. and W. H. Schlesinger. 1985. *Forest Ecosystems: Concepts and Management.* Academic Press, Inc., Orlando, FL, 340 p.

Winter, T. C. 1981. Uncertainties in estimating the water balance of lakes. Water Resources Bull. 17(1):82-115.

Winter, T. C., D. O. Rosenberry and A. M. Sturrock. 1995. Evaluation of 11 equations for determining evaporation for a small lake in the north central United States. Water Resour. Res. 31(4):983-993.

Woo, M. and J. Valverde. 1981. Summer streamflow and water level in a midlatitude forested swamp. Forest Sci. 27(1):177-189.

Yin, Z. and G. A. Brook. 1992. Evapotranspiration in the Okefenokee Swamp watershed: a comparison of temperature-based and water balance methods. J. Hydrol. 131:293-312.

Zinke, P. J. 1967. Forest interception studies in the United States. In *International Symposium on Forest Hydrology*, W. E. Sopper and H. W. Lull, eds., Pergamon Press, New York, NY, pp. 137-161.